# EFFECT OF ARC DEPOSITION AND HIGH POWER IMPULSE MAGNETRON SPUTTER COATINGS ON THE PERFORMANCE OF TOOLS FOR MACHINING VARIOUS FERROUS MATERIALS AND Ti6AL4V ALLOYS

**A Thesis Submitted to**
**the Graduate School of Engineering and Sciences of**
**İzmir Institute of Technology**
**in Partial Fulfillment of the Requirements for the Degree of**

**MASTER OF SCIENCE**

**in Materials Science and Engineering**

**by**
**Mine NOHUZ**

**July 2023**
**İZMİR**

We approve the thesis of Name **Mine NOHUZ,**

Examining Committee Members:

**Assist. Prof. Dr. Kemal DAVUT**

Department of Materials Science and Engineering, İzmir Institute of Technology

**Assoc. Prof. Dr. Onur ERTUĞRUL**

Department of Metallurgical and Materials Engineering, İzmir Kâtip Çelebi University

**Assoc. Prof. Dr. Sinan KANDEMİR**

Department of Mechanical Engineering, İzmir Institute of Technology

**21/07/2023**

**Assist. Prof. Dr. Kemal DAVUT**

Supervisor, Materials Science and Engineering,

İzmir Institute of Technology

**Prof. Dr. Sedat AKKURT**

Head of the Department of

Material Science and Engineering

**Prof. Dr. Mehtap EANES**

Dean of Graduate School

of Engineering and Science

# ACKNOWLEDGMENTS

First of all, I would like to thank my supervisor Assist. Prof. Kemal DAVUT for his help and support during my master studies and this thesis.

I would like to thank the examining committee members Assist Prof. Dr. Onur Ertuğrul and Assist. Prof. Dr. Sinan KANDEMİR for their valuable comments.

I would like to thank the research and development teams of Karcan Cutting Tools. The Center for Materials Research of IZTECH is gratefully acknowledged for SEM and EDS analysis of the samples.

I would like to thank Ali SATICI for his unique friendship and special motivation in challenging times. But most of all I would like to thank my family for everything they have done.

# ABSTRACT


## EFFECT OF CATHODIC ARC DEPOSITION AND HIGH POWER IMPULSE MAGNETRON SPUTTER COATINGS ON THE PERFOMANCE OF TOOLS FOR MACHINING VARIOUS FERROUS MATERIALS AND Ti6Al4V ALLOY

In this thesis, the performance of different coating techniques in machining various steels and Ti6Al4V is investigated. Currently, most of the carbide tools with the coating because of the tool life. In order to increase the productivity of the manufacturing processes and to use new materials, the research on the coating of cutting tools has been increased. Recently, the interest in physical vapor deposition has increased because the tool life is increased for many difficult-to-machine materials and difficult machining conditions. Two types of PVD coating were used in this work. The surfaces of the coated tools were examined under scanning electron microscope. The effects of cathodic arc deposition and high pulse magnetron sputtering on tool performance were investigated on various workpieces such as 4140 and CK45 steels, D2 tool steel (60HRC), GG25 cast iron and also on Ti6Al4V alloy. In the performance tests, the cutting forces were measured over a period of time and the wear patterns were recorded. The results indicate that HIPIMS coated tools perform better in operations where normal load is low and torsion forces are high. Those tools also work better in materials harder than 250 BHN. The better performance of HIPIMS coated tools were attributed to their less smooth and droplet free surfaces.

# ÖZET

## ÇEŞİTLİ DEMİR ALAŞIMLARI VE Ti6AL4V ALAŞIMINI İŞLEMEK İÇİN KULLANILAN TAKIMLARIN PERFORMANSINA ARK BİRİKTİRME VE YÜKSEK GÜÇLÜ İTKİLİ MANYETRON PÜSKÜRTÜMLÜ KAPLAMALARIN ETKİSİ

Bu tezde, çeşitli çelik ve Ti6Al4V'nin işlenmesi sırasında farklı kaplama tekniklerinin performansı incelenmiştir. Karbür takımların büyük bir kısmı fiziksel buharlaşma yöntemi ile kaplanmaktadır. Kaplama takım ömrünü arttıran önemli bir faktördür. Günümüzde üretim süreçlerinde ve kullanılan yeni iş parçası malzemelerinde verimliliği artırabilmek için kesici takımların kaplanması ile ilgili araştırmalar artmıştır. İşlenmesi zor birçok malzeme için takım ömrü ve zor işleme koşulları nedeniyle fiziksel buhar biriktirme yöntemi ile kesici takım kaplama konusuna olan ilgi son zamanlarda artmaktadır. Bu tezde, PVD kaplama tekniğinin iki üyesi olan katodik ark buharlaştırma tekniği ve yüksek itkili magnetron püskürtme yöntemi kullanılmıştır. 4140 ve CK45 çelikleri, D2 takım çeliği (60HRC), GG25 dökme demir ve Ti6Al4V alaşımı gibi farklı iş parçalarında katodik ark biriktirme ve yüksek darbeli magnetron püskürtmenin alet performansı üzerindeki etkisi araştırılmıştır. Kaplanan takımların yüzeyleri taramalı electron mikroskobunda incelenmiştir. Performans testleri sırasında belli bir süre kesme kuvvetleri ölçülerek aşınma miktarı görüntüler üzerinden belirlenmiştir. Sonuçlar, HIPIMS kaplamalı takımların normal yükün düşük ve burulma kuvvetlerinin yüksek olduğu operasyonlarda daha iyi performans gösterdiğini ortaya koymaktadır. Bu takımlar ayrıca 250 BHN'den daha sert malzemelerde daha iyi çalışmaktadır. HIPIMS kaplamalı takımların daha iyi performans göstermesi, daha pürüzsüz ve damlacıksız yüzeylerine bağlanmıştır.

# TABLE OF CONTENTS

LIST OF FIGURES ..... viii

LIST OF TABLES ..... xii

ABBREVIATIONS ..... xiv

CHAPTER 1. INTRODUCTION ..... 1

1.1 Machining and Its Importance ..... 1
1.2 Machining Methods ..... 2
1.3 Machinability Concept ..... 3
1.3.1 Machinability and Factors Effecting It ..... 4
1.3.2 Machinability of Ferrous Material ..... 4
1.3.3 Machinability of Ti6Al4V ..... 5
1.4 Design and Manufacture of Tools ..... 5
1.4.1 Raw Material Selection ..... 6
1.4.2 Tool Design and Simulation ..... 7
1.4.3 Prototype Manufacturing ..... 11
1.5 Coating of Tools ..... 13
1.5.1 Types and Performance of Tool Coating ..... 14
1.5.2 Types of Coating Technologies ..... 15
1.6 Literature Research ..... 19
1.7 Objective and Scope of Thesis ..... 20

CHAPTER 2. EXPERIMENTAL ..... 21

2.1 Materials for Machining ..... 21
2.2 Machining Performance Test ..... 23
2.3 Coated Tool Surface Analysis ..... 27

CHAPTER 3. RESULTS ..... 28

3.1. Coating Quality ..... 29
3.1.1 Surface Roughness Measurement ..... 29
3.1.2 Edge Preparation Values ..... 30
3.1.3 SEM and EDS Analysis ..... 31

3.2. Machining Performance ..... 41
3.2.1 Test Parameters ..... 42
3.2.2 Spike Results ..... 44
3.2.3 Tool wear ..... 52
3.2.4 Chip Images ..... 64

CHAPTER 4. DISCUSSIONS ..... 68

CHAPTER 5. CONCLUSIONS ..... 87

REFERENCES ..... 88

# LIST OF FIGURES

**Figure** **Page**

Figure 1.1. Schematic representation of holes ..... 2
Figure 1.2. Schematic Representation of Shoulder and Slot Milling[6] ..... 3
Figure 1.3. Schematic representation of self-hardening ..... 5
Figure 1.4. Geometric design of tool 1 and 2 ..... 7
Figure 1.5. Geometric design of tool 3 and 4 ..... 7
Figure 1.6. Geometric design of tool 5 and 6 ..... 8
Figure 1.7. Geometric design of tool 7 and 8 ..... 8
Figure 1.8. Geometric design of tool 9 and 10 ..... 8
Figure 1.9. Geometric design of tool 11 and 12 ..... 9
Figure 1.10. Simulation Image of tool 1 and 2 ..... 9
Figure 1.11. Simulation Image of tool 3 and 4 ..... 9
Figure 1.12. Simulation Image of tool 5 and 6 ..... 10
Figure 1.13. Simulation Image of tool 7 and 8 ..... 10
Figure 1.14. Simulation Image of tool 9 and 10 ..... 10
Figure 1.15. Simulation Image of tool 11 and 12 ..... 10
Figure 1.16. 5-axis Reinecker WZS70 CNC Machine ..... 11
Figure 1.17. Effect of Edge Preparation ..... 12
Figure 1.18. Drag Finish Machine ..... 12
Figure 1.19. Example of edge preparation report from Alicona ..... 13
Figure 1.20. Types of CVD coatings[24] ..... 16
Figure 1.21. PVD techniques for tool coating ..... 16
Figure 1.22. Schematic Representation of Cathodic Arc Deposition[28] ..... 17
Figure 1.23. Schematic Representation of HIPIMS ..... 18
Figure 2.1. Mikron VCP800 3 axis CNC machine ..... 23
Figure 2.2. Image of Lang Clamp ..... 23
Figure 2.3. Image of the blum laser ..... 24
Figure 2.4. Image of Cooling unit of CNC Machine ..... 24
Figure 2.5. Milling Example of Hypermill Simulation ..... 25
Figure 2.6. Milling Example of Hypermill Simulation ..... 25

**Figure** **Page**

Figure 2.7. Image of Spike Mobile Holder ..... 27
Figure 3.1. Alicona Infinite Focus G5 ..... 29
Figure 3.2. Ra and Sa calculation formulas ..... 30
Figure 3.3. SEM micrographs of coated surfaces of SM-PVD and SM-HIPIMS samples taken at 2500x and 5000x magnifications with SEI and BSD detectors. ..... 32
Figure 3.4. SEM micrographs of coated surfaces of SLT-PVD and SLT- HIPIMS samples taken at 2500x and 5000x magnifications with SEI and BSD detectors ..... 32
Figure 3.5. SEM micrographs of coated surfaces of DRL-PVD and DRL-HIPIMS samples taken at 2500x and 5000x magnifications with SEI and BSD detectors ..... 33
Figure 3.6. SEM micrographs of coated surfaces of GEO1-Ti6Al4V-PVD and GEO1-Ti6Al4V-HIPIMS samples taken at 2500x and 5000x magnifications with SEI and BSD detectors ..... 33
Figure 3.7. SEM micrographs of coated surfaces of GEO2-Ti6Al4V-PVD and GEO2-Ti6Al4V-HIPIMS samples taken at 2500x and 5000x magnifications with SEI and BSD detectors ..... 34
Figure 3.8. SEM micrographs of coated surfaces of D2-PM-PVD and D2-PM-HIPIMS samples taken at 2500x and 5000x magnifications with SEI and BSD detectors ..... 34
Figure 3.9. EDS spectrum of Group 1 PVD coated tools (SM-PVD) ..... 35
Figure 3.10. EDS spectrum of Group 1 HIPIMS coated tools (SM-HIPIMS) ..... 35
Figure 3.11. EDS spectrum of SLT-PVD tools ..... 36
Figure 3.12. EDS spectrum of SLT-HIPIMS tools ..... 36
Figure 3.13. EDS spectrum of DRL-PVD tools ..... 37
Figure 3.14. EDS spectrum of DRL-HIPIMS tools ..... 37
Figure 3.15. EDS spectrum of GEO1-Ti6Al4V-PVD tools ..... 38
Figure 3.16. EDS spectrum of GEO1-Ti6Al4V-HIPIMS tools ..... 38
Figure 3.17. EDS spectrum of GEO2-Ti6Al4V-PVD tools ..... 39
Figure 3.18. EDS spectrum of GEO2-Ti6Al4V-HIPIMS tools ..... 39
Figure 3.19. EDS spectrum of D2-PM-PVD tools ..... 40
Figure 3.20. EDS spectrum of D2-PM-HIPIMS tools ..... 40

**Figure** **Page**

Figure 4.1. Interaction plot of bending moment (a)Test end (b) Avarage (c) Max (d) Max-min of group 1 (cont. on next page) ..... 68
Figure 4.2. Main effect plot of bending moment and a) deposition method b) workpieces method ..... 69
Figure 4.3. Interaction plot of normal load (a)Test end (b) Avarage (c) Max (d) Max-min of group 1 ..... 70
Figure 4.4. Main effect plot of normal load and a) deposition method b) workpieces method..... 70
Figure 4.5. Interaction plot of torsion force (a)Test end (b) Average (c) Max (d) Max-min of group 1 ..... 71
Figure 4.6. Main effect plot of torsion force and a) deposition method b) workpieces method ..... 72
Figure 4.7. Interaction Plot of wear amount of group 1 ..... 73
Figure 4.8. Main effect plot of wear amount and a) deposition method b) workpieces materials..... 73
Figure 4.9. Interaction plot of bending moment (a)Test end (b) Average (c) Max (d) Max-min of group 2 ..... 74
Figure 4.10. Main Effect plot of bending moment and a) deposition method b) operation type..... 74
Figure 4.11. Interaction plot of normal load (a)Test end (b) Average (c) Max (d) Max-min of group 2 ..... 75
Figure 4.12. Main effect graph of normal load and a) deposition method b) operation type..... 76
Figure 4.13. Interaction plot of torsion force (a)Test end (b) Average (c) Max (d) Max-min of group 2 (cont. on next page) ..... 76
Figure 4.15. Main effect plot of torsion force and a) deposition method b) operation type..... 77
Figure 4.16. Interaction Plot of Wear Rate of group 2..... 78
Figure 4.17. Main effect plot of wear amount and a) deposition method b) operation type..... 78
Figure 4.18. Interaction plot of bending moment (a)Test end (b) Average (c) Max (d) Max-min of group 3 ..... 79

**Figure** **Page**

Figure 4.19. Main effect plot of bending moment and a) deposition method b) tool geometry ..... 79
Figure 4.20. Interaction plot of normal load (a)Test end (b) Average (c) Max (d) Max-min of group 3 ..... 80
Figure 4.21. Main effect plot of normal load and a) deposition method b) tool geometry ..... 81
Figure 4.22. Interaction plot of torsion force (a)Test end (b) Average (c) Max (d) Max-min of group 3 (cont. on next page) ..... 81
Figure 4.24. Main effect plot of torsion forces and a) deposition method b) tool geometry ..... 82
Figure 4.25. Interaction Plot of Wear Rate of group 3 ..... 83
Figure 4.26. Main effect of wear amount and a) deposition method b) tool geometry .. 83
Figure 4.27. Column chart of group 4 bending moment ..... 84
Figure 4.28. Column chart of group 4 normal load ..... 85
Figure 4.29. Column chart of group 4 torsion force ..... 85
Figure 4.30. Column chart of group 4 wear ..... 86

# LIST OF TABLES

**Table** **Page**

Table 1.1. Properties of Raw Materials ..... 6
Table 1.2. Advantages and disadvantages of cathodic arc and high-power impulse magnetron sputtering techniques ..... 19
Table 2.1. Chemical Composition of 4140 material (wt%) ..... 21
Table 2.2. Chemical Composition of CK45 material (wt%) ..... 22
Table 2.3. Chemical Composition of GG25 material (wt%) ..... 22
Table 2.4. Chemical Composition of 2379 material (wt%) ..... 22
Table 2.5. Chemical Composition of Ti6Al4V material (wt%) ..... 22
Table 2.6. Hardness values of workpieces material ..... 22
Table 2.7. Performance test plan ..... 26
Table 3.1. Distribution of tests to group 1 ..... 28
Table 3.2. Distribution of tests to group 2 ..... 28
Table 3.3. Distribution of tests to group 3 ..... 28
Table 3.4. Distribution of tests to group 4 ..... 29
Table 3.5. Surface roughness values of tools ..... 30
Table 3.6. Edge preparation values of the tools before and after coating ..... 31
Table 3.7. Chemical composition of coatings ..... 41
Table 3.8. Test parameter of group 1 ..... 42
Table 3.9. Test parameter of group 2 ..... 43
Table 3.10. Test parameter of group 3 ..... 43
Table 3.11. Test parameter of group 4 ..... 43
Table 3.12. Flank wear images of 4140-SM-PVD, CK45-SM-PVD and GG25-SM-PVD ..... 53
Table 3.13. Rake wear images of 4140-SM-PVD, CK45-SM-PVD and GG25-SM-PVD ..... 54
Table 3.14. Flank wear images of 4140-SM-HIPIMS, CK45SM-HIPIMS and GG25- SM-HIPIMS ..... 55

**Table** **Page**

Table 3.15. Rake wear images of 4140-SM-HIPIMS, CK45SM-HIPIMS and GG25-SM-HIPIMS ..... 56
Table 3.16. Flank wear images of 4140-SLT-PVD, 4140-SLT-HIPIMS ..... 57
Table 3.17. Rake wear images of 4140-SLT-PVD, 4140-SLT-HIPIMS ..... 58
Table 3.18. Front wear images of 4140-DRL-PVD, 4140-DRL-HIPIMS ..... 59
Table 3.19. Flank wear images of Geo1_HFM-Ti6Al4V-PVD, Geo1_HFM-Ti6Al4V-HIPIMS ..... 59
Table 3.20. Rake wear images of Geo1_HFM-Ti6Al4V-PVD, Geo1_HFM-Ti6Al4V-HIPIMS ..... 60
Table 3.21. Flank wear images of Geo2_HFM-Ti6Al4V-PVD, Geo2_HFM-Ti6Al4V-HIPIMS ..... 61
Table 3.22. Rake wear of Geo2_HFM-Ti6Al4V-PVD, Geo2_HFM-Ti6Al4V-HIPIMS ..... 63
Table 3.23. Front wear images of D2-PM-PVD, D2-PM-HIPIMS ..... 64
Table 3.24. Chip Images of Group 1 tests ..... 65
Table 3.25. Chip images of group 2 tests ..... 66
Table 3.26. Chip images of group 3 tests ..... 67

# ABBREVIATIONS

| | |
|---|---|
| **PVD** | Physical Vapour Deposition |
| **HIPIMS** | High Impulse Magnetron Sputtering |
| **Ø** | Diameter |
| **Ti6Al4V** | Titanium grade 5 |
| **HRA** | Rocwell Hardnees |
| **TiAlN** | Titanium aluminum nitride |
| **ZrN** | Zirconium Nitrate |
| **TiSiN** | Titanium silicon nitride |
| **AlCrN** | Aluminum chrome nitride |
| **Ra** | The roughness calculation on a line |
| **Sa** | The roughness calculation made within an area |
| **µm** | Micrometer |
| **SEM** | Scanning Electron Microscope |
| **EDS** | Energy-dispersive X-ray spectroscopy |

# CHAPTER 1

# INTRODUCTION

Machining is an especially important process that plays a role in manufacturing industries such as automotive, aviation, space, medical and electronics. For these industries, it is necessary to produce parts in the desired size, shape, and quality with a high tool life[1,2].

The coating of cutting tools with physical vapor deposition (PVD) coating is also a process that increases tool life. PVD coatings help to reduce the friction coefficient and wear on the tools. PVD do not show the same performance for all materials. By choosing the appropriate coating for the workpiece processed by the cutting tools, friction is reduced and thus tool wear can be reduced.

In addition to the correct coating, water vapor accumulation that is known as 'droplet' occurs on the surface of the tools during coating. This droplet affects tool performance by increasing wear on the tool. Many coating companies add post-coating operations to their coatings to prevent this situation. However, with newer coating techniques, it is possible to minimize this situation without a need for any post-coating operation.

Within the scope of this project, the effects of ARC deposition and HIPIMS technologies on tool performance will be examined on different workpieces. While making this comparison, materials that are widely used in the industries such as 4140 and CK45 steels, D2 tool steel, GG25 cast iron and Ti6Al4V alloy will be used.

## 1.1. Machining and Its Importance

Machining is the process of giving the desired geometric shape by removing chips of different shapes and sizes on the part, by referring to the projected technical drawing of a designed workpiece in accordance with the standards. The biggest importance of machining is that products with more precise tolerance ranges can be produced compared to other manufacturing technologies.

Machining helps to produce various geometries with varied sizes. Uniform dimensions and surfaces qualities can be achieved with machining.

Nowadays, manufacturing is automated. Processes are generally controlled by robots or computers; this results in decreases production cost and require less human labor. Therefore, the second important advantage of machining is the high productivity because the process is intended to do a lot of work in a brief time. After the machining, the products are very close to the shape of the design despite the high rate of the production[3].

## 1.2. Machining Methods

Machining proses can be divided into several types of technologies like turning, drilling, milling, grinding, planning, sawing, broaching, electrical discharge machining, and electro chemical machining[4]. Drilling and milling operations will be used within the scope of this project.

First of all, drilling is a machining process that creates holes. Drilling is a complex process that may seem simple but can have significant consequences if the tool fails and is used beyond its capacity. Important things in drilling are hole, hole type and hole quality[5].

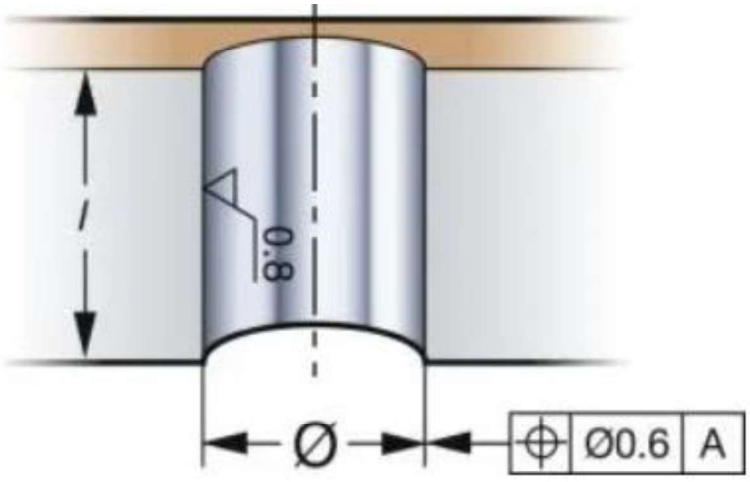


Figure 1.1. Schematic representation of holes[6]

Secondly, Milling has become a machining method with a very wide working range.

It is the process of removing chips from the workpiece that moves forward with a rotating tool. There are lots of diverse types of milling. These are shoulder milling,

slot milling, trochoidal milling, face milling etc[7]. In figure 1.2. Schematic representation of slot and shoulder milling are given. In this thesis, the shoulder, slot milling and also high-performance milling with shoulder milling operation method will be used.

It is a shoulder milling operation applied to the machining of an edge and its contouring with various tool passes. It creates two surfaces simultaneously.

One of the most important requirements is to create a 90° edge. For shoulder milling, solid carbide end mills and indexable end mills can be used[8].

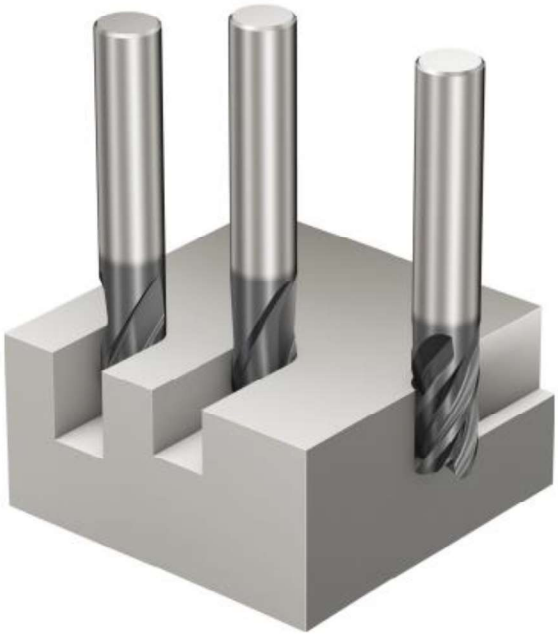

Figure 1.2. Schematic Representation of Shoulder and Slot Milling[6]

## 1.3. Machinability Concept

Machinability can be defined as the material's susceptibility to stock removal. Machinability shows different properties with different material while the manufacturing even if all other parameters are the same. For example, some materials create long continuous chips, some remove chips intermittently (cast iron), while the surface of some is smooth enough that no additional processing is required, the surface of the other may be covered with scratches[9].

### 1.3.1. Machinability and Factors Effecting It

Machinability can be defined as how easily the material can reach its final shape. Also, the factor that can affect it can be divided into two as material variables and machining variables10.

Microstructure of material, chemical composition of materials, mechanical properties and heat treatment can be considered as material variables.

For example, the machinability of a heat-treated material is much more difficult than steel based on the microstructure of material. On the other hand, tool geometry, cutting parameters, coolant type, rigidity of fixture and tool can be considered as machining variables. According to the material to be processed, the most suitable machining variables should be determined, respectively.

### 1.3.2. Machinability of Ferrous Material

The machinability of ferrous alloys can be difficult due to the material characteristic like microstructure and mechanical properties like high strength, low thermal conductivity, high ductility, and high work hardening tendency while the machining[11]. In the microstructure carbon is the most important alloying element. Alloying and trace elements can affect the machinability of steels because of changes in microstructure. They can form some carbides, nitrides, oxides, or intermetallic phases that can affect machinability. Some of the alloying elements affect the machinability negatively while some affect positively. For instance, Sulfur makes machinability easer due to the forms of stable sulfides. On the other hand, aluminum, silicon, or calcium are reduce the machinability of ferrous metals because it forms some oxides[12].

Heat treatment process is also an important process that effect machinability. This process changes the arrangement of constituent, shapes of grains and their quantity; therefore, mechanical properties of material are also influenced by machinability. Heat treated materials always harder the machine than without heat treated materials[13]

### 1.3.3. Machinability of Ti6Al4V

Based on high tensile strength, low ductile yield, lower elastic modulus, and lower thermal conductivity makes Ti6Al4V material relatively hard to machine material[14]. Especially low thermal conductivity makes machinability of Ti6Al4V difficult due to the self-hardening. Self-hardening means that while the machining heat generation occurs between tool and workpiece material therefore workpiece material undergoes plastic deformation. This situation is like a heat treatment at lower temperatures[15].

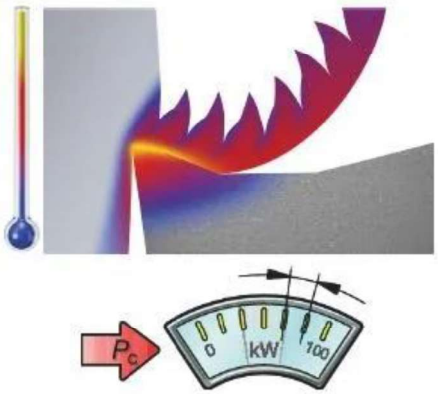


Figure 1.3. Schematic representation of self-hardening[16]

## 1.4. Design and Manufacture of Tools

The tool manufacturing process starts with the design of the tool and the creation of the technical drawing. The feasibility of the tools whose technical drawings are created is carried out in the simulation. It will be designed in 2D in Auto-CAD program, considering the geometric details of the product and the demands in the market. It can be updated after the finite element analyzes to determine the tool life.

It will be tried to provide the desired life by changing the raw material properties and coating types in the same geometric dimensions with the literature review and the information received from the suppliers.

### 1.4.1. Raw Material Selection

The choice of cutting tool material and grade is a crucial factor to consider when planning a successful machining process. Basic information about each cutting tool material and performance is important for making the right choice.

Considerations for each operation include the workpiece material to be machined, part type and shape, machining conditions and surface quality level. Cutting tool materials have different combinations of hardness, toughness and wear resistance and are divided into multiple grades with specific properties. Cemented Carbide will be used as raw material in this project, and they supply from the Ceratizit company.

Table 1.1 gives the raw material to be used in this thesis and its properties. For general machining of ferrous metal GU20E recommended, for high performance machining CTS24Z and CTS20D recommended for high heat resistant properties. Lastly, for heat treated material machining CTS12D grade recommended[17]. When designing the tool, it is very important to know which material and under what conditions it will work.

Table 1.1. Properties of Raw Materials[17]

| | GRADE | ISO CODE | GRAIN SIZE | BINDER AMOUNT | HARDNESS (HRA) | DENSITY g/cm³ | Transverse rupture strength TRS N/mm² |
|---|---|---|---|---|---|---|---|
| Tool 1-6 | GU20E | K20-K40 | 0,7 | 10 | 91,9 | 14.4 | 3800 |
| Tool 7 | CTS24Z | K20-K40 | 0.5-0.8 | 12 | 91.7 | 14.1 | 4000 |
| Tool 8 | | | | | | | |
| Tool 9 | CTS20D | K20-K40 | 0.5-0.8 | 10 | 91.9 | 14.38 | 4000 |
| Tool 10 | | | | | | | |
| Tool 11 | CTS12D | K05-K10 | 0.5-0.8 | 6 | 93.1 | 14.8 | 3600 |
| Tool 12 | | | | | | | |

## 1.4.2. Tool Design and Simulation

While choosing the tool design, the most preferred tools for ferrous metals, titanium alloys and hardened steels were selected within the Karcan cutting tool. Geometrically, 5 different milling cutters and 1 drill were selected. The two-dimensional images of the designed tools are below.

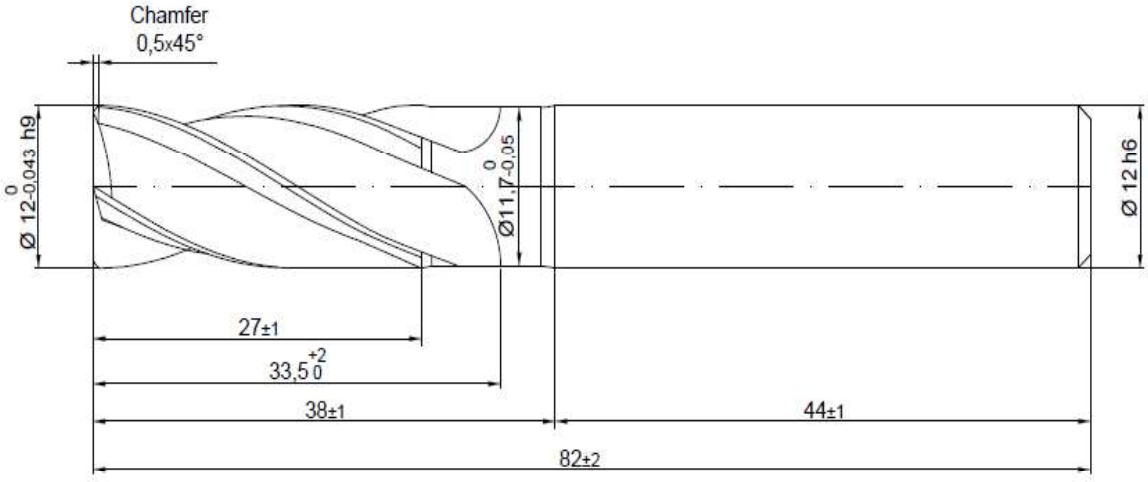


Figure 1.4. Geometric design of tool 1 and 2

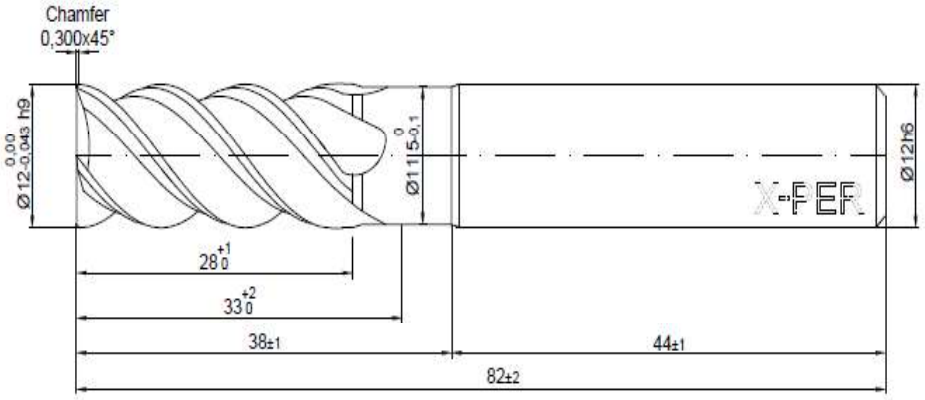


Figure 1.5. Geometric design of tool 3 and 4

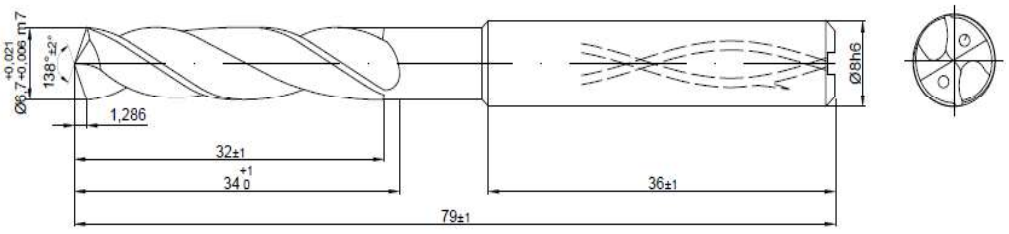


Figure 1.6. Geometric design of tool 5 and 6

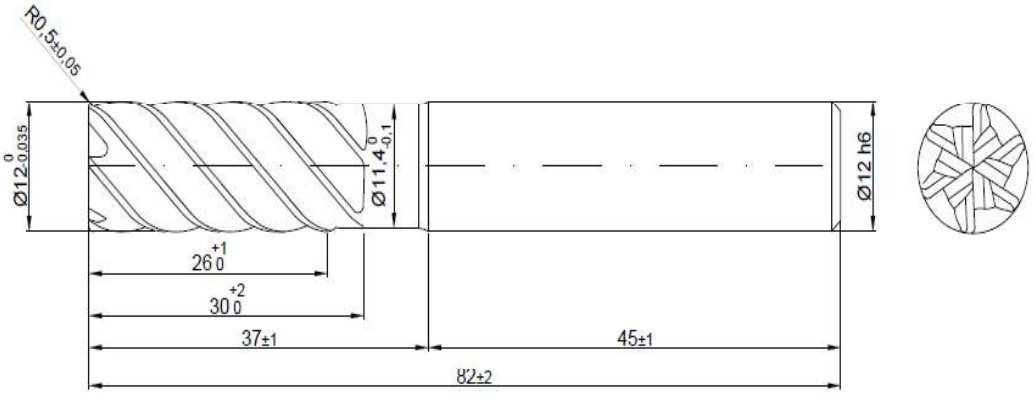


Figure 1.7. Geometric design of tool 7 and 8

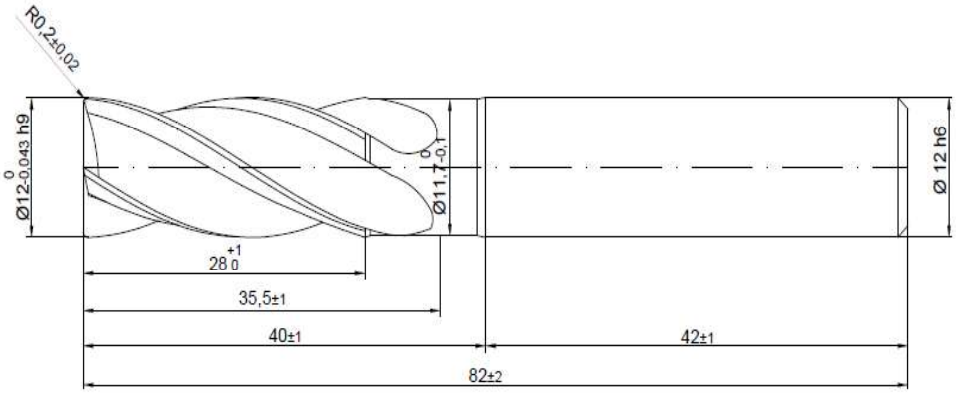


Figure 1.8. Geometric design of tool 9 and 10

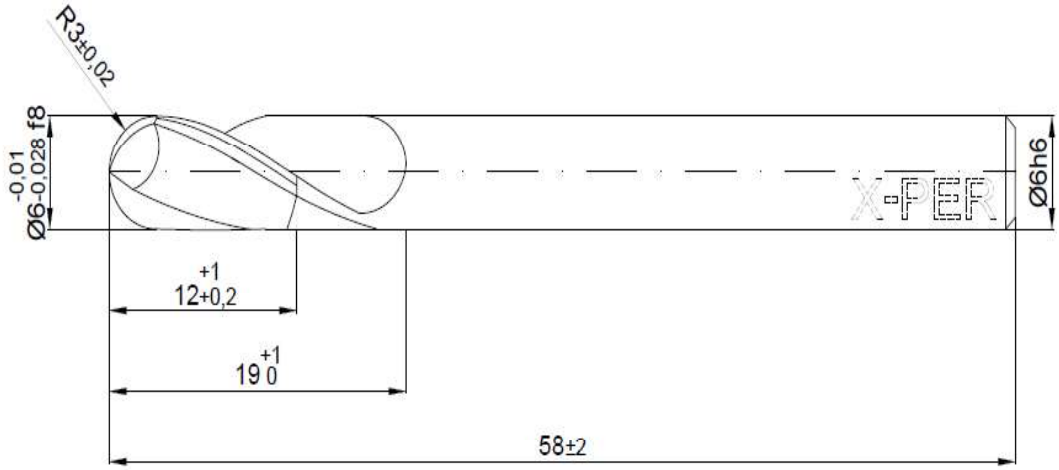


Figure 1.9. Geometric design of tool 11 and 12

Also, Tool simulation is basically the process of testing the production capabilities and manufacturability of the designed tool in a computer environment. Tool simulations was created with in the Numroto program. Each color in the simulation belongs to certain elements determined in the geometry of the tool.

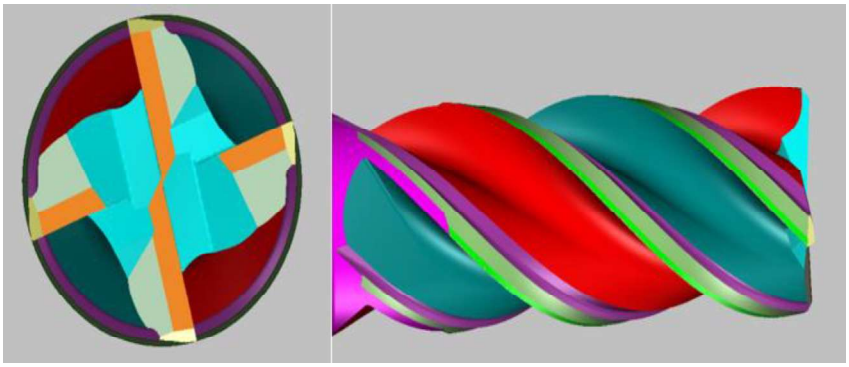

Figure 1.10. Simulation Image of tool 1 and 2

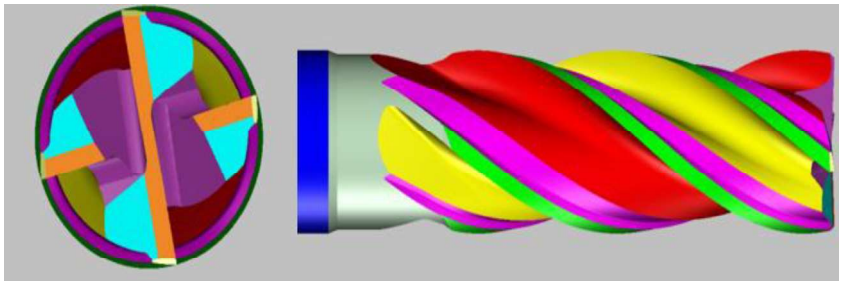

Figure 1.11. Simulation Image of tool 3 and 4

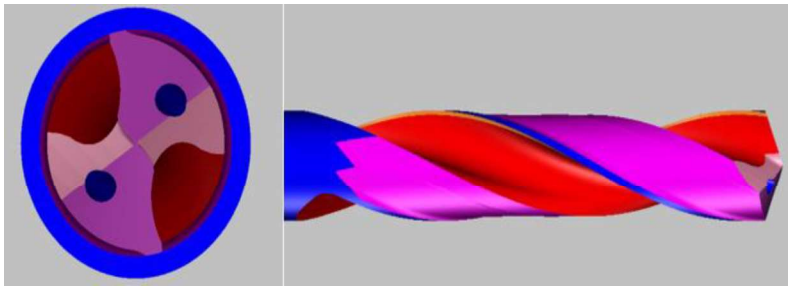

Figure 1.12. Simulation Image of tool 5 and 6

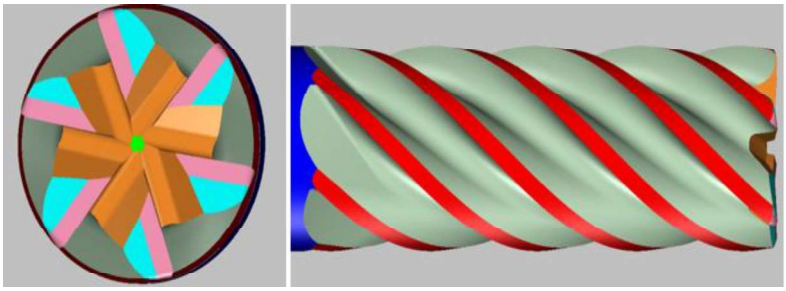

Figure 1.13. Simulation Image of tool 7 and 8

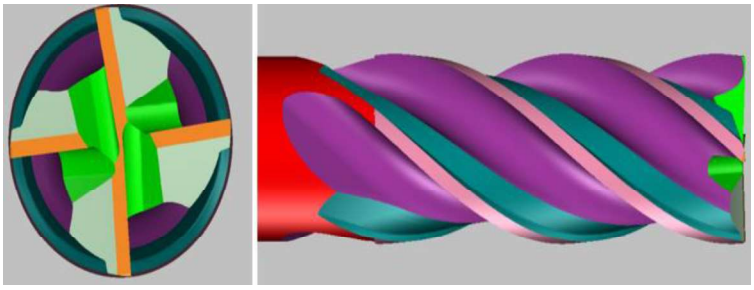

Figure 1.14. Simulation Image of tool 9 and 10

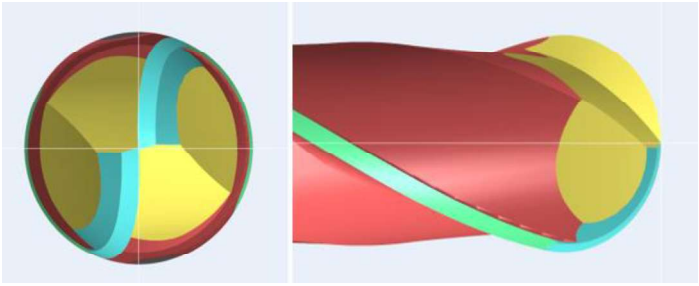

Figure 1.15. Simulation Image of tool 11 and 12

### 1.4.3. Prototype Manufacturing

All the prototype productions were produced on the Reinecker WZS70 machine, which is a 5-axis CNC machine. The shaping of the tools was carried out by grinding operation on the basis of grinding. Diamond wheels of different geometry were used for each operation. Operations such as groove, radius, pre-grinding and backing seen in the tools were simulated using the CAD/CAM program Numroto and processed on a 5-axis CNC machine. During tool manufacturing, first the channels are opened, then the back of the channel is discharged, and then the grinding operations of the surfaces to be cut together with the corner radius at the front are performed**.**

Figure 1.16. 5-axis Reinecker WZS70 CNC Machine

### 1.4.4. Edge Preparation

Cutting edge geometry affects the performance of the tool and impacts many other things like proses parameters, chip formation, tool wear etc. Edge preparation is a mechanical process of rolling the cutting edge. There are many processes to obtain homogenous edge rounding like blasting, drag finish, brushing. This process applied tool before the coating process.

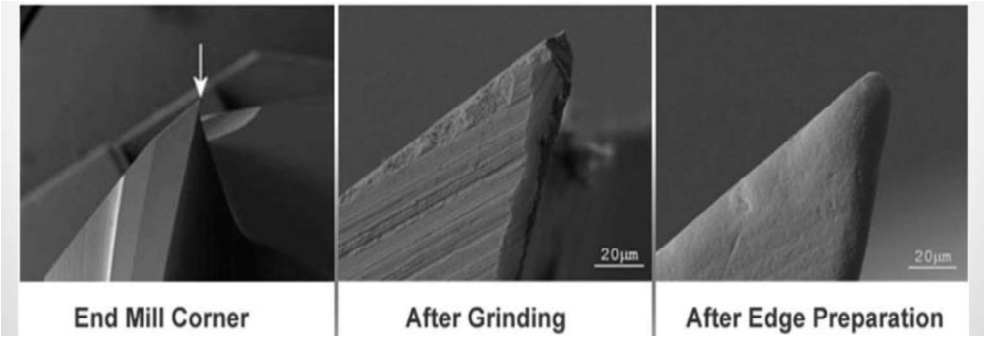


Figure 1.17. Effect of Edge Preparation[18]

In figure 1.18, drag finish machine in Karcan Cutting tools given; drag finish is a technique that used for rounding of the cutting edges. Also, cutting edge radius can be between 5 and 200 microns with this technique. The tool clamps to the holder and then it drags in some grinding media. Edge preparation process is completed by spinning the tool, tool table and the media at high speeds.

Figure 1.18. Drag Finish Machine

The edge preparation value is measured with the Alicona Infinite focus G5 device. An example about edge preparation measurement is given in Figure 1.19. Clerance and rake surfaces represent two angles that cut, and the edge preparation value is the radius at the micron level where these two angles meet.

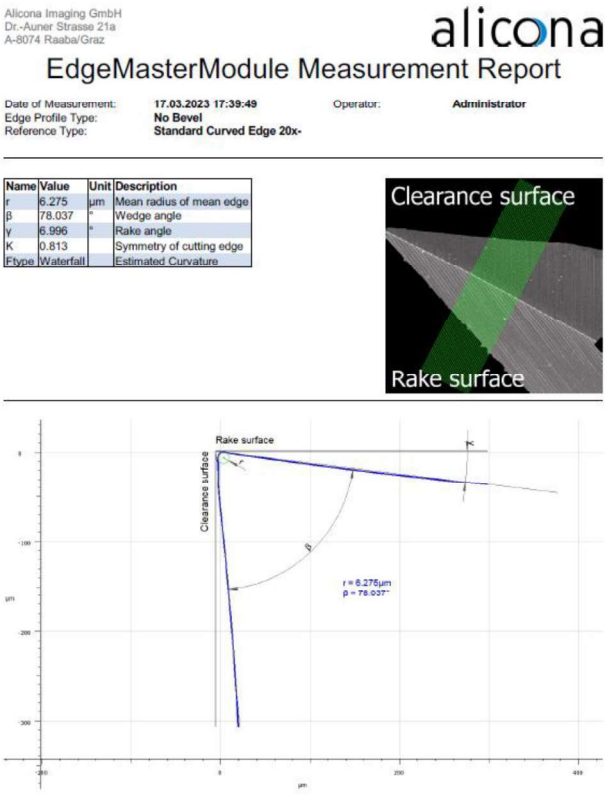


Figure 1.19. Example of edge preparation report from Alicona

## 1.5. Coating of Tools

The cutting tools with coating have a compound material structure that gives better performance than the uncoated tools. Coating gives the tool different properties like anti friction Surface, chemically inert layer, thermal insulation layer, also it gives several micron thicknesses.

During the machining, the coated tools give better protection to thermal and mechanical loads, reduces interaction between tool and workpiece material thus reduces friction therefore wear resistance increase[19]. Thus, lots of coating types and technology develop in time.

### 1.5.1. Types and Performance of Tool Coating

All research of coating and coating technologies are aimed to protect cutting tool from abrasive and adhesive wear. Nevertheless, the research is still going on to develop coatings that gives better performance[20].

There are many different coatings for different applications of cutting tools. The most important properties of coatings for cutting tools are given below:

Wear Resistance: High wear resistance decreases the material loss of tools.

Thermal Resistance: High thermal resistance reduces heat generation between material and tool.

Lubricity: Reduces the friction between tool and workpiece material.

TiAlN, ZrN, TiSiN and AlCrN are the most used coatings in cutting tools. They have different distinguishing characteristics.

#### 1.5.1.1. Properties of TiAlN

The aluminum oxide layer provides the tool with longer life and advantages in high temperature applications. Although this type of coating is more suitable for carbide tools, it is also preferred when little or no coolant is used. The excess of aluminum in the composition provides more hardness on the surface[21]. It is generally used in drills and reamers.

#### 1.5.1.2. Properties of ZrN

Although this coating, which is generally used in the medical industry, is a thin coating, it is a high hard coating. Being a thin coating, it protects the sharp edge needed for cutting soft metals such as aluminum, brass, copper. At the same time, this coating, which has a low coefficient of friction, is a type of coating that is recommended for cutting non-ferrous metals[22].

### 1.5.1.3. Properties of TiSiN

In this coating, which is formed by the combination of titanium and silicium, Titanium adds hardness to the coating, while silicium provides high oxidation resistance and prevents chemical reactions that may occur.

TiSiN-based coatings are known for their ability to work in harsh conditions. They can show high performance eve n when no cooler is used[23].

### 1.5.1.4. Properties of AlCrN

Known for its chemical stability (high oxidation resistance), this coating is recommended for applications where Build-up edge is observed on the cutting edge. A build-up edge means the workpiece material is being pressure welded to the cutting tool. At the same time, it is resistant to thermal stresses that may occur in this coating, which has high thermal shock resistance. However, due to the high stresses, shearing can be observed in the coatings[24]. It is generally used in end mills.

Among all coatings, AlCrN coating is relatively new coating and thanks to the amount of Cr in the structure, the tools with this coating can be used at high speeds and feed rates. Briefly, it protects the tools more than others. Therefore, AlCrN coating will be used in this thesis.

## 1.5.2. Types of Coating Technologies

As mentioned, paragraph 1.5.1, several tool coatings have been advanced in years. Coating materials are deposited on the cutting tool material. Deposition methods are divided into 2 groups physical vapor deposition (PVD) and chemical vapor deposition (CVD). There are several types of CVD process, including atmospheric pressure chemical vapor deposition, metal-organic chemical vapor deposition, low pressure chemical vapor deposition, laser chemical vapor deposition, photochemical vapor deposition, chemical vapor infiltration etc.

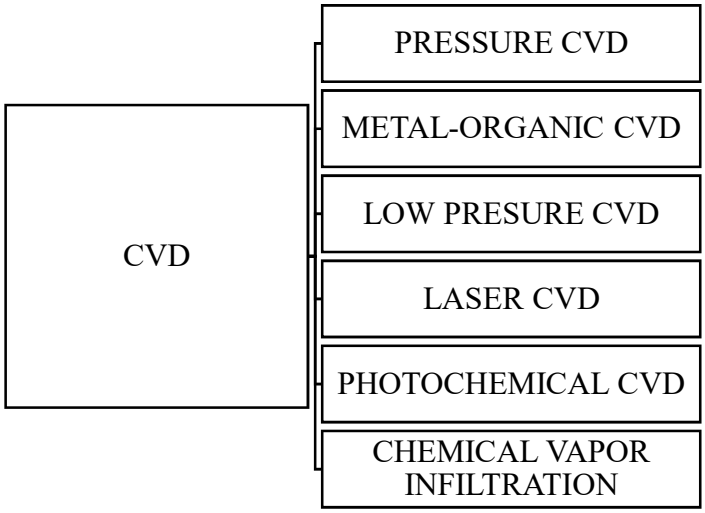


Figure 1.20. Types of CVD coatings[24]

Between these two techniques, the biggest differences are that PVD (around 250°C~450°C) occurs lower temperature range than CVD (around 450°C~1050°C)[25]. The second difference is the cost. PVD is a cheaper technique than CVD. PVD methods are given in Figure 1.21.

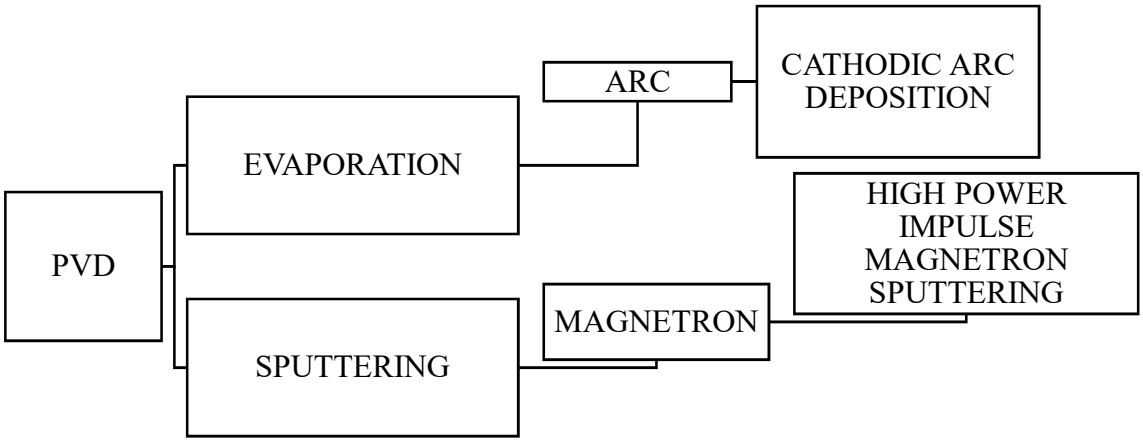


Figure 1.21. PVD techniques for tool coating[26]

PVD techniques can be divided into 2 groups as sputtering and evaporation. In sputtering technique vaporization formed by of a solid substance by bombarding it with ion energy[27]. It uses plasma as a source. On the other hand, evaporation technique uses as a source temperature which decreases the number of high-speed atoms[28].

Cathodic arc deposition technique also known as an Arc-PVD technology that is a member of PVD technique. In this technique electric arc is used to vaporize material from a cathode target. then it condenses on a substrate material[29].

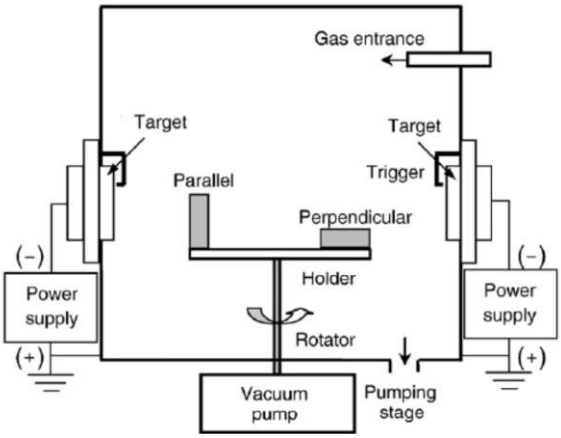


Figure 1.22. Schematic Representation of Cathodic Arc Deposition[28]

In figure 1.22. Schematic representation of cathodic arc deposition technique given. Firstly, evaporation starts on the cathode Surface with high current, low voltage arc. Therefore, localized temperature is generated that results in the vaporized cathode material. Then the cathode part self-extinguishes and re-ignites in a new area. This behavior causes the apparent motion of the arc. The arc has high power density, which leads to high ionization. When a reactive substance encounters this evaporation process, dissociation takes place, and compounds are formed on the substrate material.

There is a disadvantage of this process that is large amount of macro particles and droplets form due to the cathode evaporations time. These droplets badly effect the performance and quality of the coating[30].

HIPIMS is a member of sputtering technique. It is based on the working principle of magnetron sputtering and provides the advantages of that technique. In this technique, sputtering rate is very high so that causes increase in plasma densities[31].

As a result of high metal concentration, multiple ionization, it provides excellent adhesion to surface material. HIPIMS completely avoid droplets. Due to the unique features of high-power discharge, it is used for a wide range of applications.

HIPIMS technology is similar process to magnetron sputtering. The power supply is different, it must create high power pulses. Figure 1.23 shows schematic representation of HIPIMS technology.

Firstly, high voltage applied between cathode and anode. Cathode is located behind the sputtering target and anode is connected to the chamber as electrically ground. This situation results in ionization atoms going anode the cathode that led to high energy collision target surface. Atoms of the target Surface ejected to the vacuum environment as a result of each collision. To facilitate as many high-energy collisions as possible - leading to increased deposition rates - the sputter gas is typically chosen as a high molecular weight gas such as argon[32]

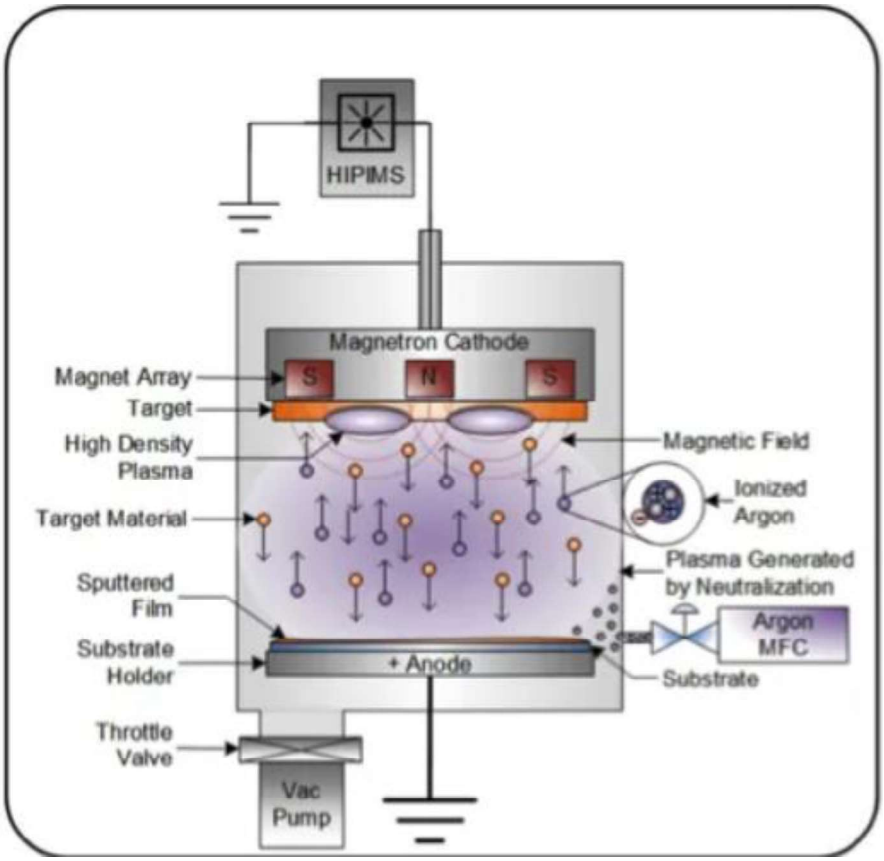


Figure 1.23. Schematic Representation of HIPIMS[33]

The biggest advantage of HIPIMS is the control of a powerful high voltage that ionizes a very high percentage of the target material without overheating, creating a dense plasma cloud with virtually no droplets. Thanks to this, coating has high performance dense coating, good adhesion, and extremely smooth surface[34]. The table summarizes the advantages and disadvantages of these two techniques.

Table 1.2. Advantages and disadvantages of cathodic arc and high-power impulse magnetron sputtering techniques

| COATING TECHNIQUE | ADVANTAGES | DISADVANTAGES |
|---|---|---|
| Cathodic Arc Technologies | -Compatibility with industry<br>-Good film adhesion<br>-Excellent stoichiometric control<br>-Low temperature<br>-Multilayer compact coating<br>-Uniform film<br>-Low voltage | -May be under excessively high compressive stress<br>-Delamination<br>-Macroparticles |
| HIPIMS | -Improved film density and adhesion<br>-Better film uniformity<br>-Increased control over film thickness and structure<br>-Greater efficiency and cost-effectiveness<br>-High voltage<br>-No droplets | -Back attraction to the target of ionized sputtered species<br>-Lower deposition rate with respect to DC at equivalent average power<br>-Start operation at very low pressure are difficult issues |

## 1.6. Literature Research

Many techniques and processes have been developed for cutting tools and these coating processes are still progressing[35]. Many types of both evaporation and magnetron sputtering techniques, which are a two member of PVD coating, are recently developing or coatings that are denser, tougher, denser, and harder[36]. There are various studies in literature to develop both cathodic coating and HIPIMS coating.

Marchin *et al.* investigated friction behavior of cutting tool which has Tisane and TiSiCN coating with optimized composition and cathodic arc deposition. They observed that Tessin coating has higher wear that TiSiCN while the coating compared to the uncoated tools coated tools performed 10 times better tool life[37].

Yi *et al.* compared the oxidation resistances of Ni and Cu-deposited AlTiN coatings for titanium material machining. They used cathodic arc technology in their work and the results they obtained are the best tool life belong to the AlTiN–Cu-coated tools due to the low cutting forces with cutting speed of 60 while AlTiN–Ni-coated outperformed with the cutting speed of 80. Briefly they obtained that oxidation resistance is related to cutting speed as well as coating[38].

He *et al.* studied tool performance of high-speed performances cutting with 5 different Al/Ti ratios coatings (cathodic arc deposition) on 304 stainless steels. They obtained that A high Al amount has shown to negatively affect tool performance. The best tool performance belongs to the Al/Ti ratios 60/40 coated tools and when the chip analysis has been done chip of this coating is smoother undersurface which means between tool and workpiece the friction is very low and this led to less sticky chip[39]. Kumar *et al.* work on the comparison of HIPIMS and DCMS (direct current magnetron sputtered) coating technology. They showed that the HIPIMS techniques has higher hardness, more dense structure and gives better adhesion than the DCMS techniques[40]. Sousa *et al.* have compared the wear Behavior and machining performance of TiAlSiN Coated material with different coating techniques which are DCMS and HIPIMS techniques. They reported that HIPIMS techniques gives better wear resistance and mechanical properties. Better mechanical properties give better performance for hard to machining alloys. Also, HIPIMS coated tool has higher compressive stress and that good for finishing operation[41]. W. Reolon *et al.* investigated the machining performance of two different coating techniques which are HIPIMS and cathodic arc Technologies during the machining of Inconel 718. When they compared these two coating methods and their properties, they obtained that HIPIMS has less porosity, high hardness, and adhesion higher than the cathodic arc evaporation. In addition, while the Inconel 718 machining the cutting load less than cathodic arc evaporation technique[42].

## 1.7. Objective and Scope of Thesis

Within the scope of this project, the effects of coating type and technologies on milling and drilling processes of various material groups were investigated. Therefore, it is anticipated that the performance of cutting tools used in the aerospace, defense and automotive industries will increase, thanks to the knowledge of the required design criteria specific to each material group. The main purpose of this thesis is to improve tool life by increasing the wear resistance of tools.

# CHAPTER 2

# EXPERIMENTAL

Carbide raw material is formed by the supplier by pouring powder in molds and sintering. Then, it is taken as carbide bar, brought to the desired diameter and h6 tolerance between the two centers and for processing. It is supplied without runout as it is ground between two centers. For comparison, the prototypes produced were machined from carbide bars of the same standard.

The same supplier of processing quality was selected when procuring workpiece materials. The workpiece materials were Ti6Al4V (3.7165), 4140 steel (1.7225), Ck45 steel (1.1191), D2 tool steel (1.2379) and GG25 cast iron, where material numbers are given in parentheses. All these materials were taken as logs with dimensions of 150x150x150mm. The dimensions in the materials have been determined to be suitable for the unit to be used in the performance test. It should also be noted that in practice it is likely that materials processed in aerospace will have thinner walls and the bonding conditions will not be as rigid as in the test conditions. Therefore, it is necessary to transfer the results obtained from performance tests to practical production with an engineering approach.

## 2.1. Materials for Machining

Workpiece materials were supplied from ‘As Çelik’ company. All these materials were taken as logs with dimensions of 150x150x150mm. Only D2 tool steel has different dimensions of 260x260x50mm. The dimensions in the materials have been determined to be suitable for the unit to be used in the performance test and according to the measurements in the purchased company. The chemical compositions and hardness value of the workpieces are given in the tables below.

Table 2.1. Chemical Composition of 4140 material (wt%)

| | C | Si | Mn | P | S | Cr | Mo | Ni | Al | Cu |
|---|---|---|---|---|---|---|---|---|---|---|
| Max-Min | 0.43-0.38 | 0.35-0.15 | 1-0.75 | <0.03 | <0.04 | 1.1-0.8 | 0.15-0.25 | <0.25 | <0.35 | |
| Actual Value | 0.41 | 0.24 | 0.83 | 0.006 | 0.006 | 0.9 | 0.18 | 0.09 | 0.014 | 0.18 |

Table 2.2. Chemical Composition of CK45 material (wt%)

| | C | Si | Mn | P | S | Cr | Mo | Al |
|---|---|---|---|---|---|---|---|---|
| Max-Min | 0.42-0.5 | <0.4 | 0.5-0.8 | <0.03 | <0.035 | <0.4 | <0.1 | |
| Actual Value | 0.485 | 0.191 | 0.753 | 0.015 | 0.005 | | | 0.031 |

Table 2.3. Chemical Composition of GG25 material (wt%)

| | C | Si | Mn | P | S |
|---|---|---|---|---|---|
| Max-Min | 2.90-3.65 | 1.80-2.90 | 0.5-0.7 | <0.1 | <0.3 |
| Actual Value | 3.43 | 1.82 | 0.567 | 0.06 | 0.012 |

Table 2.4. Chemical Composition of 2379 material (wt%)

| | C | Si | Mn | P | S | Cr | Mo | V |
|---|---|---|---|---|---|---|---|---|
| Max-Min | 1.40-1.60 | 0.10-0.6 | 0.1-0.6 | 0.03 | <0.03 | <0.03 | 0.70-1.20 | 0.5-1.0 |
| Actual Value | 1.43 | 0.13 | 0.23 | 0.006 | 0.013 | 12.Haz | 0.89 | 0.92 |

Table 2.5. Chemical Composition of Ti6Al4V material (wt%)

| | Ti | Al | V | Fe | C | N | H | O |
|---|---|---|---|---|---|---|---|---|
| Max-Min | <90 | 6.75-5.5 | 4.5-3.5 | <0.4 | <0.08 | <0.05 | <0.015 | <0.2 |
| Actual Value | 89.50 | 6.May | 4 | 0.14 | 0.025 | 0.007 | 0.016 | 0.172 |

Table 2.6. Hardness values of workpieces material

| **Workpieces Material** | **Hardness Values (BHN)** |
|---|---|
| 4140 | 280-300 |
| CK45 | 190-201 |
| GG25 | 125-200 |
| Ti6Al4V | 330-340 |
| D2 Tool Steel | 630-700 |

## 2.2. Machining Performance Test

In this thesis 3 axis CNC machine used for performance tests Mikron VCP800 seen in Figure 2.1 is the workbench.

Figure 2.1. Mikron VCP800 3 axis CNC machine

The billet is clamped to the CNC machine with the Lang clamp as shown in Figure 2.2 Before being clamped in the vise, the surface of the billet is leveled with the scanning head and the surfaces to be clamped in the vise. It is flattened with an end mill in order not to be squeezed as a curve.

Figure 2.2. Image of Lang Clamp

When the machine is first connected to the machine, the tool length, diameter, and runout are automatically measured with the help of the blum laser shown in figure 2.3 Blum laser detects the tool geometry with its unique method and processes values such as length, diameter, runout and offset that it automatically measures on the machine tool sheet accordingly. It is an especially important method to minimize errors.

Figure 2.3. Image of the blum laser

The cooling unit used in the CNC machine, where the tests are performed, is shown in figure 2.4 There is a coolant pressure of 10-70 bar for internal cooling and up to 30 bar for external cooling. Castrol Hysol SL 45 XBB brand boron oil was used as coolant.

Figure 2.4. Image of Cooling unit of CNC Machine

Simulation of the tests are prepared in the Hypermill program, shown in Figure 2.5 and 2.6 Hypermill; In determining the tool paths, starting from the chip thickness, aiming at the shortest time and the most efficient machining, and using high performance cutting tools; It is a CAM program used for 3, 4, 5 axis CNC milling and drilling.

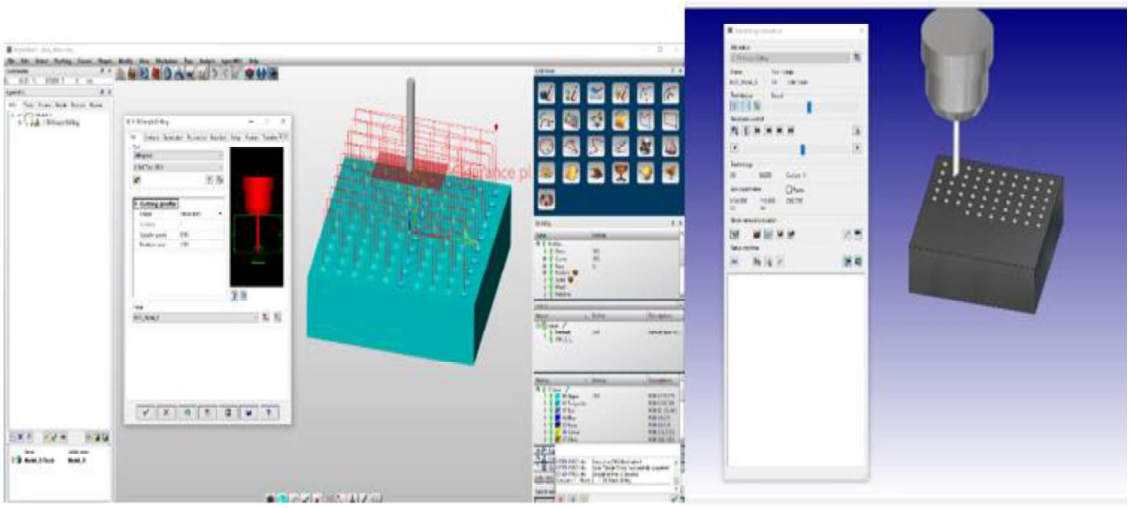

Figure 2.5. Milling Example of Hypermill Simulation

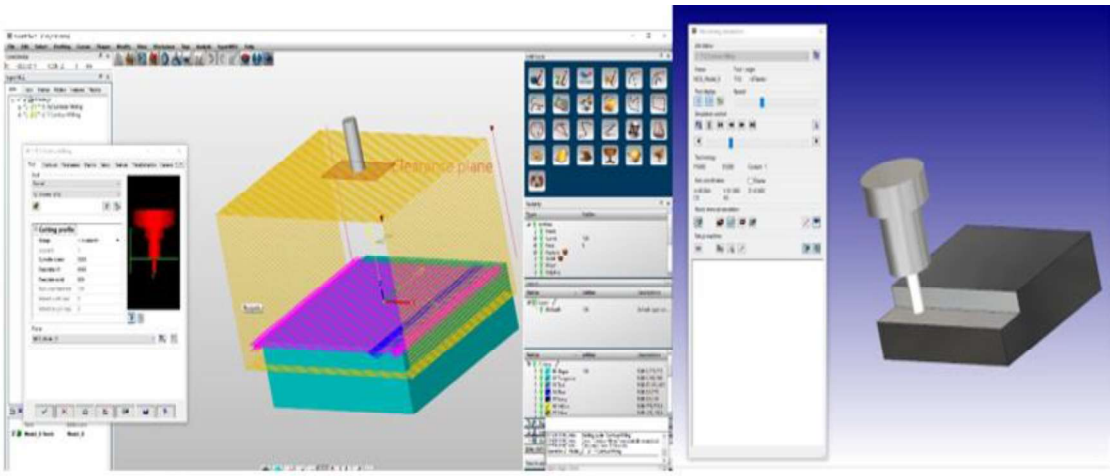

Figure 2.6. Milling Example of Hypermill Simulation

The tests will be completed on 4 different workpieces for different tools and for each designed tool, 2 different coating methods were tried. In this thesis, cathodic arc technology and high-power impulse magnetron sputtering techniques will be used. While cathodic arc is a widely used method in technology cutting tool coating, HIPIMS is a new technique. In addition, 4 different operation types that are shoulder milling, slotting, drilling and high-performance milling are used to observe the different loads on the tool and also these operation types are the most common operation types used .

A total of 16 performance tests were carried out. The following table gives the test plan of this thesis.

Table 2.7. Performance test plan

| NAME OF TEST | TOOL | COATING TECHNOLOGY | OPERATION TYPE | WORKPIECE MATERIAL |
|---|---|---|---|---|
| **4140-SM-PVD** | Tool 1 | CATHODIC-ARC | Shoulder Milling | 1.7225 (4140) |
| **CK45-SM-PVD** | | | Shoulder Milling | CK45 |
| **GG25-SM-PVD** | | | Shoulder Milling | 0.6025-GG25 |
| **4140-SM-HIPIMS** | Tool 2 | HIPIMS | Shoulder Milling | 1.7225 (4140) |
| **CK45-SM-HIPIMS** | | | Shoulder Milling | CK45 |
| **GG25-SM-HIPIMS** | | | Shoulder Milling | 0.6025-GG25 |
| **4140-SLT-PVD** | Tool 3 | CATHODIC-ARC | Slot | 1.7225 (4140) |
| **4140-SLT-HIPIMS** | Tool 4 | HIPIMS | Slot | 1.7225 (4140) |
| **4140-DRL-PVD** | Tool 5 | CATHODIC-ARC | Drilling | 1.7225 (4140) |
| **4140-HPM-HIPIMS** | Tool 6 | HIPIMS | Drilling | 1.7225 (4140) |
| **Geo1_HFM-Ti6Al4V-PVD** | Tool 7 | CATHODIC-ARC | High Feed Milling | Ti6Al4V |
| **Geo1_HFM-Ti6Al4V-HIPIMS** | Tool 8 | HIPIMS | High Feed Milling | Ti6Al4V |
| **Geo2_HFM-TiAl4V-PVD** | Tool 9 | CATHODIC-ARC | High Feed Milling | Ti6Al4V |
| **Geo2_HFM-Ti6Al4V-HIPIMS** | Tool 10 | HIPIMS | High Feed Milling | Ti6Al4V |
| **D2-PM-PVD** | Tool 11 | CATHODIC-ARC | High Feed Milling | 1.2379 (X155CrVMo12-1) 60HRC |
| **D2-PM-HIPIMS** | Tool 12 | HIPIMS | High Feed Milling | 1.2379 (X155CrVMo12-1) 60HRC |

With in the scope of this thesis, 4140-SM-PVD, CK45-SM-PVD, GG25-SM-PVD, 4140-SM-HIPIMS, CK45-SM-HIPIMS and GG25-SM-HIPIMS coating comparison on different workpiece, 4140-SM-PVD, 4140-SM-HIPIMS, 4140-SLT-PVD, 4140-SLT-HIPIMS, 4140-DRL-PVD, 4140-DRL-HIPIMS coating comparison in different operations, D2-PM-PVD and D2-PM-HIPIMS coating behavior on hard materials, GEO1_HFM-Ti6Al4V-PVD, GEO1_HFM-Ti6Al4V-HIPIMS, GEO2_HFM-Ti6Al4V-PVD and GEO2_HFM-Ti6Al4V-HIPIMS coating behavior at high cutting speed on tı6al4v material comparisons have been made.

A special spike mobile holder, shown on figure 2.7 was used during these tests. This holder shows the loads during the machining like bending moment, normal load, and normal loads.

Figure 2.7. Image of Spike Mobile Holder

## 2.3. Coated Tool Surface Analysis

The surfaces of coated tools were examined under Zeiss EVO MA-15 scanning electron microscope (SEM). Before the SEM examination the surface of all tools were cleaned with acetone. The SEM examinations were performed with 20 kV accelerating voltage at 2500x and 5000x magnifications using secondary electron (SEI) and back-scatter electron detectors. Moreover, the compositions of coatings were determined using EDAX Apollo energy dispersive X-ray spectroscopy (EDS) system.

# CHAPTER 3

# RESULTS

All tests performed were compared in 4 main groups. In the first group, 2 different coatings on 3 different materials were compared with a shoulder milling operation. In the second group, 2 different coatings using a single material were compared with 2 different machining operations such as slot milling and drilling. In the third comparison, two different tools and coatings in a single material will be compared in a high feed milling operation. Finally, as a fourth comparison, coating performances on hardened steel with one tool of two coatings and one face milling operation were examined. In table 3.1-3.2-3.3-3.4 shows which test will be compared in which group.

Table 3.1. Distribution of tests to group 1

| **NUMBER OF GROUP** | **GROUP 1** | | | | | |
|---|---|---|---|---|---|---|
| **NUMBER OF TEST** | 4140-SM-PVD | CK45-SM-PVD | GG25-SM-PVD | 4140-SM-HIPIMS | CK45-SM-HIPIMS | GG25-SM-HIPIMS |

Table 3.2. Distribution of tests to group 2

| **NUMBER OF GROUP** | **GROUP 2** | | | | | |
|---|---|---|---|---|---|---|
| **NUMBER OF TEST** | 4140-SM-PVD | 4140-SM-HIPIMS | 4140-SLT-PVD | 4140-SLT-HIPIMS | 4140-DRL-PVD | 4140-SM-PVD |

Table 3.3. Distribution of tests to group 3

| **NUMBER OF GROUP** | **GROUP 3** | | | |
|---|---|---|---|---|
| **NUMBER OF TEST** | GEO1_HFM-Ti6Al4V-PVD | GEO1_HFM-Ti6Al4V-HIPIMS | GEO2_HFM-Ti6Al4V-PVD | GEO2_HFM-Ti6Al4V-HIPIMS |

Table 3.4. Distribution of tests to group 4

| NUMBER OF GROUP | GROUP 4 | |
|---|---|---|
| NUMBER OF TEST | D2-PM-PVD | D2-PM-HIPIMS |

## 3.1. Coating Quality

Coating quality was measured as surface quality and corner preparation values. These measurements were made with the Alicona Infinite Focus G5 measuring instrument shown in figure 3.1.

Figure 3.1. Alicona Infinite Focus G5

### 3.1.1. Surface Roughness Measurement

Surface roughness can be defined as the non-uniform quality of a surface. The Surface roughness measured by Sa and Ra values. The Ra value is the roughness calculation on a line. Sa value is the roughness calculation made within an area. These Ra and Sa values calculated formulas given in figure 3.2.

$$Ra = \frac{1}{l_r}\int_{l_r} |z(x)|dx \qquad Sa = \frac{1}{A}\iint_{A} |z(x,y)|dxdy$$

Figure 3.2. Ra and Sa calculation formulas

In Table 3.5, the surface roughness values of the tools are given. When looking at the values, both Ra and Sa measurements of the tools coated with the HIPIMS technique are better than the ARC technology. The test responses of the tools are given in table 3.1 in chapter 2.

Table 3.5. Surface roughness values of tools

| | **Tool 1 (SM-PVD)** | **Tool 2 (SM-HIPIMS)** | **Tool 3 (SLT-PVD)** | **Tool 4 (SLT-HIPIMS)** | **Tool 5 (DRL-PVD)** | **Tool 6 (DRL-HIPIMS)** |
|---|---|---|---|---|---|---|
| **Ra (µm)** | 0.869 | 0.298 | 0.728 | 0.491 | 0.427 | 0.381 |
| **Sa (µm)** | 0.419 | 0.354 | 0.536 | 0.527 | 0.522 | 0.401 |
| | Tool 7 (GEO1-PVD) | Tool 8 (GEO1-HIPIMS) | Tool 9 (GEO2-PVD | Tool 10 (GEO2-HIPIMS) | Tool 11 (D2-PVD) | Tool 12 (D2-HIPIMS) |
| **Ra (µm)** | 0.133 | 0.127 | 0.198 | 0.139 | 0.536 | 0.456 |
| **Sa (µm)** | 0.234 | 0.225 | 0.173 | 0.171 | 0.553 | 0.439 |

## 3.1.2. Edge Preparation Values

As mentioned in section 1.4.4, edge preparation is a process that generally increases tool life, but excessive edge preparation affects negatively, so the optimum amount should be determined. The coating affects these edge preparation values and can make a slight change on the performance of the tool.

The effect of edge preparation values on tool performance is dependent on the workpiece and operation. For example, for hard material like stainless steel, the tool must have edge preparation around 10 microns. On the other hand, materials relatively softer than others like aluminum alloys do not need too much edge preparation and their edge preparation values are around 2 microns.

When optimum values are determined according to the operation and material, when the edge preparation of the tool is lower than this value, it may be subject to sudden breaks, while being high causes reductions in tool life. In table 3.6, edge preparation values are given before and after coating. Tools coated with HIPIMS technology give more edge preparations value than ARC technology.

Table 3.6. Edge preparation values of the tools before and after coating

| | **Tool 1 (SM-PVD)** | **Tool 2 (SM-HIPIMS)** | **Tool 3 (SLT-PVD)** | **Tool 4 (SLT-HIPIMS)** | **Tool 5 (DRL-PVD)** | **Tool 6 (DRL-HIPIMS)** |
|---|---|---|---|---|---|---|
| **Before Coating (µm)** | 4.495 | | 6.964 | | 11.496 | |
| **After Coating (µm)** | 4.629 | 6.275 | 9.420 | 13.014 | 13.572 | 20.392 |
| | Tool 7 (GEO1-PVD) | Tool 8 (GEO1-HIPIMS) | Tool 9 (GEO2-PVD | Tool 10 (GEO2-HIPIMS) | Tool 11 (D2-PVD) | Tool 12 (D2-HIPIMS) |
| **Before Coating (µm)** | 4.106 | | 5.446 | | 5.918 | |
| **After Coating (µm)** | 5.612 | 8.826 | 8.423 | 5.526 | 7.771 | 7.786 |

### 3.1.3. SEM and EDS Analysis

In figure 3.3, SEM images of tools covered with HIPIMS, and cathodic arc technology used in group 1 tests are given. When the images are examined, the droplet amounts are quite low in HIPIMS coated tools. Looking at Figure 3.4, SEM images of the tools used in the slot test which belong s to the group 2 test are given. As shown in figure 3.4, the HIPIMS coating has fewer droplets.

| | **Magnification:** 2500x<br>**Signal:** Secondary electron | **Magnification:** 5000x<br>**Signal:** Back-scatter electron |
|---|---|---|
| **SM-PVD** | 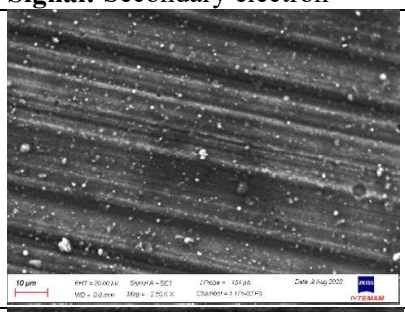 | 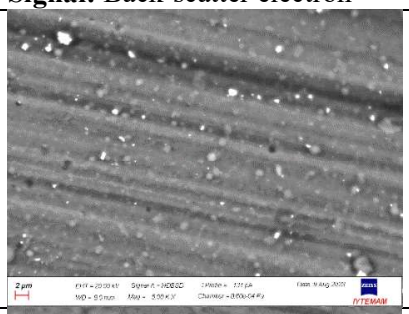 |
| **SM-HIPIMS** | 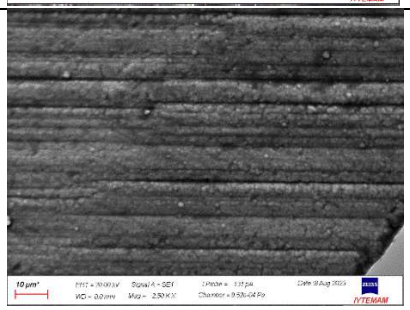 | 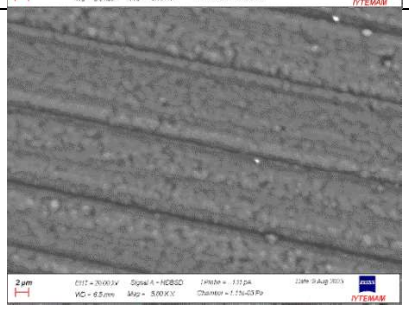 |

Figure 3.3. SEM micrographs of coated surfaces of SM-PVD and SM-HIPIMS samples taken at 2500x and 5000x magnifications with SEI and BSD detectors.

| | **Magnification:** 2500x<br>**Signal:** Secondary electron | **Magnification:** 5000x<br>**Signal:** Back-scatter electron |
|---|---|---|
| **SLT-PVD** | 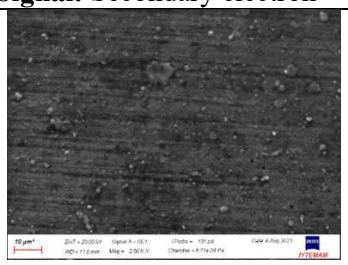 | 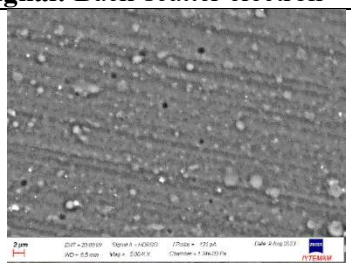 |
| **SLT-HIPIMS** | 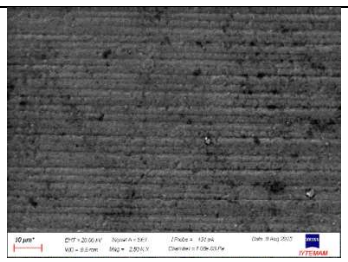 | 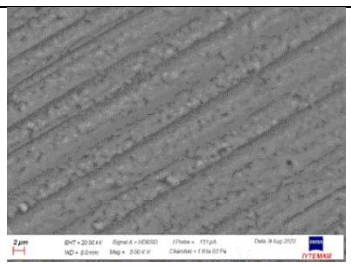 |

Figure 3.4. SEM micrographs of coated surfaces of SLT-PVD and SLT-HIPIMS samples taken at 2500x and 5000x magnifications with SEI and BSD detectors

The group 2 test are given in figures 3.5, the HIPIMS coating has fewer droplets. In figure 3.6, SEM images of geometry 1, coating comparison of group 3 are given. It is clear that in figures 3.6, the HIPIMS coating has fewer droplets.

| | **Magnification:** 2500x<br>**Signal:** Secondary electron | **Magnification:** 5000x<br>**Signal:** Back-scatter electron |
|---|---|---|
| **DRL-PVD** | 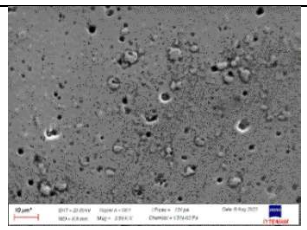 | 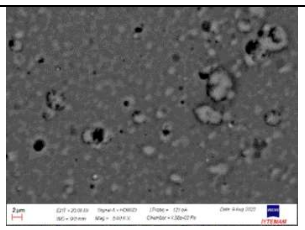 |
| **DRL-HIPIMS** | 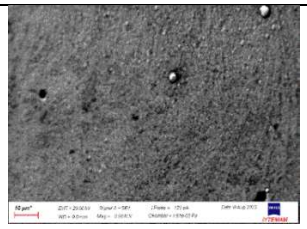 | 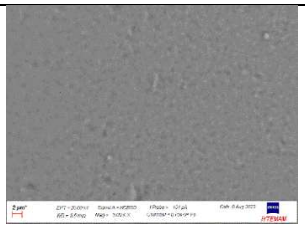 |

Figure 3.5. SEM micrographs of coated surfaces of DRL-PVD and DRL-HIPIMS samples taken at 2500x and 5000x magnifications with SEI and BSD detectors

| | **Magnification:** 2500x<br>**Signal:** Secondary electron | **Magnification:** 5000x<br>**Signal:** Back-scatter electron |
|---|---|---|
| **GEO1-Ti6Al4V-PVD** | 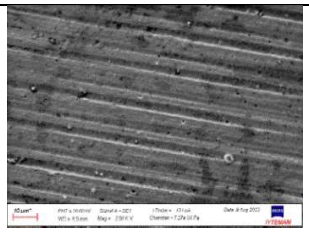 | 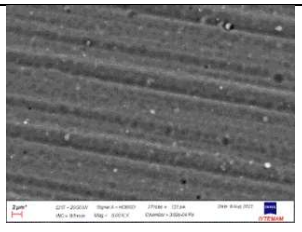 |
| **GEO1-Ti6Al4V-HIPIMS** | 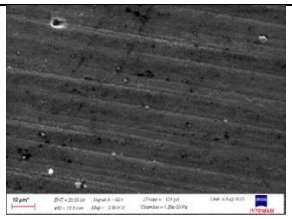 | 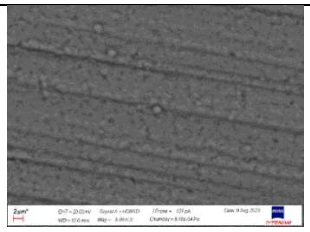 |

Figure 3.6. SEM micrographs of coated surfaces of GEO1-Ti6Al4V-PVD and GEO1-Ti6Al4V-HIPIMS samples taken at 2500x and 5000x magnifications with SEI and BSD detectors

In figure 3.7, there is no specific difference in droplet between two coating technologies. It is clear that in figures 3.8, the HIPIMS coating has fewer droplets than cathodic arc deposition.

| | **Magnification: 2500x**<br>**Signal: Secondary electron** | **Magnification: 5000x**<br>**Signal: Back-scatter electron** |
|---|---|---|
| **GEO2-Ti6Al4V-PVD** | 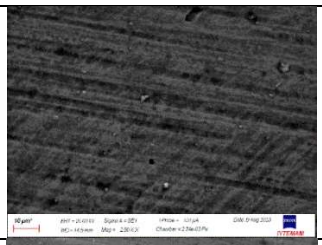 | 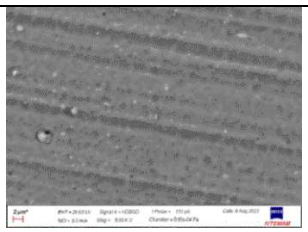 |
| **GEO2-Ti6Al4V-HIPIMS** | 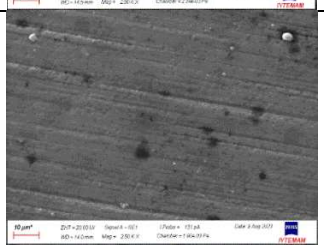 | 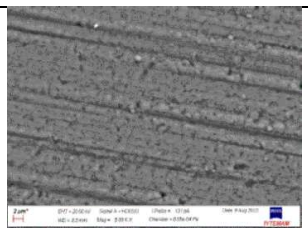 |

Figure 3.7. SEM micrographs of coated surfaces of GEO2-Ti6Al4V-PVD and GEO2-Ti6Al4V-HIPIMS samples taken at 2500x and 5000x magnifications with SEI and BSD detectors

.

| | **Magnification:** 2500x<br>**Signal:** Secondary electron | **Magnification:** 5000x<br>**Signal:** Back-scatter electron |
|---|---|---|
| **D2-PM-PVD** | 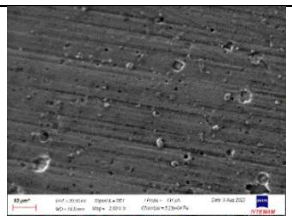 | 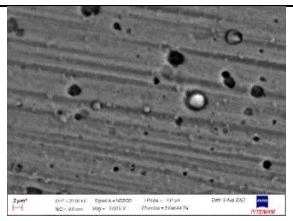 |
| **D2-PM-HIPIMS** | 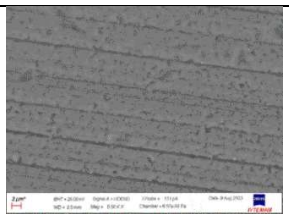 | 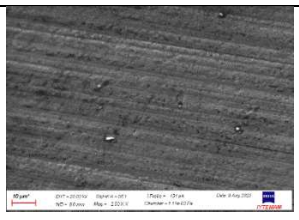 |

Figure 3.8. SEM micrographs of coated surfaces of D2-PM-PVD and D2-PM-HIPIMS samples taken at 2500x and 5000x magnifications with SEI and BSD detectors

The following graphs are the EDS analysis of the tools used in the tests. EDS results indicate the chemical composition of the coatings. When comparing results of group 1 tests, cathodic arc deposition and HIPIMS techniques both use AlCrN based coating as shown in figures 3.9 and 3.10, and in figures 3.11 and 3.12, The tool used in the slot operation was used with the same coating with the two techniques and AlCrN based coating was used. On the other hand, looking at figure 3.13 and 3.14, the tool used in the drilling operation was used with the AlTiN based coating with cathodic arc deposition techniques while HIPIMS was used with AlCrN based coating.

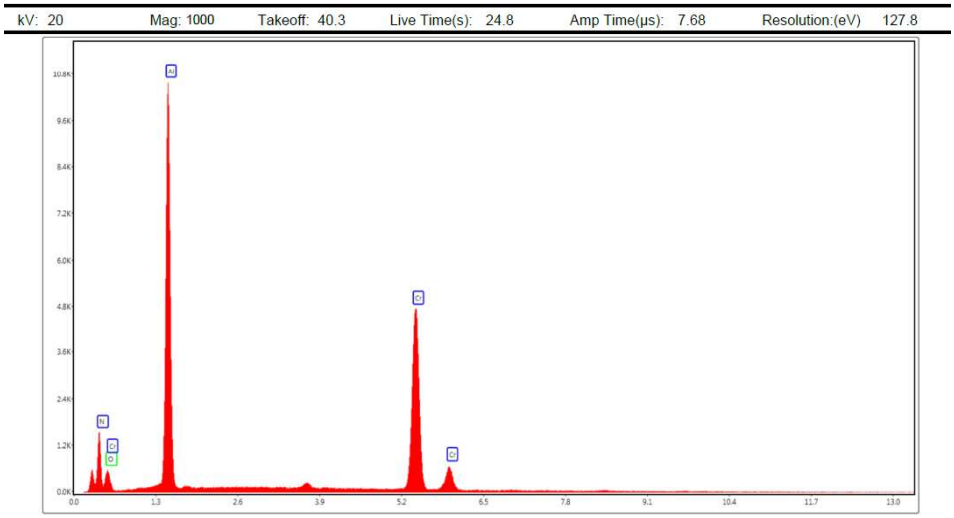


Figure 3.9. EDS spectrum of Group 1 PVD coated tools (SM-PVD)

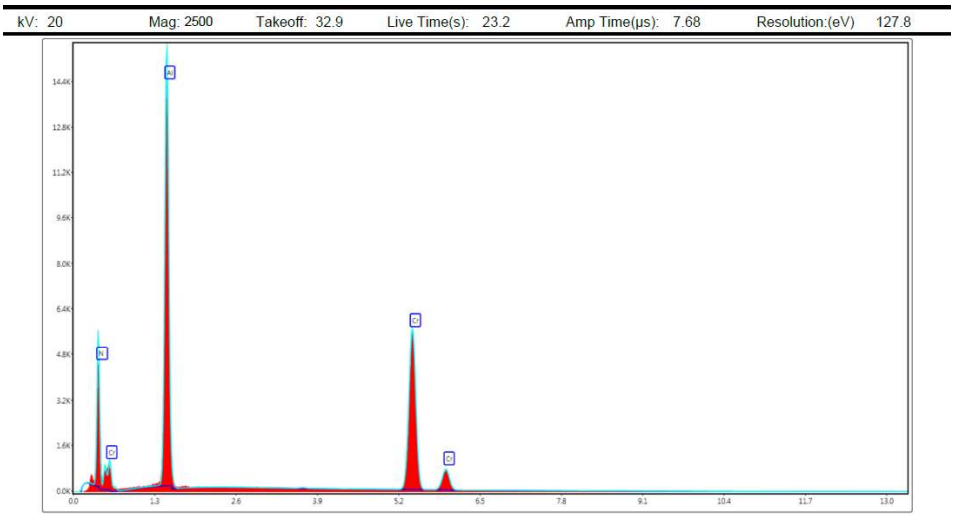


Figure 3.10. EDS spectrum of Group 1 HIPIMS coated tools (SM-HIPIMS)

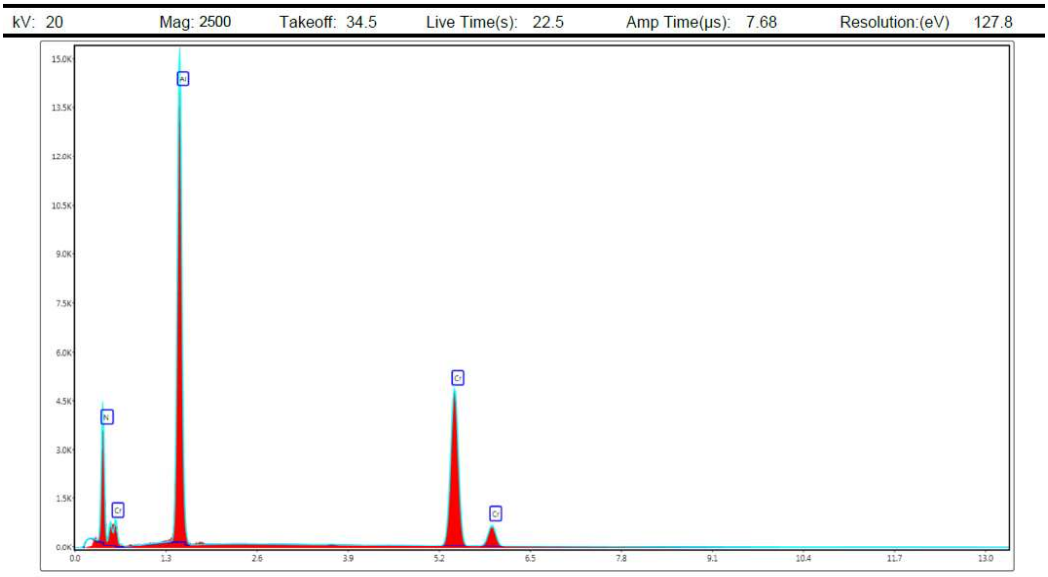


Figure 3.11. EDS spectrum of SLT-PVD tools

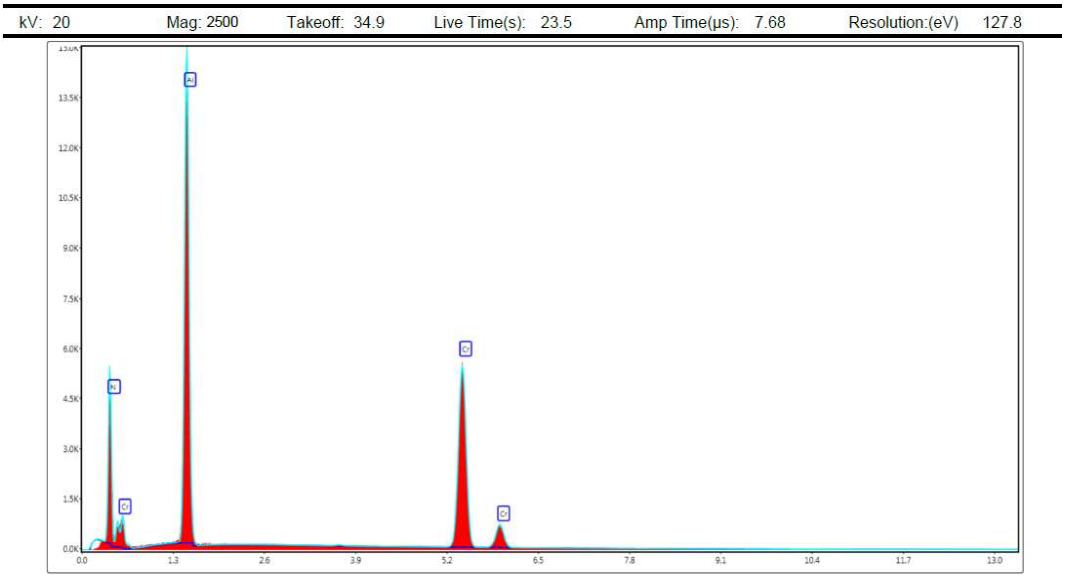


Figure 3.12. EDS spectrum of SLT-HIPIMS tools

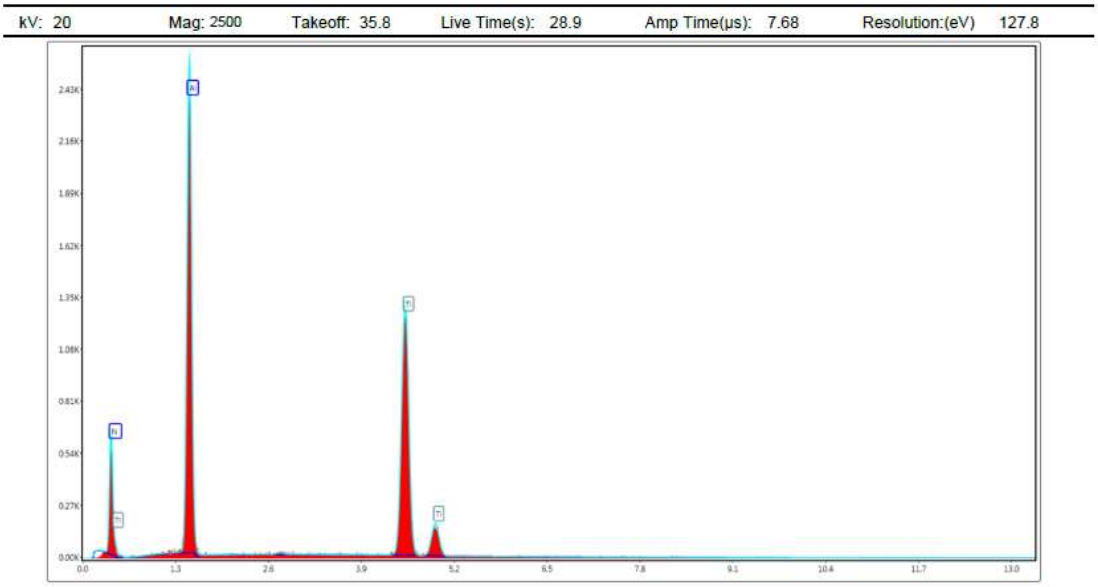


Figure 3.13. EDS spectrum of DRL-PVD tools

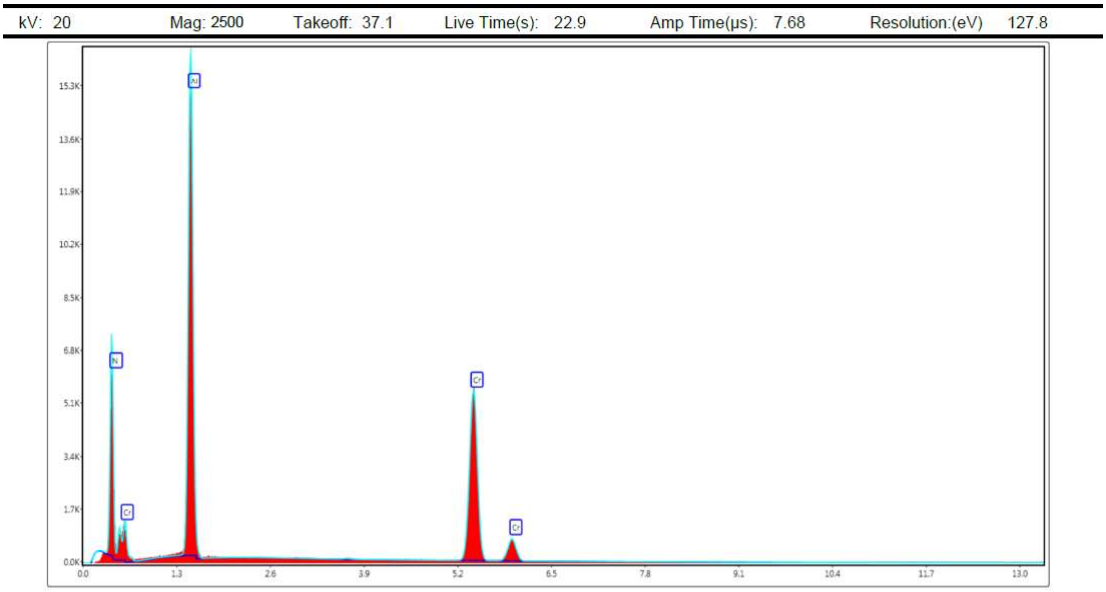


Figure 3.14. EDS spectrum of DRL-HIPIMS tools

Looking at the figures 3.15, 3.16, 3.17 and 3.18, EDS results of group 3 tests are given. For geometry 1, AlCrN based coating is used for cathodic arc deposition techniques and AlTiSiN based coating is used in HIPIMS techniques. Also, for geometry 2, AlCrN based coating used for cathodic arc deposition techniques and AlTiSiN based coating used in HIPIMS techniques.

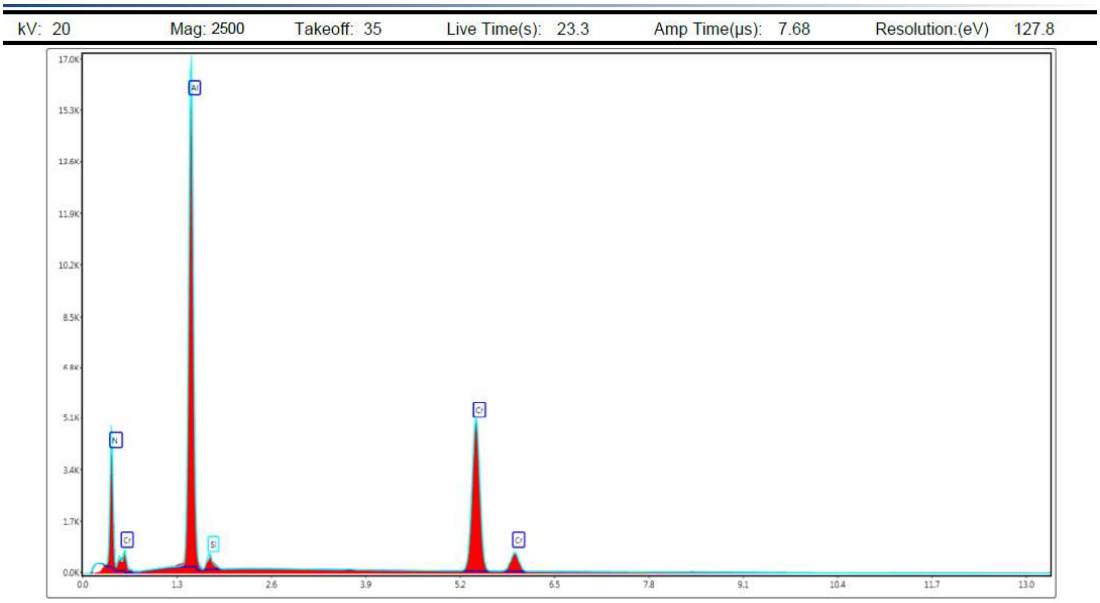


Figure 3.15. EDS spectrum of GEO1-Ti6Al4V-PVD tools

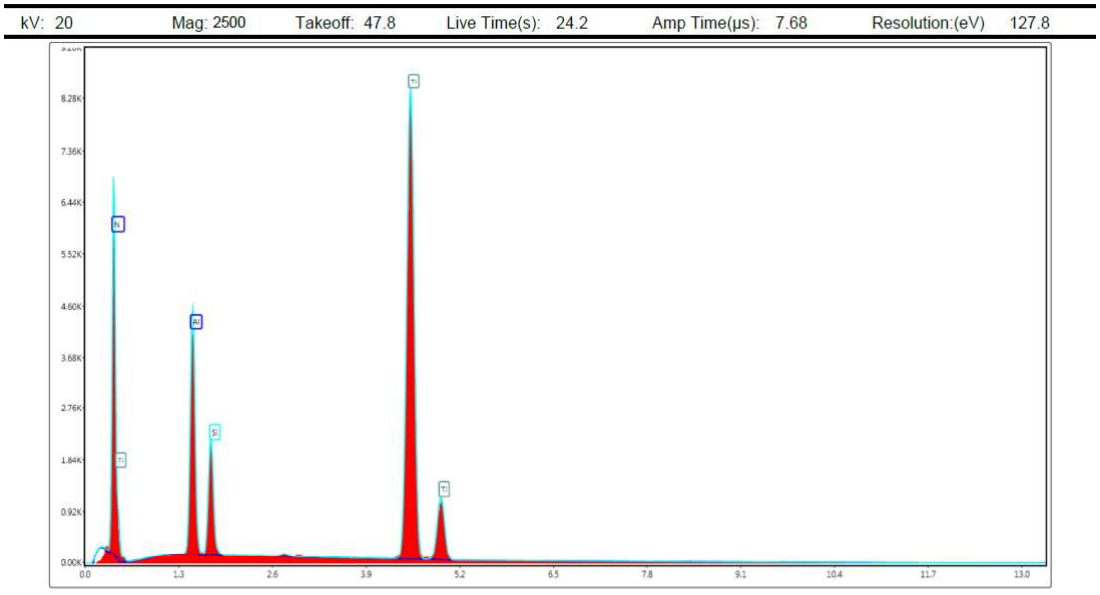


Figure 3.16. EDS spectrum of GEO1-Ti6Al4V-HIPIMS tools

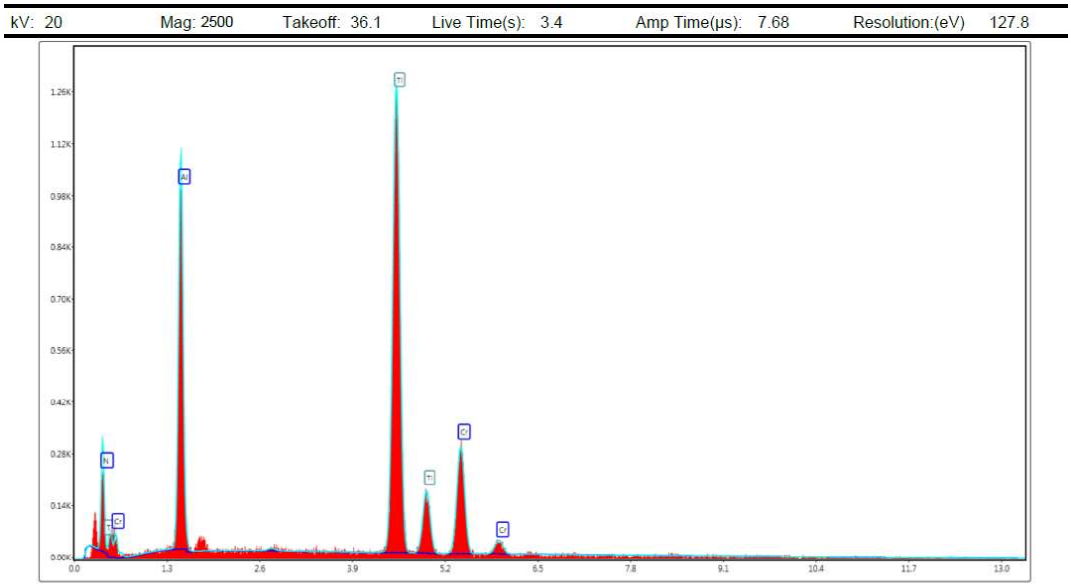


Figure 3.17. EDS spectrum of GEO2-Ti6Al4V-PVD tools

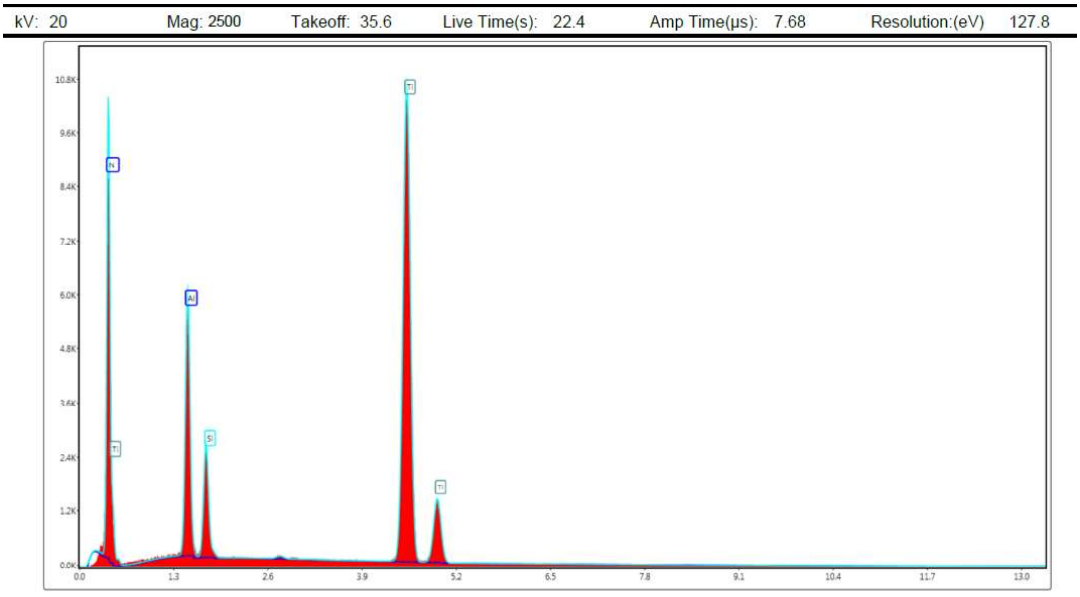


Figure 3.18. EDS spectrum of GEO2-Ti6Al4V-HIPIMS tools

Looking at figures 49 and 50 EDS, results of group 4 tests are given. For different coating techniques, same coatings are used, AlTiSiN based coating used for cathodic arc deposition techniques and HIPIMS techniques.

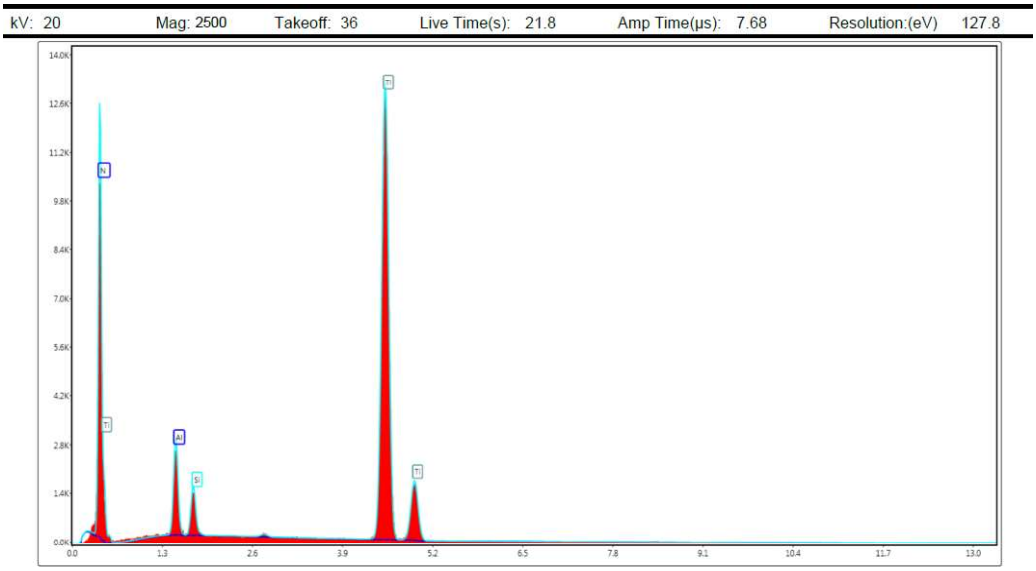


Figure 3.19. EDS spectrum of D2-PM-PVD tools

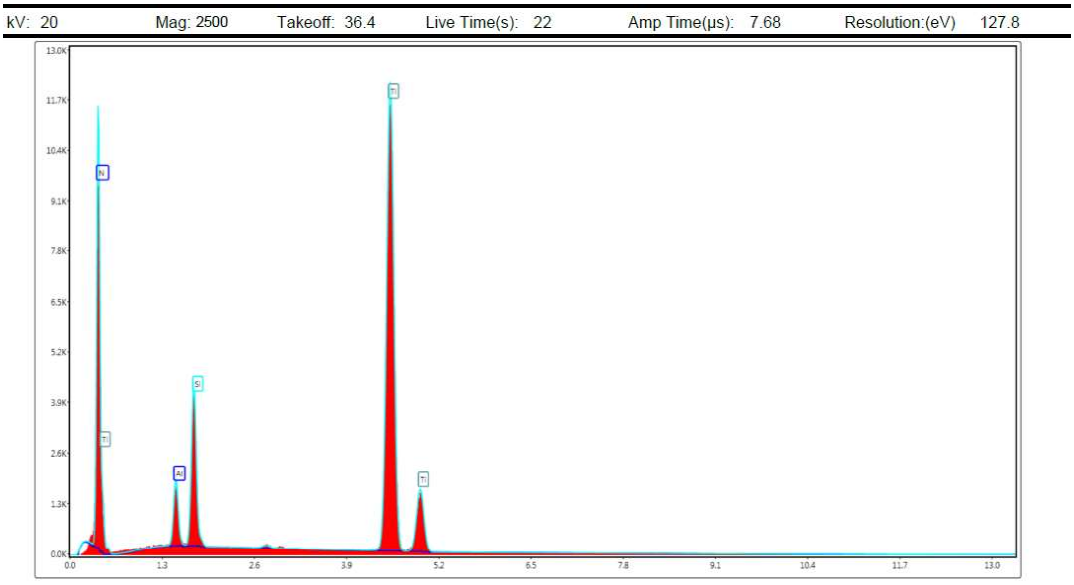


Figure 3.20. EDS spectrum of D2-PM-HIPIMS tools

The chemical compositions of the coatings used in this thesis are given in Table 3.7. Acocording to this table, in general AlCrN, AlTiSiN and AlCrN based coating materials are used in this thesis.

Table 3.7. Chemical composition of coatings (W:Weight, A: Atomic)

| | N | | O | | Al | | Cr | | Si | | Ti | |
|---|---|---|---|---|---|---|---|---|---|---|---|---|
| | W % | A % | W % | A % | W % | A % | W % | A % | W % | A % | W % | A % |
| **Group1 SM-PVD** | 12.4 | 27.18 | 1.74 | 3.35 | 34.25 | 38.99 | 51.61 | 30.48 | X | X | X | X |
| **Group1 SM-HIPIMS** | 27.93 | 50.48 | X | X | 31.97 | 30 | 40.99 | 19.52 | X | X | X | X |
| **4140 SLT-PVD** | 25.36 | 46.81 | X | X | 34.88 | 33.42 | 39.76 | 19.77 | X | X | X | X |
| **4140 SLT-HIPIMS** | 27.21 | 49.69 | X | X | 31.83 | 30.17 | 40.96 | 20.15 | X | X | X | X |
| **4140 DRL-PVD** | 17.85 | 35.84 | X | X | 34.97 | 36.45 | 47.18 | 27.7 | X | X | X | X |
| **4140 DRL-HIPIMS** | 30.91 | 54.02 | X | X | 30.84 | 27.98 | 38.25 | 18 | X | X | X | X |
| **GEO1 Ti6Al4V-PVD** | 25.56 | 46.72 | X | X | 34.97 | 33.19 | 37.92 | 18.67 | 1.55 | 1.41 | X | X |
| **GEO1 Ti6Al4V-HIPIMS** | 22.25 | 45.58 | X | X | 11.75 | 12.5 | X | X | 5.62 | 574 | 60.38 | 36.18 |
| **GEO2 Ti6Al4V-PVD** | 9.76 | 24.27 | X | X | 19.8 | 25.58 | 19.38 | 12.99 | X | X | 51.07 | 37.16 |
| **GEO2 Ti6Al4V-HIPIMS** | 28.41 | 53.36 | X | X | 12.32 | 12.01 | X | X | 5.35 | 5.01 | 53.92 | 29.62 |
| **D2-PM-PVD** | 26.8 | 53.46 | X | X | 5.92 | 6.13 | X | X | 2.79 | 2.78 | 64.49 | 37.63 |
| **D2-PM-HIPIMS** | 27.83 | 54.14 | X | X | 3.6 | 3.64 | X | X | 8.03 | 7.79 | 60.54 | 34.44 |

## 3.2. Machining Performance

While the tools were tested on the material, the Spike spindle type dynamometer seen in was used. Spike is a dynamometer that can measure the amount of loading in each cutting edge in the tool, figure 3.21 shows the forces on the tool.

These are bending and torsional moments of the tool while working, Tool test data was collected by Spike spindle type dynamometer. These data are measured with the help of the dynamometer inside the spike holder and transferred to the computer via wireless.

Figure 3.21. Schematic representation of promicron spike dynamometer holder

### 3.2.1. Test Parameters

In order to use the tool in the most efficient way during machining, parameters must be selected most suitable for the workpiece and tool geometry. In this thesis, the most suitable parameters were determined with the experience of the Karcan cutting tool in machining over time. Parameters used in this thesis are given in the table. The cutting parameters are spindle speed (S), feed rate (F), radial depth of cut (Ae) and axial depth of cut (Ap).

Table 3.8. Test parameter of group 1

| | **4140-SM-PVD** | **CK45-SM-PVD** | **GG25-SM-PVD** | **4140-SM-HIPIMS** | **CK45-SM-HIPIMS** | **GG25-SM-HIPIMS** |
|---|---|---|---|---|---|---|
| **Workpiece Material** | 4140 | CK45 | GG25 | 4140 | CK45 | GG25 |
| **Operation** | Shoulder Milling | Shoulder Milling | Shoulder Milling | Shoulder Milling | Shoulder Milling | Shoulder Milling |
| **S (rpm)** | 3200 | 4000 | 4000 | 3200 | 4000 | 4000 |
| **F (mm/dev)** | 700 | 750 | 1250 | 700 | 750 | 1250 |
| **Ae (mm) / Ap (mm)** | 2.4 / 18 | 2.4 / 18 | 2.4 / 18 | 2.4 / 18 | 2.4 / 18 | 2.4 / 18 |
| **Coolant** | Air | Air | Air | Air | Air | Air |

Table 3.9. Test parameter of group 2

| | 4140-SLT-PVD | 4140-SLT-HIPIMS | 4140-DRL-PVD | 4140-DRL-HIPIMS |
|---|---|---|---|---|
| **Workpiece Material** | 4140 | 4140 | 4140 | 4140 |
| **Operation** | Slot Milling | Slot Milling | Drilling | Drilling |
| **S (rpm)** | 3979 | 3979 | 6250 | 6250 |
| **F (mm/dev)** | 796 | 796 | 1250 | 1250 |
| **Ae (mm) / Ap (mm)** | 12 / 18 | 12 / 18 | 6.7 / 20 | 6.7 / 20 |
| **Coolant** | Air | Air | Internal Cooling (~ 66 bar) | Internal Cooling (~ 66 bar) |

Table 3.10. Test parameter of group 3

| | **GEO1_HFM-Ti6Al4V-PVD** | **GEO1_HFM-Ti6Al4V-HIPIMS** | **GEO2_HFM-Ti6Al4V-PVD** | **GEO2_HFM-Ti6Al4V-HIPIMS** |
|---|---|---|---|---|
| **Workpiece Material** | Tİ6Al4V | Tİ6Al4V | Tİ6Al4V | Tİ6Al4V |
| **Operation** | High Feed Milling | High Feed Milling | High Feed Milling | High Feed Milling |
| **S (rpm)** | 2653 | 2653 | 3000 | 3000 |
| **F (mm/dev)** | 2500 | 2500 | 2500 | 2500 |
| **Ae (mm) / Ap (mm)** | 1.2 / 18 | 1.2 / 18 | 1.5 / 15 | 1.5 / 15 |
| **Coolant** | Internal Cooling (~ 20 bar) | Internal Cooling (~ 20 bar) | Internal Cooling (~ 20 bar) | Internal Cooling (~ 20 bar) |

Table 3.11. Test parameter of group 4

| | **D2-PM-PVD** | **D2-PM-HIPIMS** |
|---|---|---|
| **Workpiece Material** | 2379 | 2379 |
| **Operation** | Face Milling | Face Milling |
| **S (rpm)** | 5800 | 5800 |
| **F (mm/dev)** | 700 | 700 |
| **Ae (mm) / Ap (mm)** | 0.3 / 0.3 | 0.3 /0.3 |
| **Coolant** | Air | Air |

### 3.2.2. Spike Results

In the spike graphs x-axis gives the number of produced units. In the milling process, 1 unit refers to a 150 mm cut for group 1-2-3 test and 260 mm cut for group 4 test. For the drilling tests, the number of produced units indicates 1 hole for 4140-DRL-PVD and 4140-DRL-HIPIMS tests. In spike graphs, looking at the bending moment while milling and the normal load while drilling gives better results on tool performance.

For the group 1 results; in figure 3.22. Bending moment graph of group 1 test are given. In tools coated with cathodic arc technique, the 4140 tool performed better.

The tool coated with HIPIMS technology showed better performance in processing. CK45 material. When compared these two tests, in terms of bending moment, the HIPIMS coated tool gave the best results in CK 45 material. In figure 3.23 Tension graph of group 1 test are given. In both techniques, HIPIMS and ARC technologies, the test performed on 4140 and CK45 respectively, in terms of material's normal loads gives the best results. When we look at the total result of normal loads, CK45 material also gave the best result in terms of tool life and torsion strength coated with HIPIMS technology. In figure 3.24, the torsion force results of the tools coated with ARC and HIPIMS technology are obtained when processing 4140, CK45 and CK45 material, and the tool coated with HIPIMS gave a better result for both material 4140 and CK45. The fluctuations in GG25 material are due to the low hardness of the material and excessive wear of the HIPIMS coating.

Briefly, for group 1 tests HIPIMS technology outperformed the cathodic arc technology. Also, the best machinable material is the CK45 materials based on tension and torsion force while the 4140 is the best based on bending moment.

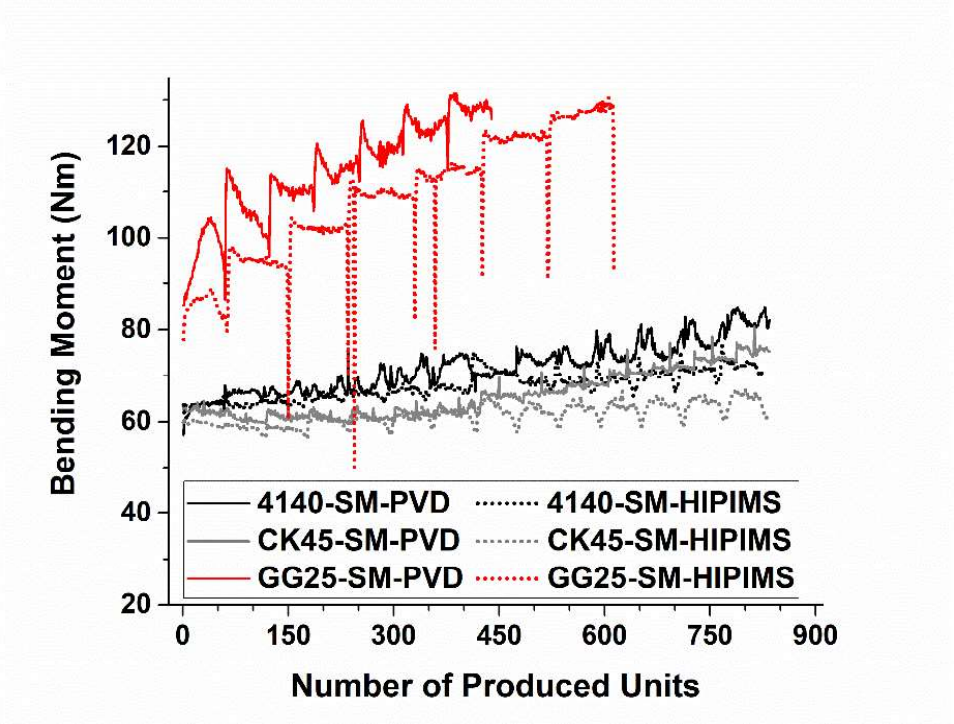


Figure 3.22. Bending moment graph of group 1 tests

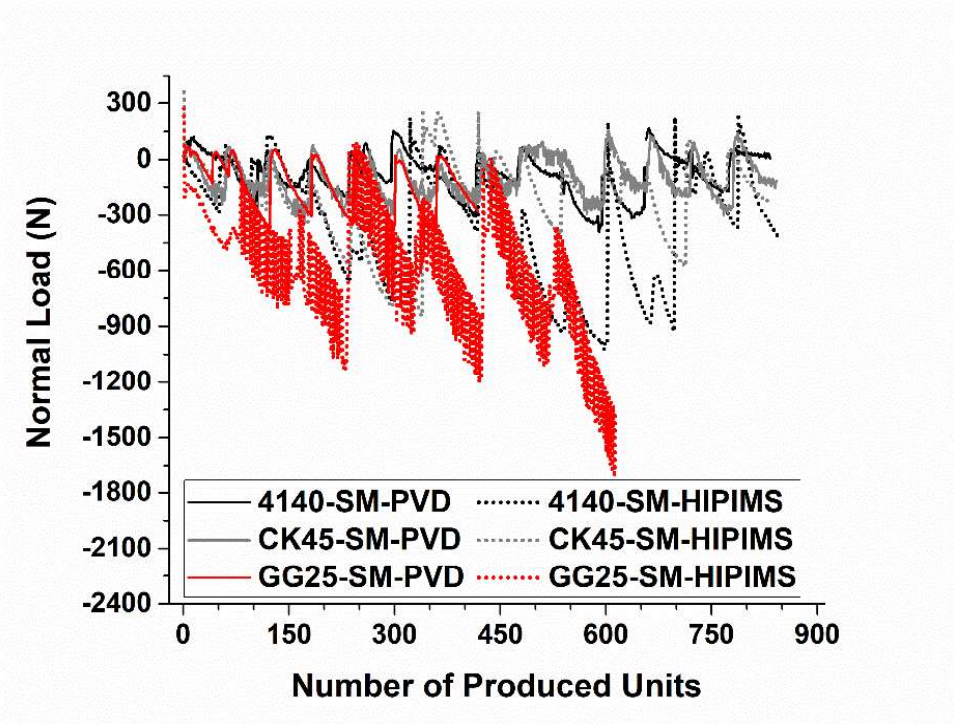


Figure 3.23. Normal load graph of group 1

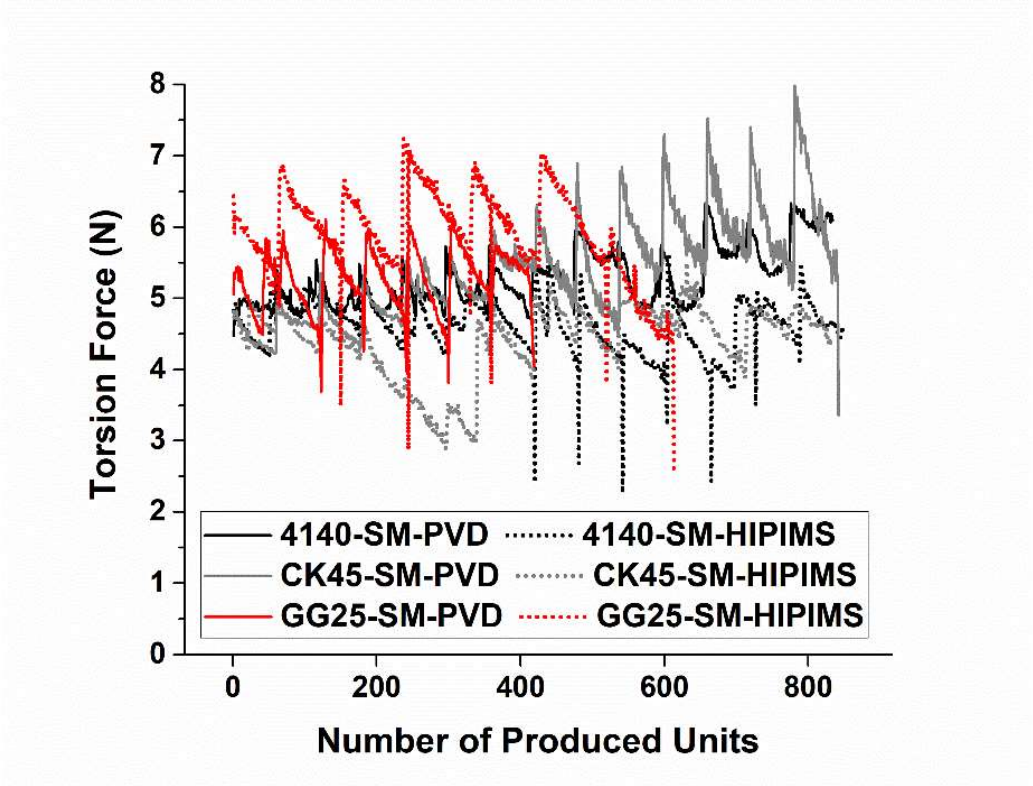


Figure 3.24. Torsion force graph of group 1

For group 2 tests spike graphs given below. In graph 3.25, considering the bending forces, the cutting tools have less bending force during the drilling process. The most stable graphic belongs to both 4140-DRL-PVD and 4140-DRL-PVD.

On the other hand, in figure 3.26, the normal loads are given, the cutting tools were exposed to less normal load during the milling process. The most stable graphic belongs to 4140-SM-HIPIMS. In graph 3.27, torsion forces are given, and the drilling process was exposed to less torsion force and the tool coated with cathodic arc technology gave better results in drilling operations.

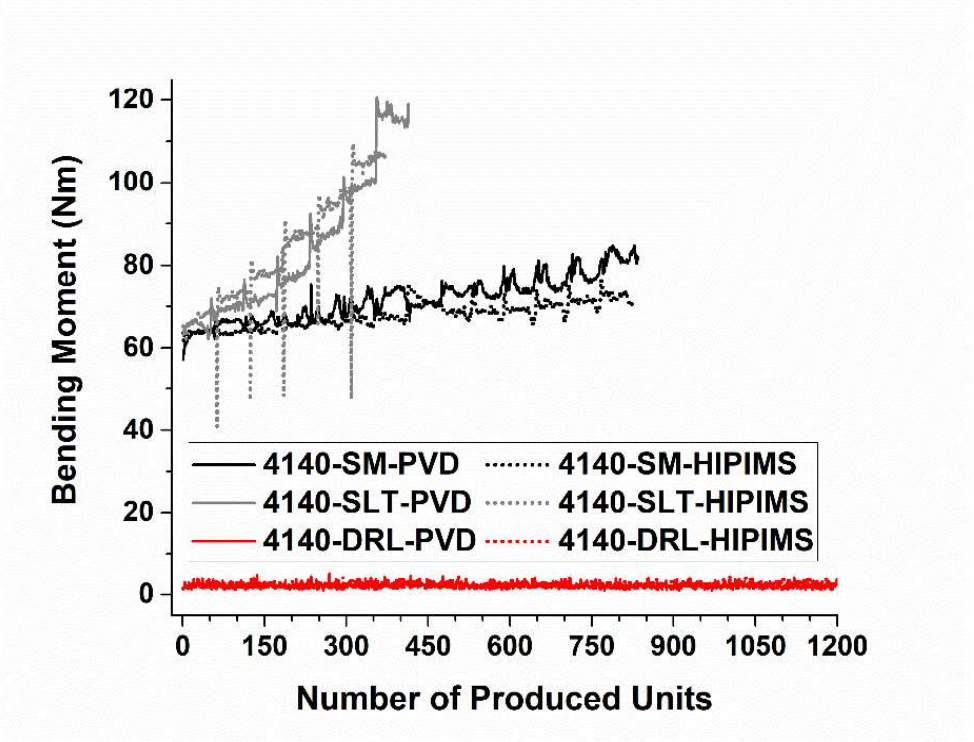


Figure 3.25. Bending moment graph of group 2 tests

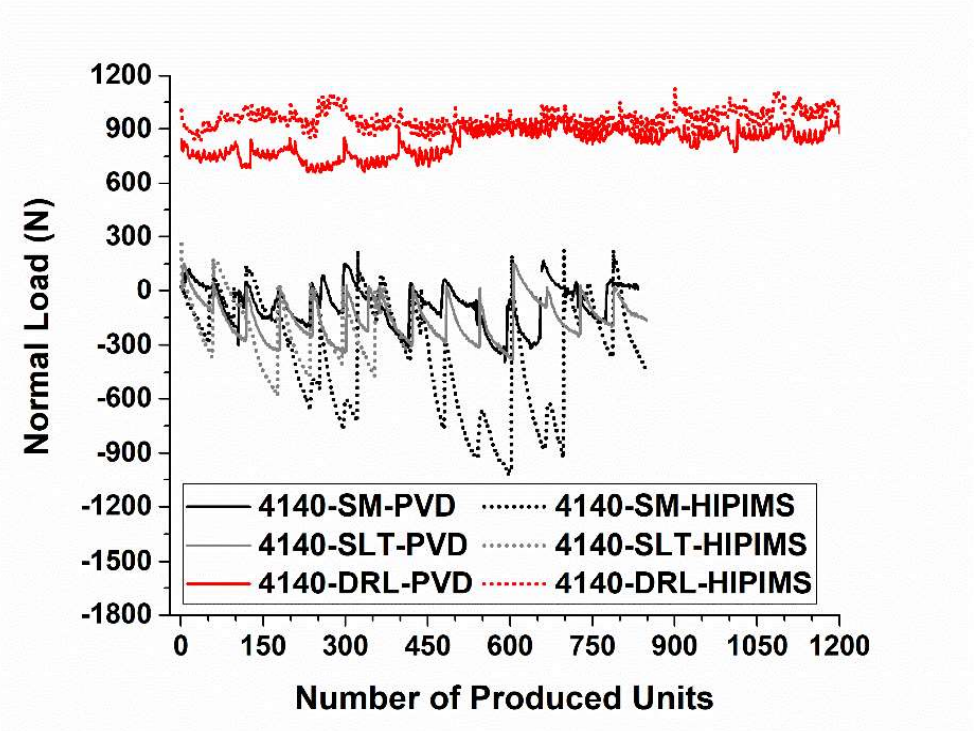


Figure 3.26. Normal loads of group 2 tests

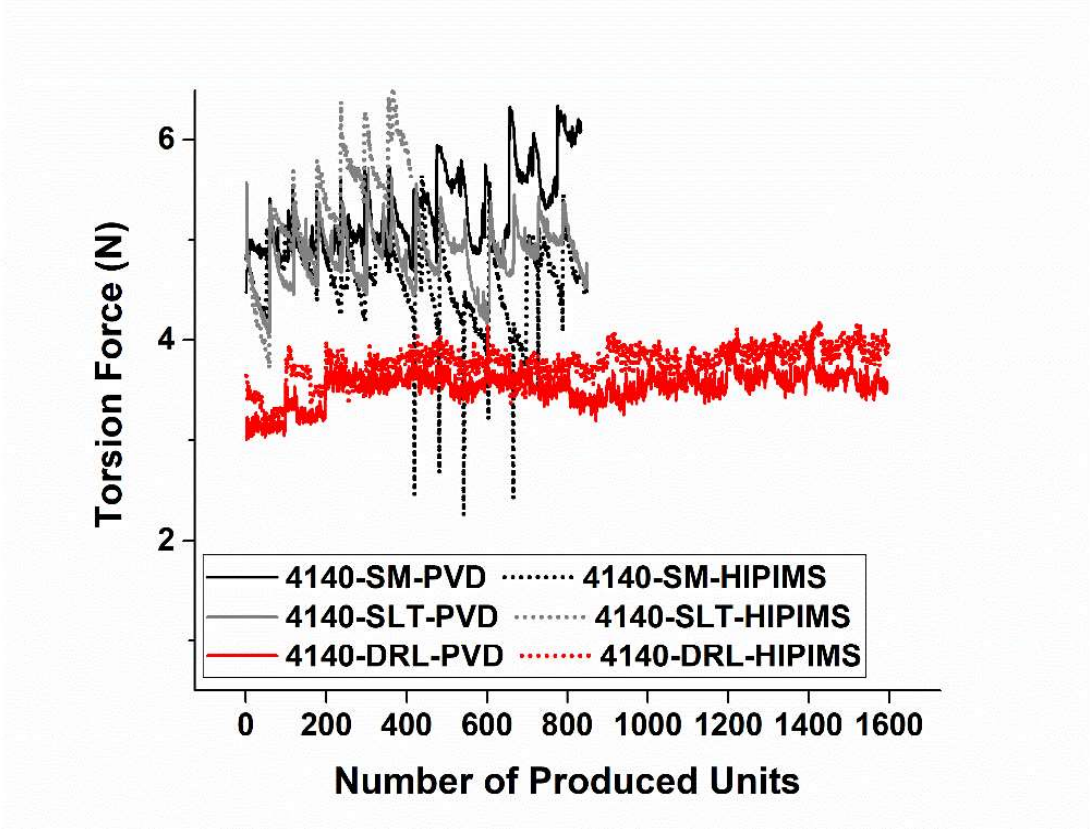


Figure 3.27. Torsion force of group 2 tests

For group 3 tests spike graphs given below. Looking at bending moment in figure 3.28, normal load in figure 2.39 and normal loads in figure 3.30, respectively. In figures 3.28 and 3.29, GEO2_HFM-Ti6Al4V-HIPIMS gives the best result while in the terms of normal load in figure 2.29, GEO2_HFM-Ti6Al4V-PVS gives better result than the others.

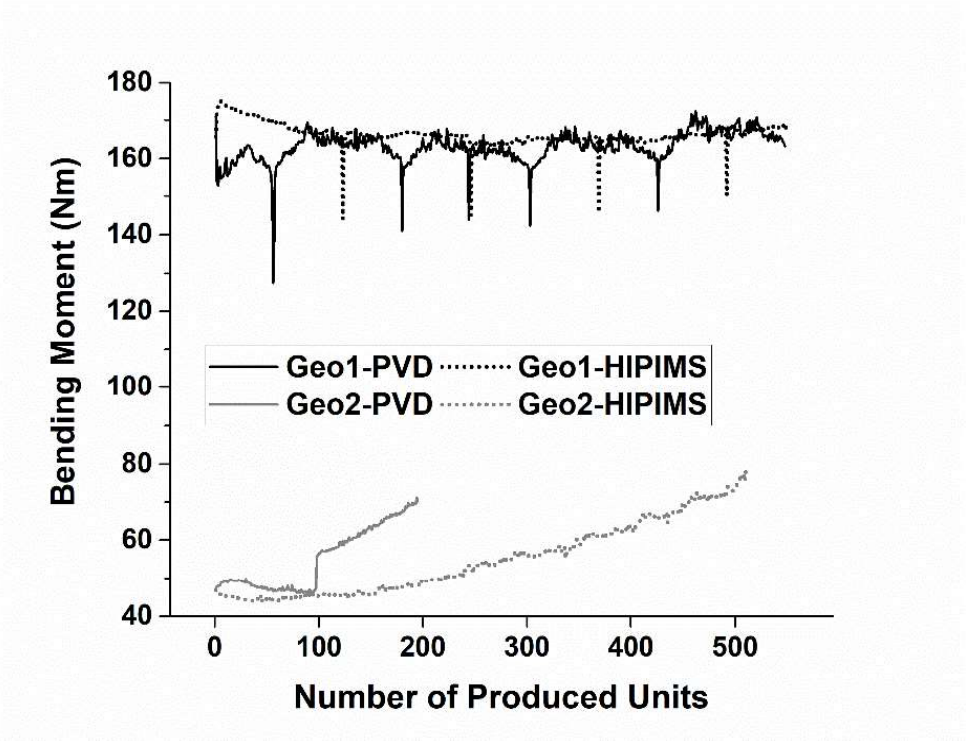


Figure 3.28. Bending moment of Group 3 tests

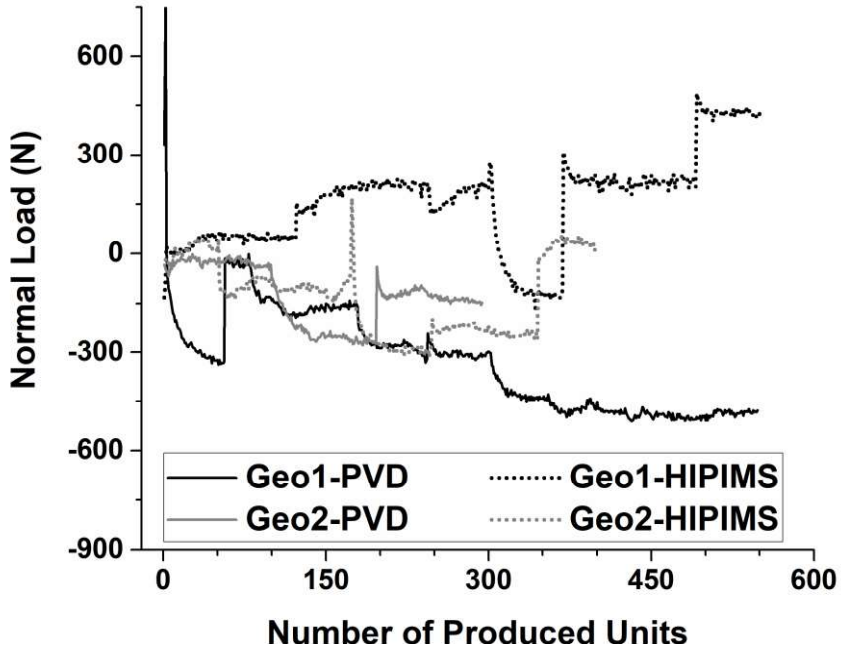


Figure 3.29. Normal load graph of group 3 tests

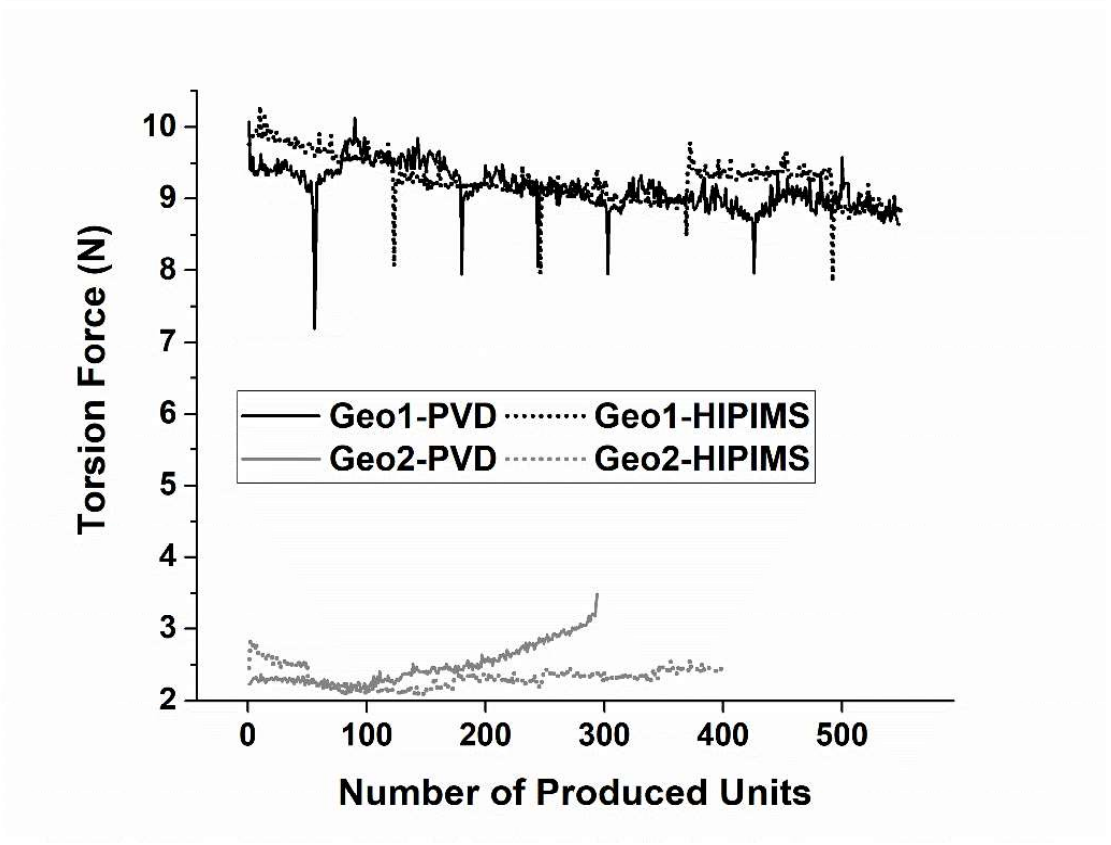


Figure 3.30. Torsion force graph of group 3 tests

For group 4 tests spike graphs given below. Looking at bending moment in the figure 3.31, normal load in the figure 3.32 and normal loads in the figure 3.33, respectively. that used tool 12 with HIPIMS coated gave the best results in all graphics. Looking at all these graphs, D2-PM-HIPIMS gave better results.

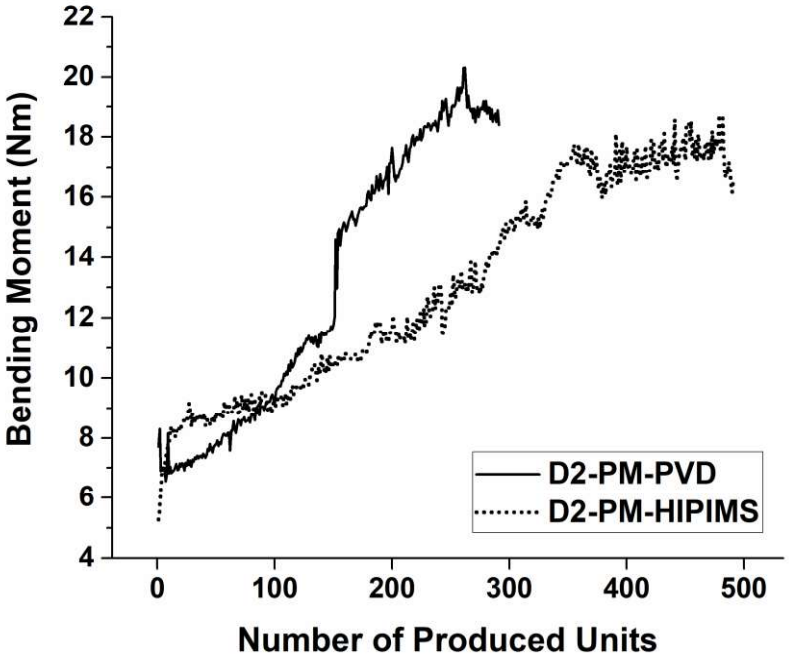


Figure 3.31. Bending moment of group 4 tests

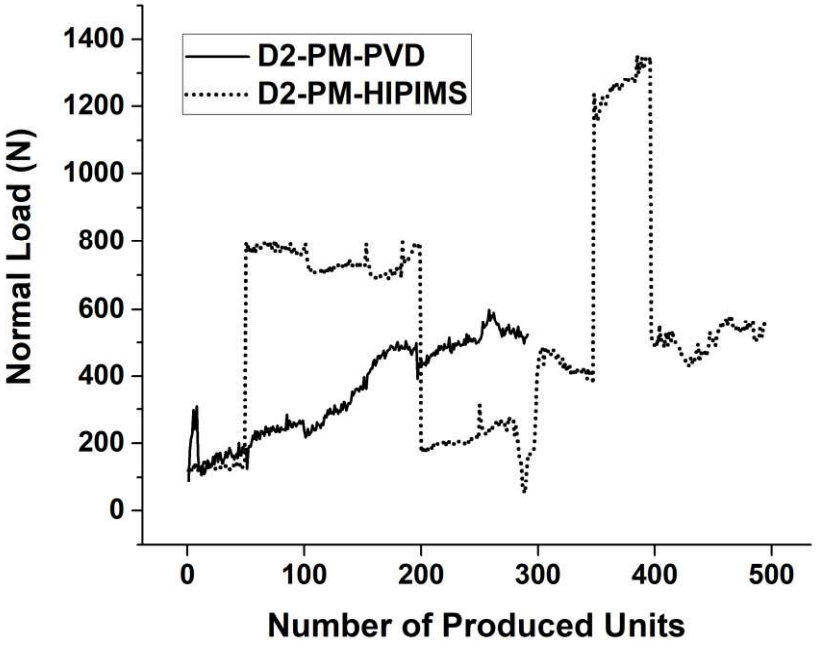


Figure 3.32. Normal load graph of group 4 tests

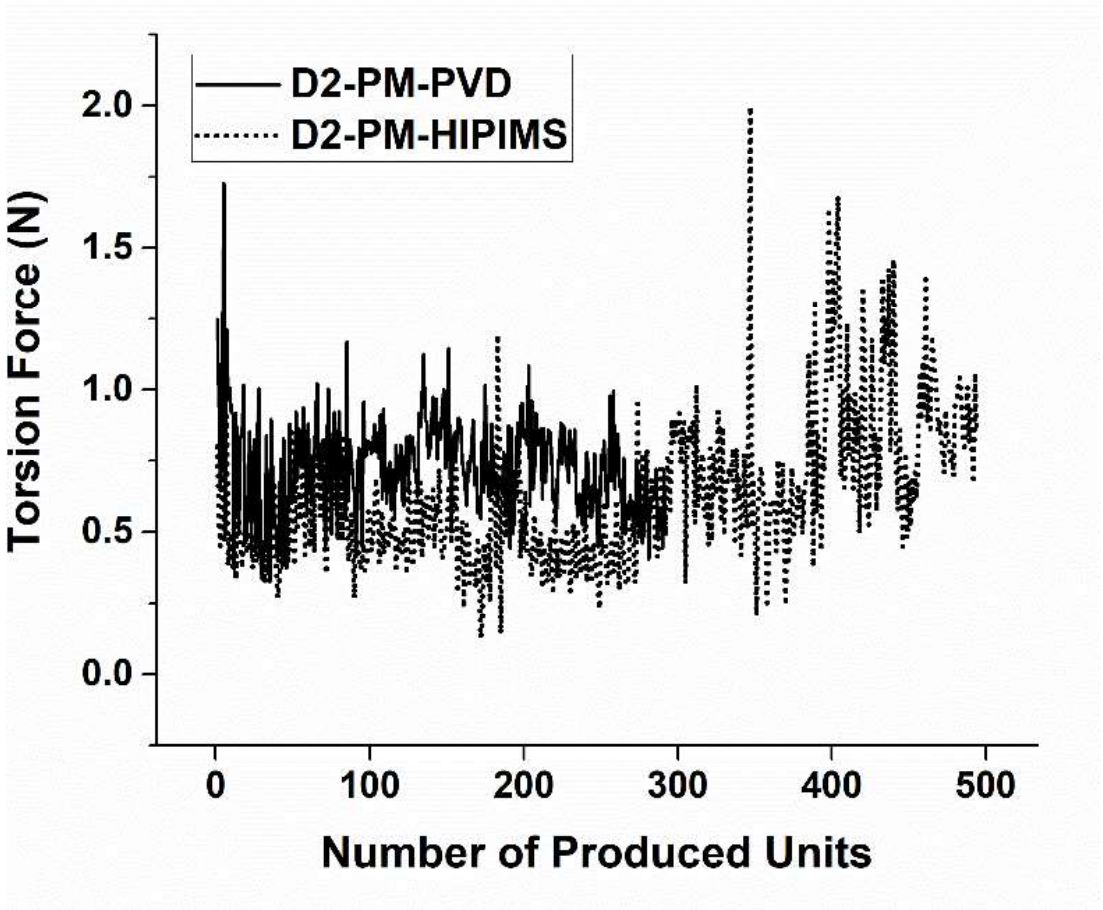


Figure 3.33. Torsion force graph of group 4 tests

### 3.2.3. Tool wear

Tool wear was measured in 2 dimensions with the help of an optical microscope. Metric program was used while measuring. Table 3.12 and 3.14 show the flank wear images of the group 1 tests. Rake wears images are given in tables 3.13 and 3.15. When these wear values are compared, GG25 material wears more in both wear types. Also, the highest amount of wear belongs to GG25-SM-HIPIMS in group 1 tests.

Table 3.12. Flank wear images of 4140-SM-PVD, CK45-SM-PVD and GG25-SM-PVD

| Tool Wear Images (Flank Wear) | | |
|---|---|---|
| **4140-SM-PVD** **~123 m cut** | **CK45-SM-PVD** **~123 m cut** | **GG25-SM-PVD** **~72m cut** |
| | | |
| | | 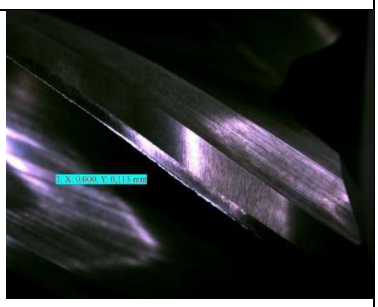 |
| 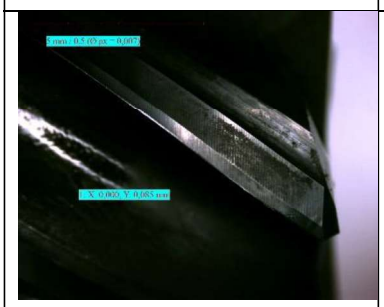 | | |
| 0.106 µ wear | 0.128 µ wear | 0.128 µ wear |

Table 3.13. Rake wear images of 4140-SM-PVD, CK45-SM-PVD and GG25-SM-PVD

| Tool Wear Images (Rake Wear) | | |
|---|---|---|
| **4140-SM-PVD**<br>**~123m cut** | **CK45-SM-PVD**<br>**~123m cut** | **GG25-SM-PVD**<br>**~72 m cut** |
| | | |
| | 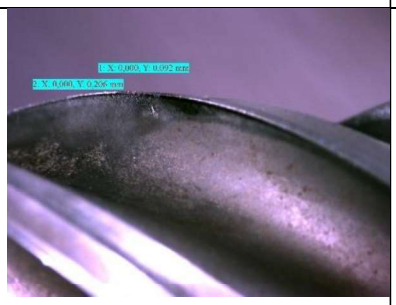 | |
| | 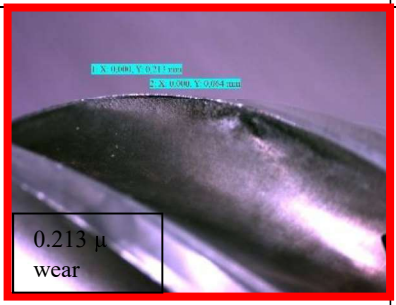 | 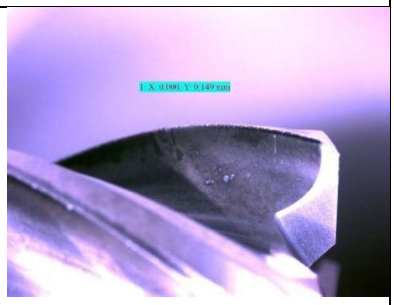 |
| 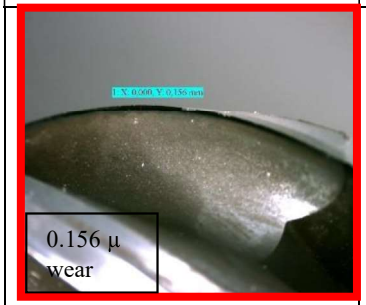 | | |

Table 3.14. Flank wear images of 4140-SM-HIPIMS, CK45SM-HIPIMS and GG25-SM-HIPIMS

| Tool Wear Images (Flank Wear) | | |
|---|---|---|
| **4140-SM-HIPIMS**<br>**~123m cut** | **CK45-SM-HIPIMS**<br>**~ 123 m cut** | **GG25-SM-HIPIMS**<br>**~90 m cut** |
| 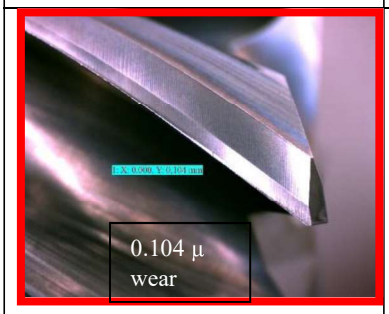 | | 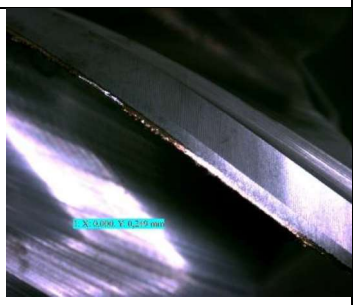 |
| 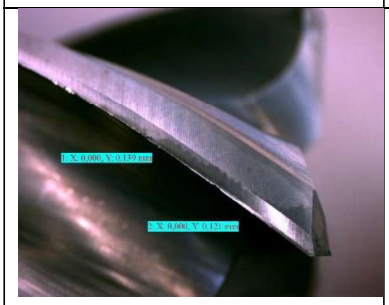 | | 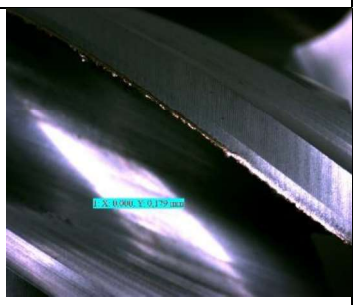 |
| | | |
| | | |

Table 3.15. Rake wear images of 4140-SM-HIPIMS, CK45SM-HIPIMS and GG25-SM-HIPIMS

| Tool Wear Images (Rake Wear) | | |
|---|---|---|
| **4140-SM-HIPIMS ~123m cut** | **CK45-SM-HIPIMS ~ 123 m cut** | **GG25-SM-HIPIMS ~90 m cut** |
| | | |
| 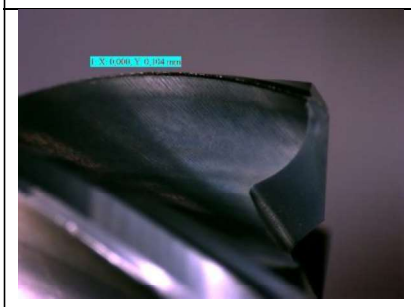 | | 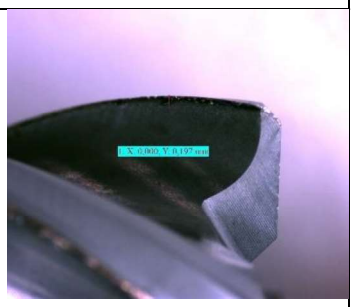 |
| 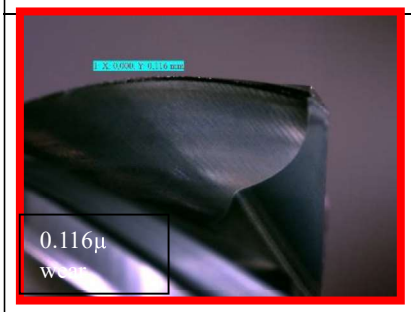 | 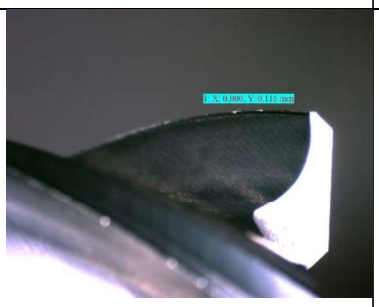 | |
| 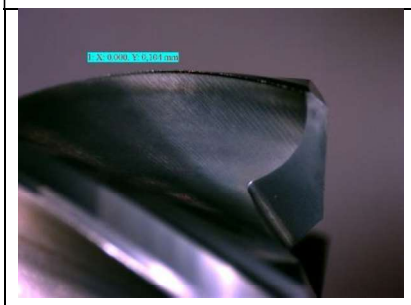 | 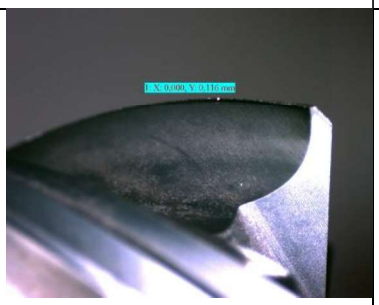 | |

Tables 3.16 and 3.17 show the flank and rake wear respectively, of the 4140-SLT-PVD and 4140-SLT-HIPIMS tests. In addition, table 2.18 shows front wear images of the 4140-DRL-PVD and 4140-DRL-HIPIMS tests. When the comparison of wear within the scope of group 2, the types of operations affect the amount of wear.

In the drilling operation, the front wear of the drill is the same amount as in slot milling. Also, slot operation wear is greater than with shoulder milling.

Table 3.16. Flank wear images of 4140-SLT-PVD, 4140-SLT-HIPIMS

| **The Wear Images (Flank Wear)** | |
|---|---|
| **4140-SLT-PVD<br>~67 m cut** | **4140-SLT-HIPIMS<br>~90 m cut** |
| 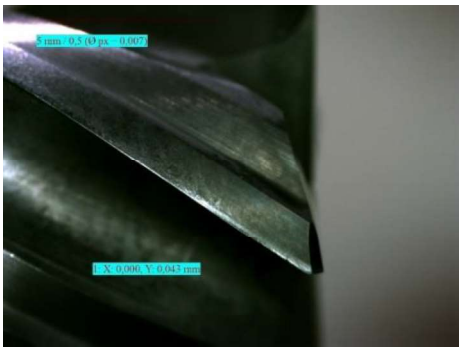 | 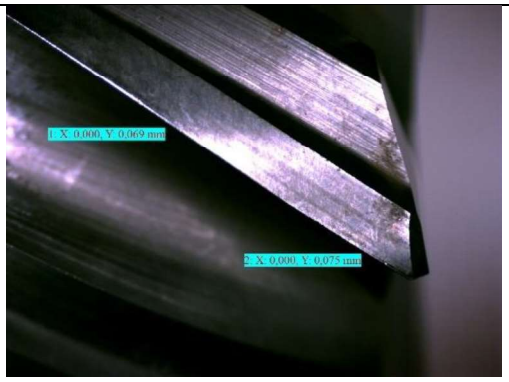 |
| | 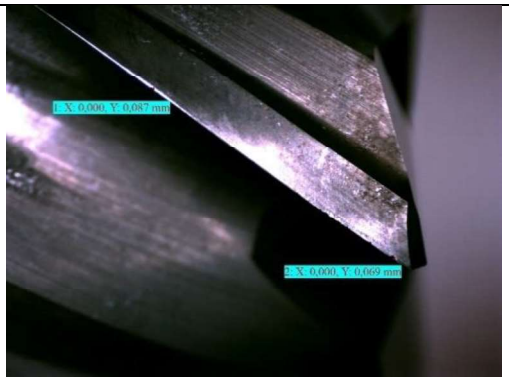 |
| | 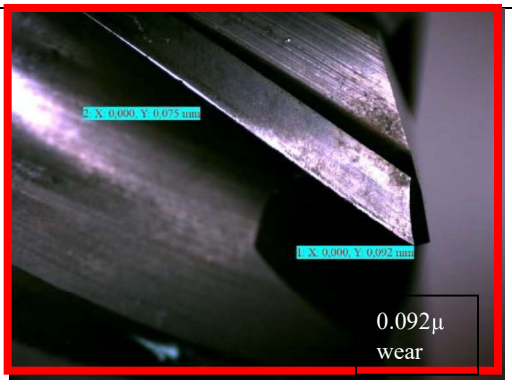 |

Table 3.17. Rake wear images of 4140-SLT-PVD, 4140-SLT-HIPIMS

| The Wear Images (Rake Wear) | |
|---|---|
| **4140-SLT-PVD ~67 m cut** | **4140-SLT-HIPIMS ~90 m cut** |
| 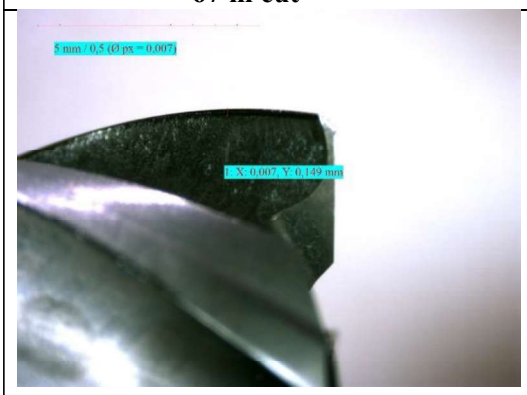 | 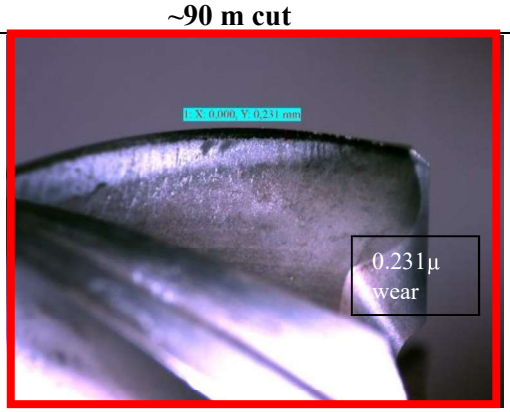  |
| | 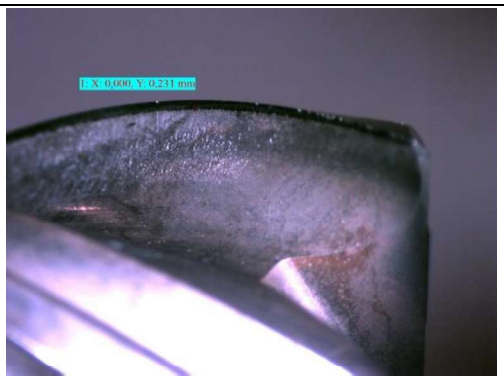 |
| | |
| | 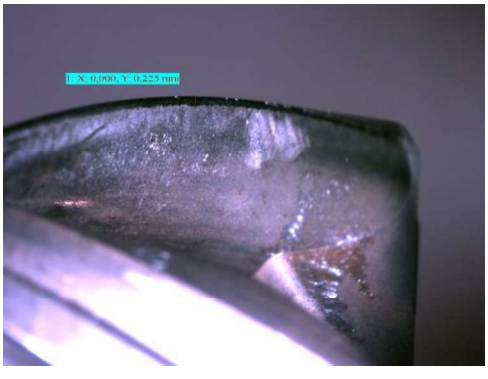 |

Table 3.18. Front wear images of 4140-DRL-PVD, 4140-DRL-HIPIMS

| **The Wear Images (Front)** | |
|---|---|
| **4140-DRL-PVD**<br>**1600 Holes** | **4140-SM-PVD0**<br>**1600 Holes** |
| | 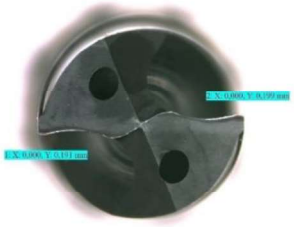 |

Flank and rake wear of group 3 tests are given in tables 3.19-3.20 and 3.21-3.22 respectively. When these wears are compared, it has been observed that geometry 2 wears more than geometry 1.

Table 3.19. Flank wear images of Geo1_HFM-Ti6Al4V-PVD, Geo1_HFM-Ti6Al4V-HIPIMS

| **The Wear Images (Flank Wear)** | |
|---|---|
| **Geo1_HFM-Ti6Al4V-PVD**<br>**~78 m cut** | **Geo1_HFM-Ti6Al4V-HIPIMS**<br>**~78 m cut** |
| | 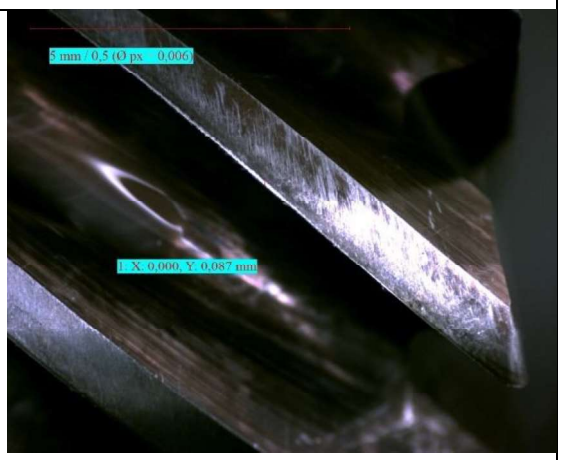 |

(cont. on next page)

Table 3.19 (cont.).

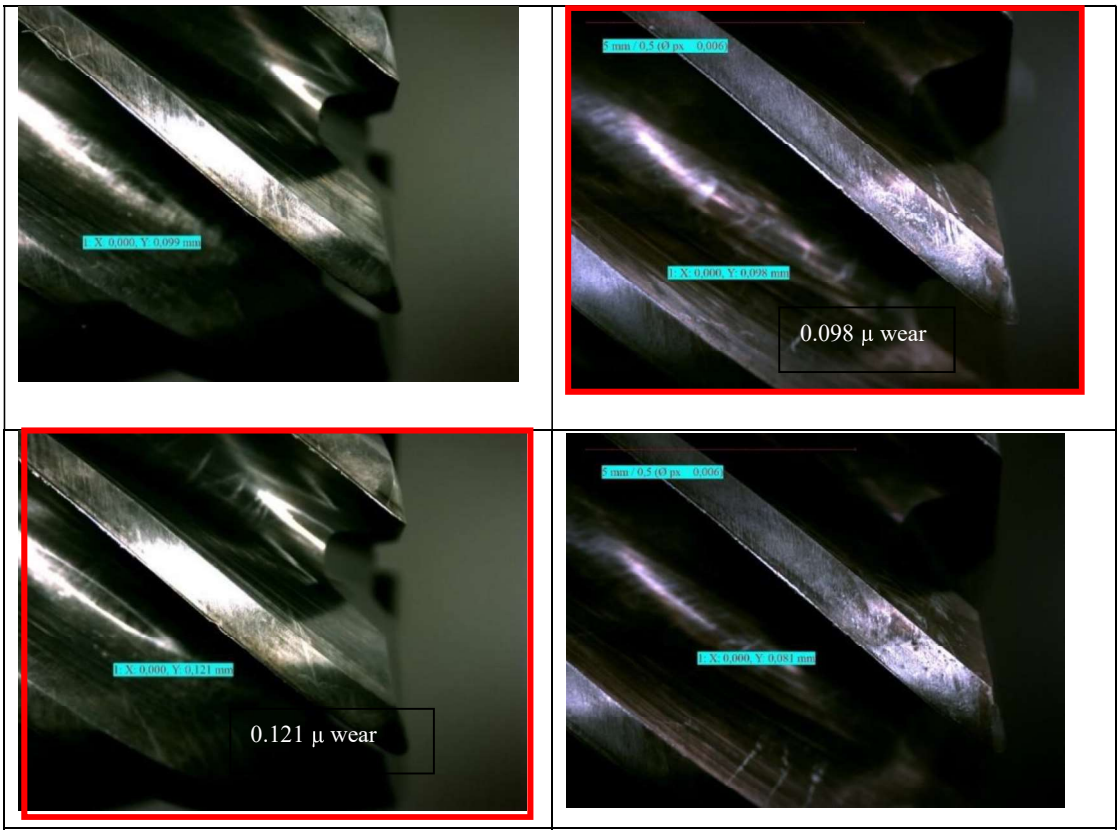


Table 3.20. Rake wear images of Geo1_HFM-Ti6Al4V-PVD, Geo1_HFM-Ti6Al4V-HIPIMS

| The Wear Images (Rake Wear) | |
|---|---|
| **Geo1_HFM-Ti6Al4V-PVD**<br>**~78 m cut** | **Geo1_HFM-Ti6Al4V-HIPIMS**<br>**~78 m cut** |
| | 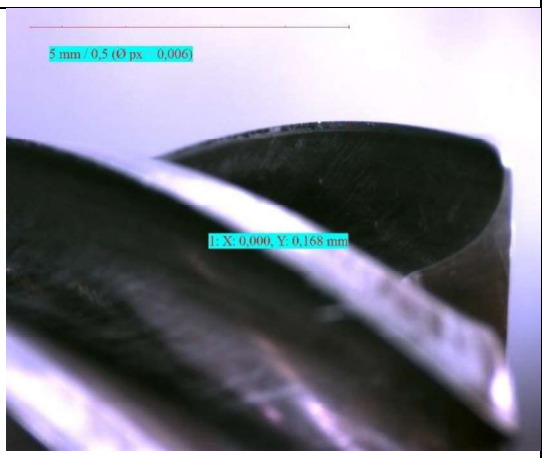 |



(cont. on next page)

Table 3.20 (cont.).

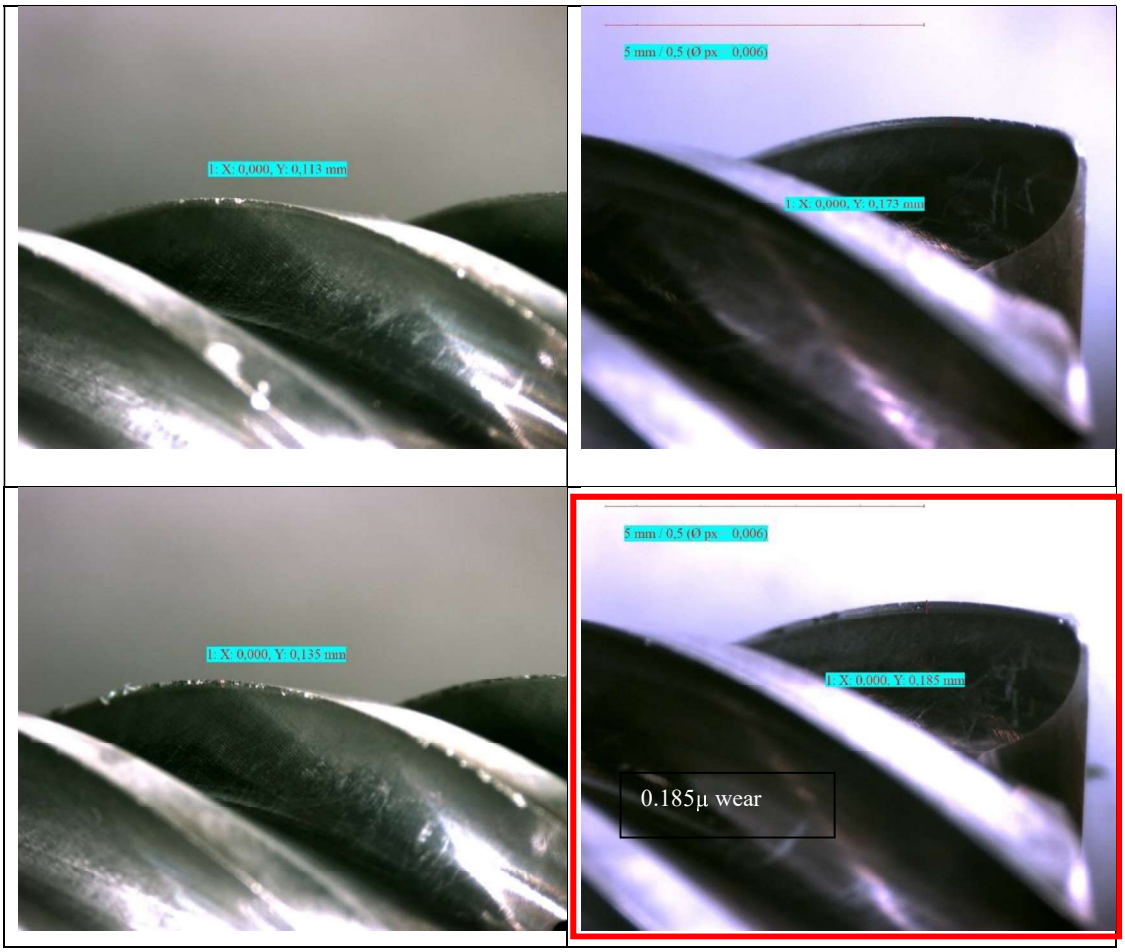


Table 3.21. Flank wear images of Geo2_HFM-Ti6Al4V-PVD, Geo2_HFM-Ti6Al4V-HIPIMS

| **The Wear Images (Flank Wear)** | |
|---|---|
| **Geo2_HFM-Ti6Al4V-PVD**<br>**~45 m cut** | **Geo2_HFM-Ti6Al4V-HIPIMS**<br>**~78 m cut** |
| 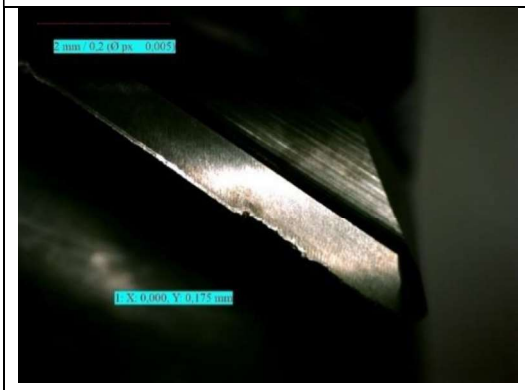 | 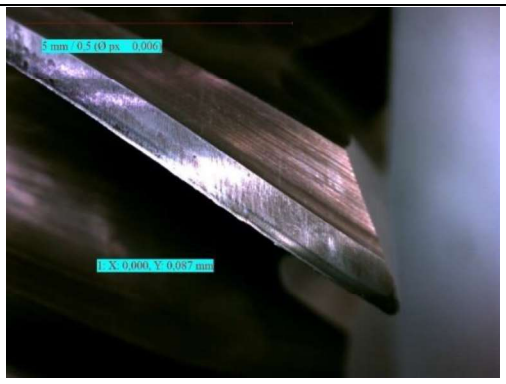 |



(cont. on next page)

Table 3.21 (cont.).

| | |
|---|---|
| 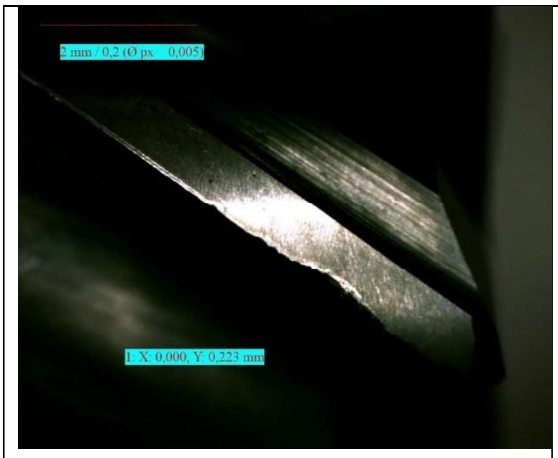 | 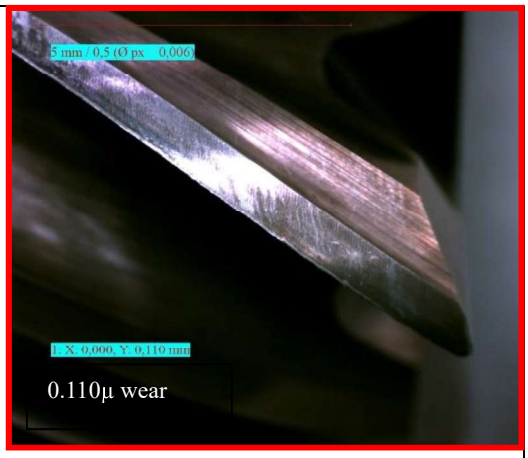 |
| | 0.110µ wear |
| 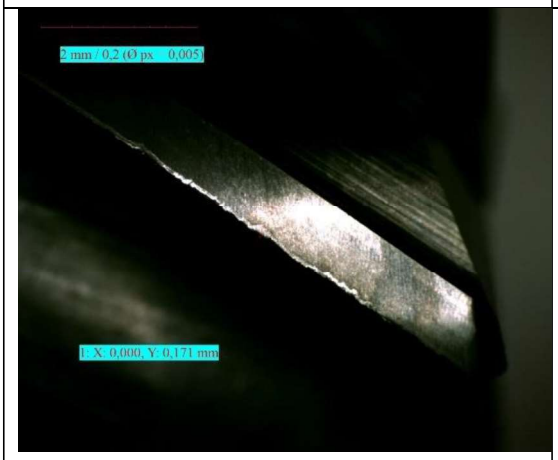 | 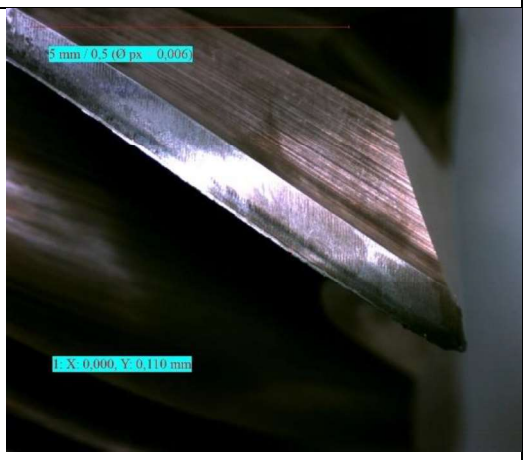 |
| 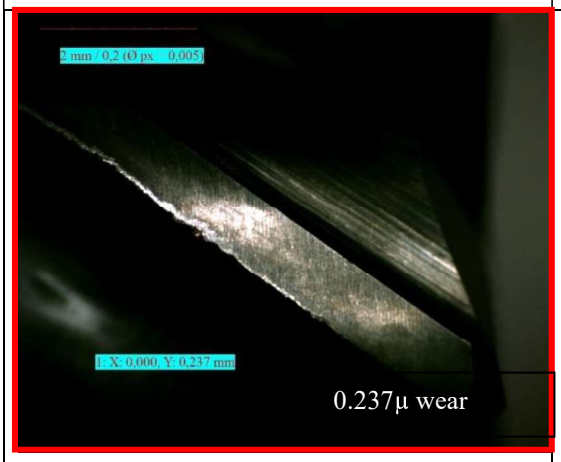 | 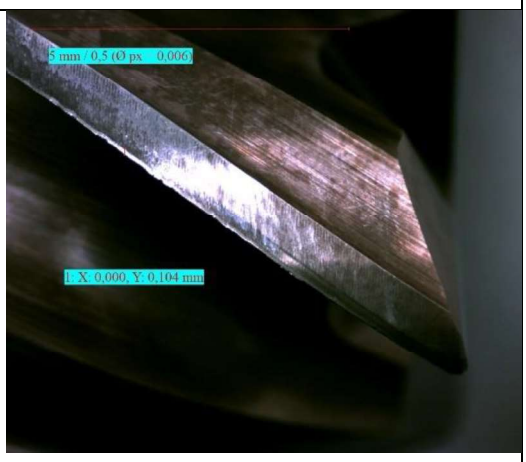 |
| 0.237µ wear | |

Table 3.22. Rake wear of Geo2_HFM-Ti6Al4V-PVD, Geo2_HFM-Ti6Al4V-HIPIMS

| **The Wear Images (Rake Wear)** | |
|---|---|
| **Geo2_HFM-Ti6Al4V-PVD**<br>**~45 m cut** | ***Geo2_HFM-Ti6Al4V-HIPIMS***<br>**~78 m cut** |
| | 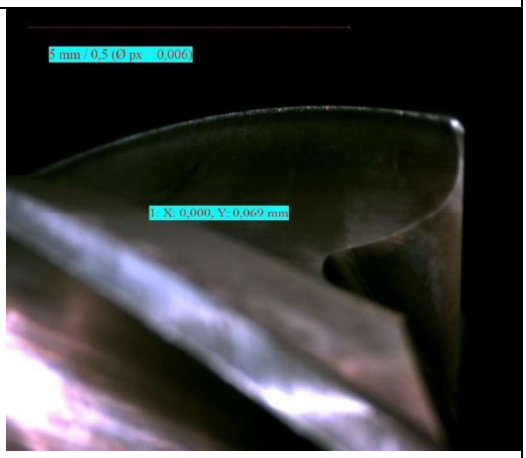 |
| | 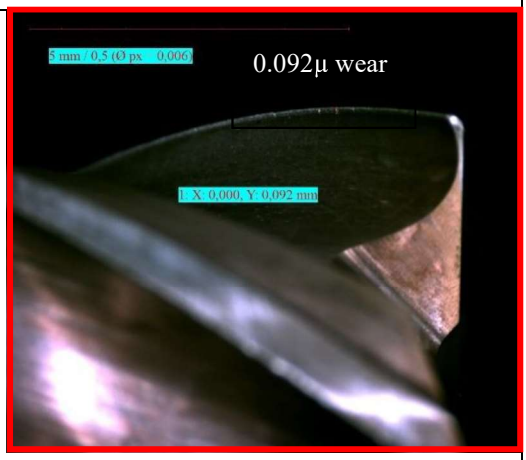 |
| 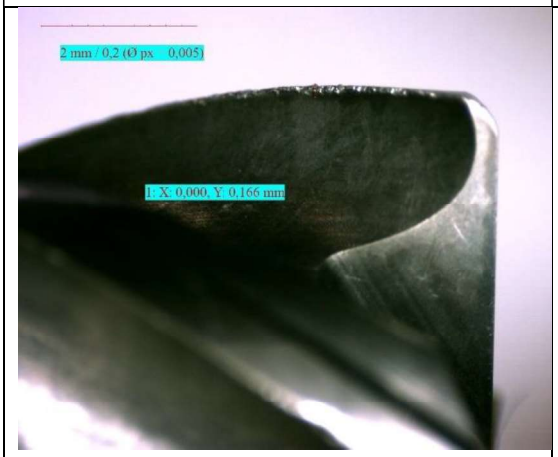 | 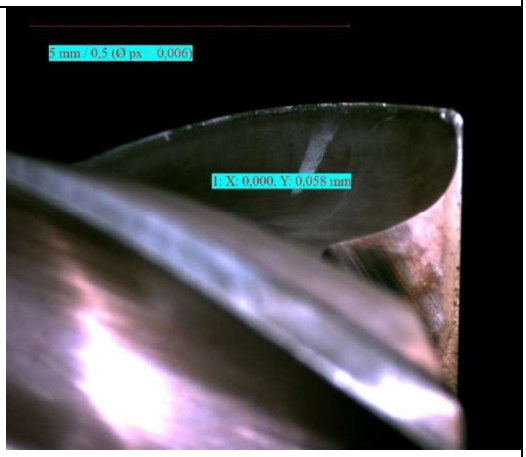 |

Table given in the below gives that the front wear image of the group 4 tests and when compared these images the D2-PM-HIPIMS is less wear than D2-PM-PVD.

Table 3.23. Front wear images of D2-PM-PVD, D2-PM-HIPIMS

| **The Wear Images (Front)** | |
|---|---|
| **D2-PM-PVD**<br>**~48 m cut** | **D2-PM-HIPIMS**<br>**~75 m cut** |
| 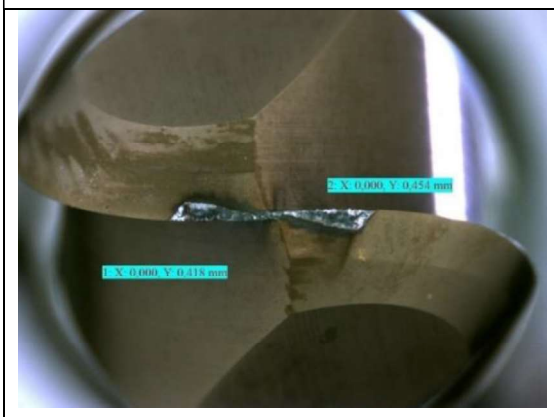 | 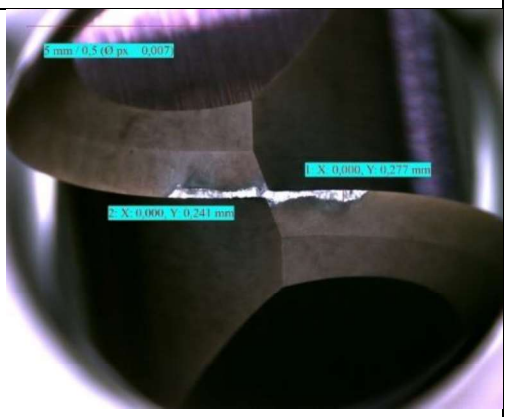 |

## 3.2.4. Chip Images

For all chip images in Tables 3.24, 3.25 and 3.26 the same scale given next to the images is used. In that scale the distance between each line represents 1 mm. Table 3.24 gives the chip images of group 1 tests. When the chip forms of each material group are compared with each other, they show similar forms, but result of HIPIMS coated tests, the chip colors are darker than the other. When we look at the chip images of the GG25 material, there is a chip that crumbles and disperses compared to the other material.

Table 3.24. Chip Images of Group 1 tests

| TEST | 4140-SM-PVD | CK45-SM-PVD | GG25-SM-PVD |
|---|---|---|---|
| CHIP IMAGES | | | |
| **TEST** | **4140-SM-HIPIMS** | **CK45-SM-HIPIMS** | **GG25-SM-HIPIMS** |
| CHIP IMAGES | | | |

Table 3.25 gives the chip images of group 2 tests. Based on these chips, slot milling has a thicker chip than shoulder milling, while drilling has a short and curved chip.

Table 3.25. Chip images of group 2 tests

| TEST | 4140-SM-PVD | 4140-SLT-PVD | 4140-DRL-PVD |
|---|---|---|---|
| CHIP IMAGES | | 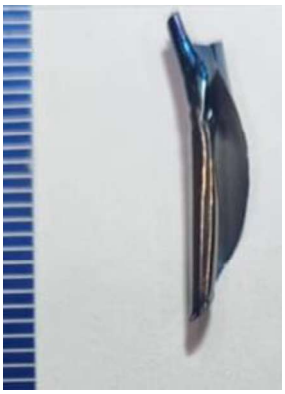 | 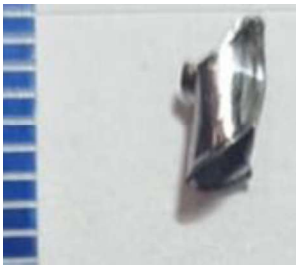 |
| **TEST** | **4140-SM-HIPIMS** | **4140-SLT-HIPIMS** | **4140-DRL-HIPIMS** |
| **CHIP IMAGES** | | | |

Table 3.26 gives examples of chips of group 3 tests. When looking at the chips, the chips of HIPIMS coated tools are closer to what they should be and in a more uniform form.

Table 3.26. Chip images of group 3 tests

| TEST | GEO1_HFM-Ti6Al4V-PVD | GEO2_HFM-Ti6Al4V-PVD |
|---|---|---|
| CHIP IMAGES | | |
| **TEST** | **GEO1_HFM-Ti6Al4V-HIPIMS** | **GEO2_HFM-Ti6Al4V-HIPIMS** |
| CHIP IMAGES | | |

In group 4, the number of passes in the vertical is very low, there was no significant chip formation. Chip comparison cannot be made for group 4.

# CHAPTER 4

# DISCUSSIONS

The design of experiment method was used to interpret the data obtained in this part. This method is a method used to determine the relationship between the inputs that affect a process and the outputs of that process. In addition, the main effect plot is used for comparison to see the effect of one independent variable on the dependent variable. Experimental design results for are given in the graphs below. Interaction plots and main effect plots were created within the scope of bending moment, torsion force and normal loads of each group, value at the end of the test, average maximum value, and maximum minus minimum value.

Firstly, the interaction plot of the group 1 tests is given in figure 4.1. Looking at figure 4.1 a, b and c there is no or little interaction between coating technologies and material but in figure 4.1 d strong interaction between coating technologies and workpiece materials.

The reason for this is related to the instant loading from spike measurement. In figure 4.2 gives the main effect plot of bending moment of group 1 test. In figures 4.2 it shows that bending moment is not affected by deposition method. In figure 4.2 bending moment effective by the material. Especially, GG25 material shows more bending moments than other material.

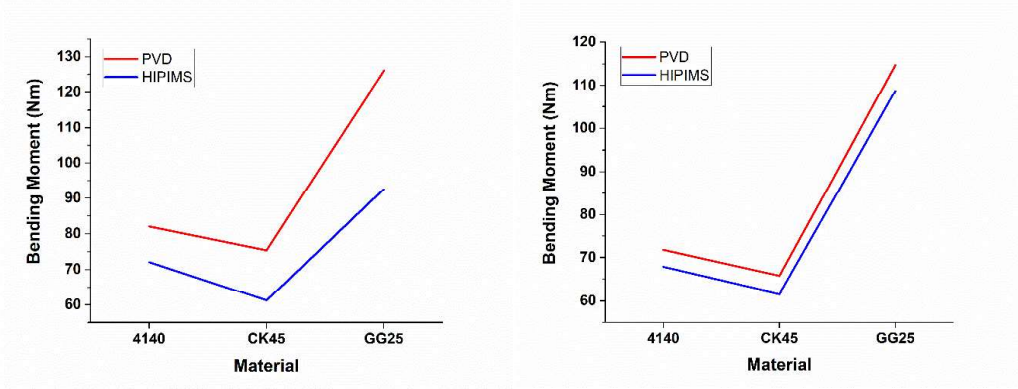


**a)** **b)**

Figure 4.1. Interaction plot of bending moment (a)Test end (b) Avarage (c) Max (d) Max-min of group 1 (cont. on next page)

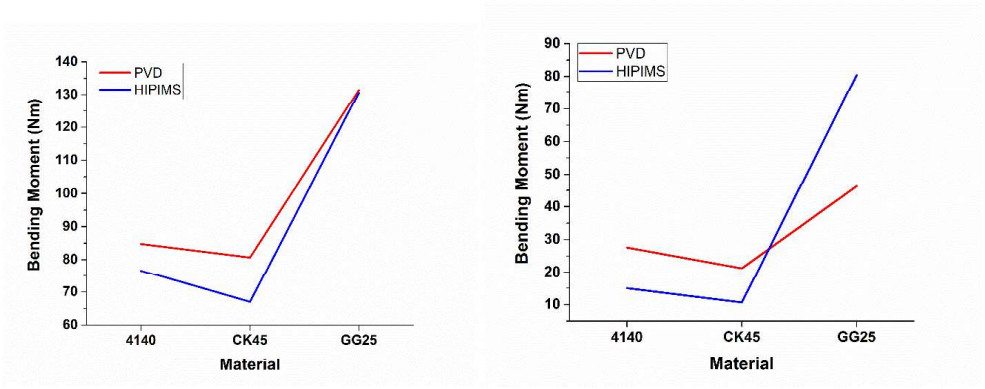


**c)** **d)**

Figure 4.1 (cont.)

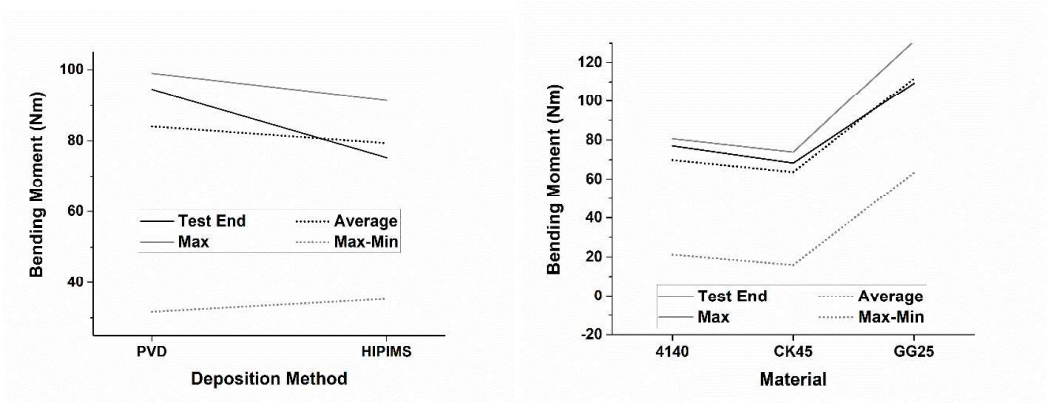


**a)** **b)**

Figure 4.2. Main effect plot of bending moment and a) deposition method b) workpieces method

Figure 4.2 gives normal load interaction plots of group 1 test. Looking at figures 4.3 a, b, c and d, there is a strong interaction between deposition method and workpieces material. In addition, figure 4.4 gives the main effect plot of both normal load-deposition method and normal load-workpieces material. In figure 4.4 a, there is a slight change in deposition methods and normal load in the terms of average, test end and maximum value of normal load but there is a significant difference max-min values which is high in the HIPIMS deposition methods. In figure 4.4 b there is a strong change in normal load when the workpiece material was changed. GG25 materials especially have lower normal load values in terms of test end, average and maximum values.

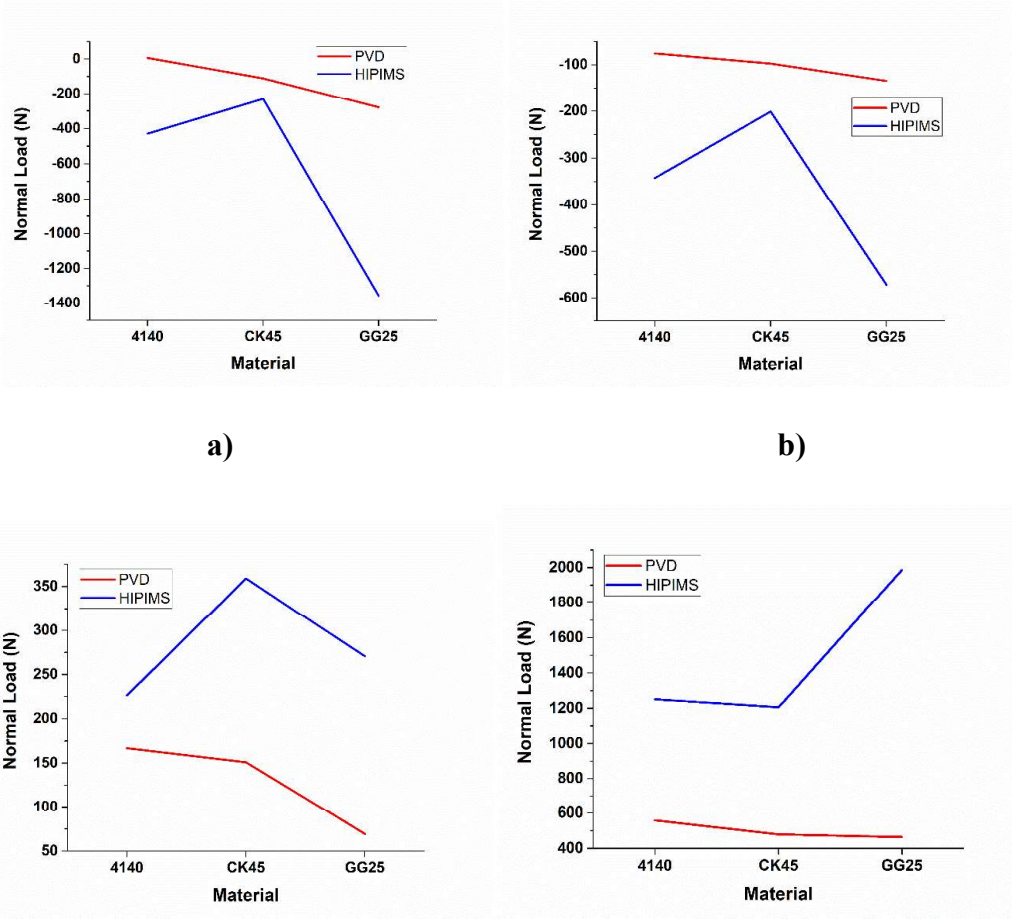


Figure 4.3. Interaction plot of normal load (a)Test end (b) Avarage (c) Max (d) Max-min of group 1

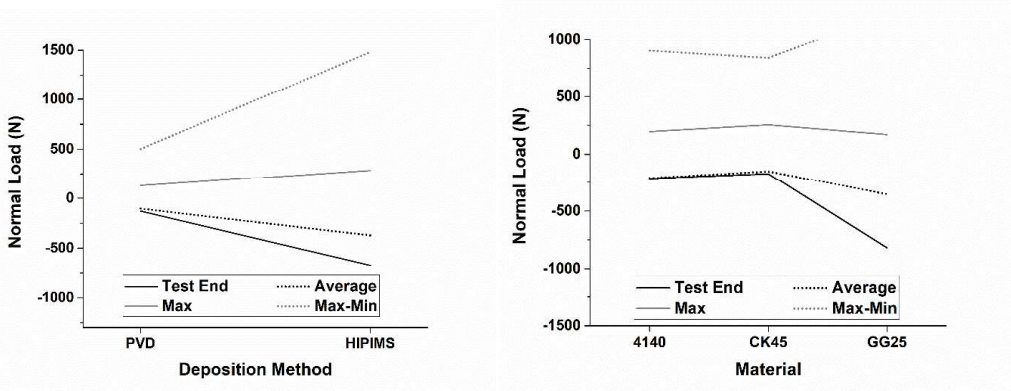


Figure 4.4. Main effect plot of normal load and a) deposition method b) workpieces method

When looking at figure 4.5 a, b, c, and d, when the torsion forces values are examined, a strong interaction is seen in all graphics of workpiece materials and coating technologies, and torsion forces and workpieces material. In figure 4.6 gives main effect plot of both torsion force-deposition method and torsion force-workpieces material. In figure 4.6 a, there is a slight change in deposition methods and normal load. In figure 4.6 b there is a strong change in torsion forces when the workpiece material was changed. GG25 material especially has higher torsion force values in terms of average, maximum and maximum-minimum values while it decreases in the test end of torsion values.

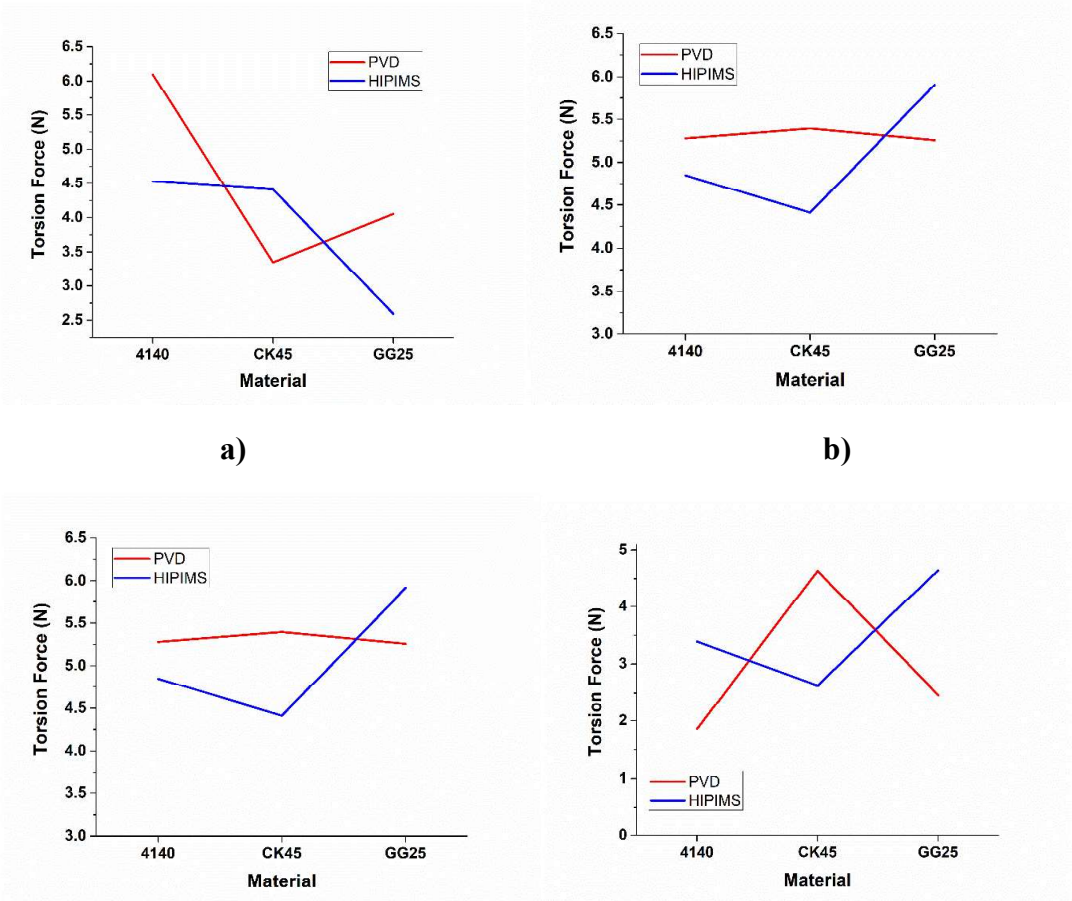


Figure 4.5. Interaction plot of torsion force (a)Test end (b) Average (c) Max (d) Max-min of group 1

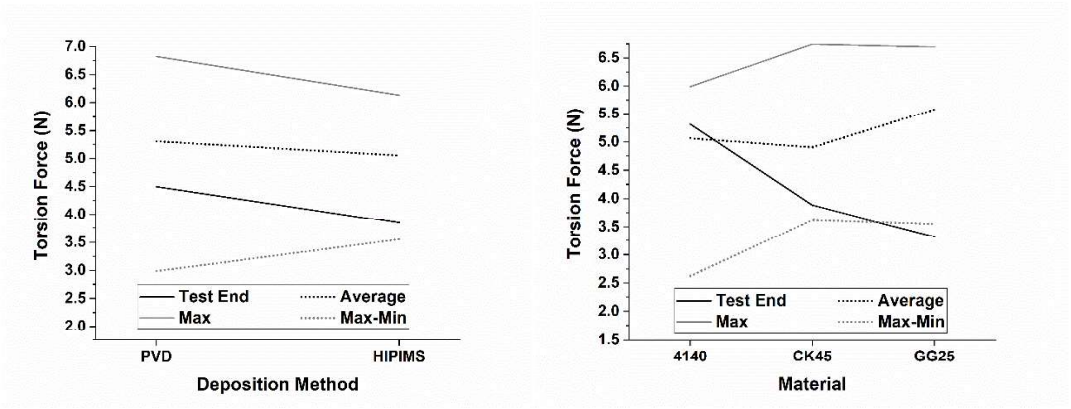


**a)** **b)**

Figure 4.6. Main effect plot of torsion force and a) deposition method b) workpieces method

Considering the wear interaction plot in figure 4.7, there is a strong interaction between the wear values and workpieces material, but this strong interaction comes from GG25 material. The graph keeps its parallelism between 4140 and CK45 material. Also, there is strong interaction between workpieces material and coating technologies due to the wear of GG25 material.

In figure 4.8 gives the main effect plot of both wear-deposition method and wear-workpieces material. In figure 4.8 a show that the wear more in HIPIMS technology.

In figure 4.8 b, it is seen that amount of wear is more in the GG25 material and in the figure 71 b wears more while the tool coated with HIPIMS Briefly, even if the HIPIMS technology shows better performance according to cutting forces, it shows inferior performance while GG25 material in the terms of wear.

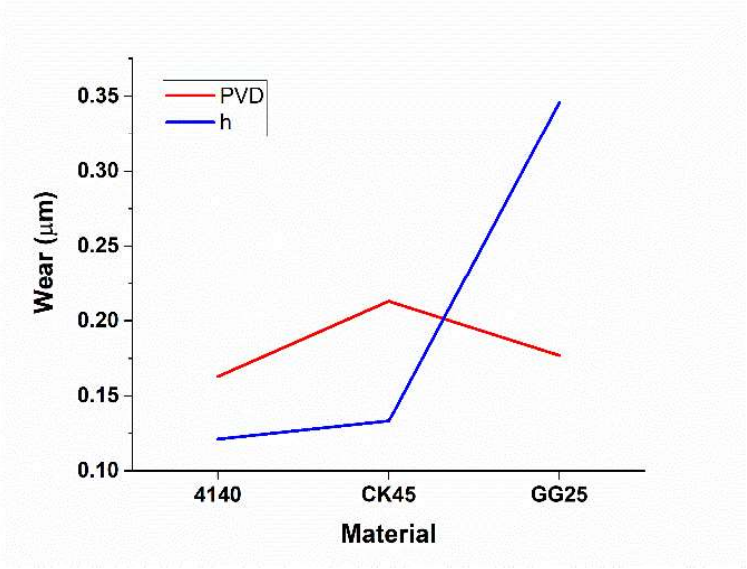


Figure 4.7. Interaction Plot of wear amount of group 1

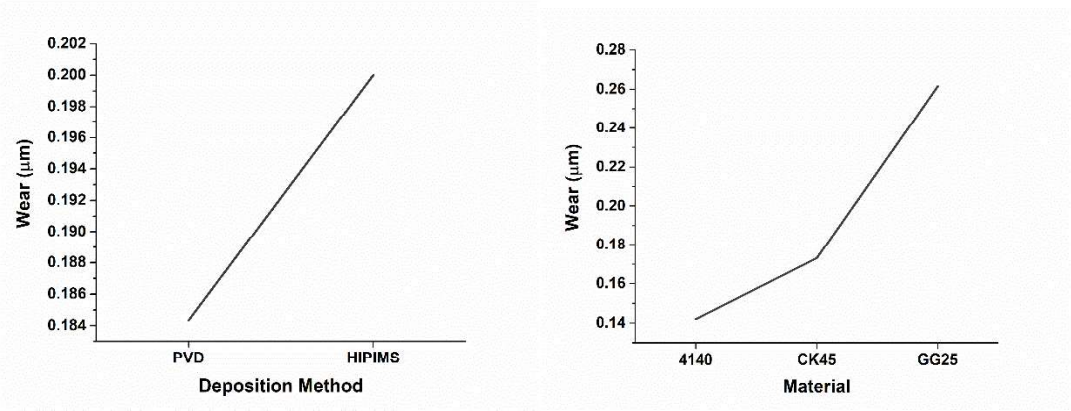


**a)** **b)**

Figure 4.8. Main effect plot of wear amount and a) deposition method b) workpieces materials

Secondly, interaction plot values are given in figure 4.9 When the comparison of bending moment interaction plots as you can see in figure 4.9 a, b, c and d there is little or no interaction between operation type and coating technology. In addition, figure 4.10 gives the main effect plot of both bending moment-deposition method and bending moment-workpieces material. In figure 4.9 a, there is a slight decrease in HIPIMS deposition methods. In figure 4.9 b there is a strong change in bending moment when the operation was changed. Slotting operation has higher bending moment while drilling has lower bending moment value.

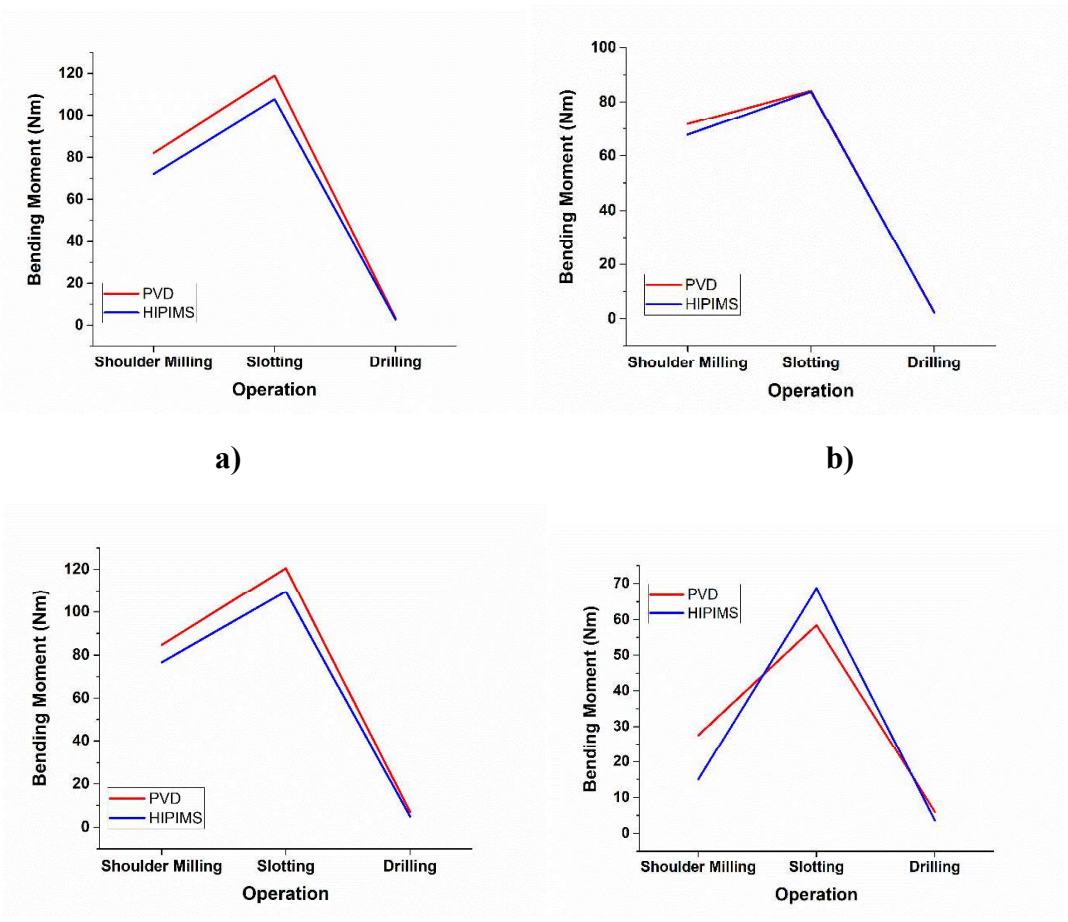


Figure 4.9. Interaction plot of bending moment (a)Test end (b) Average (c) Max (d) Max-min of group 2

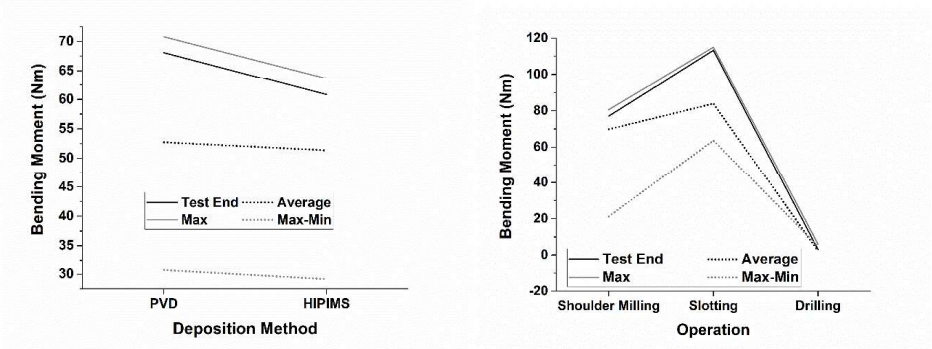


Figure 4.10. Main Effect plot of bending moment and a) deposition method b) operation type

When the comparison of normal load interaction plots as you can see in figure 4.11 a, b c and d there is little or no interaction between operation type and coating technologies. As it can see in figure 4.12, normal load is not much effective by the deposition method, but the operation type is highly effective. The drilling operation gives a more normal load.

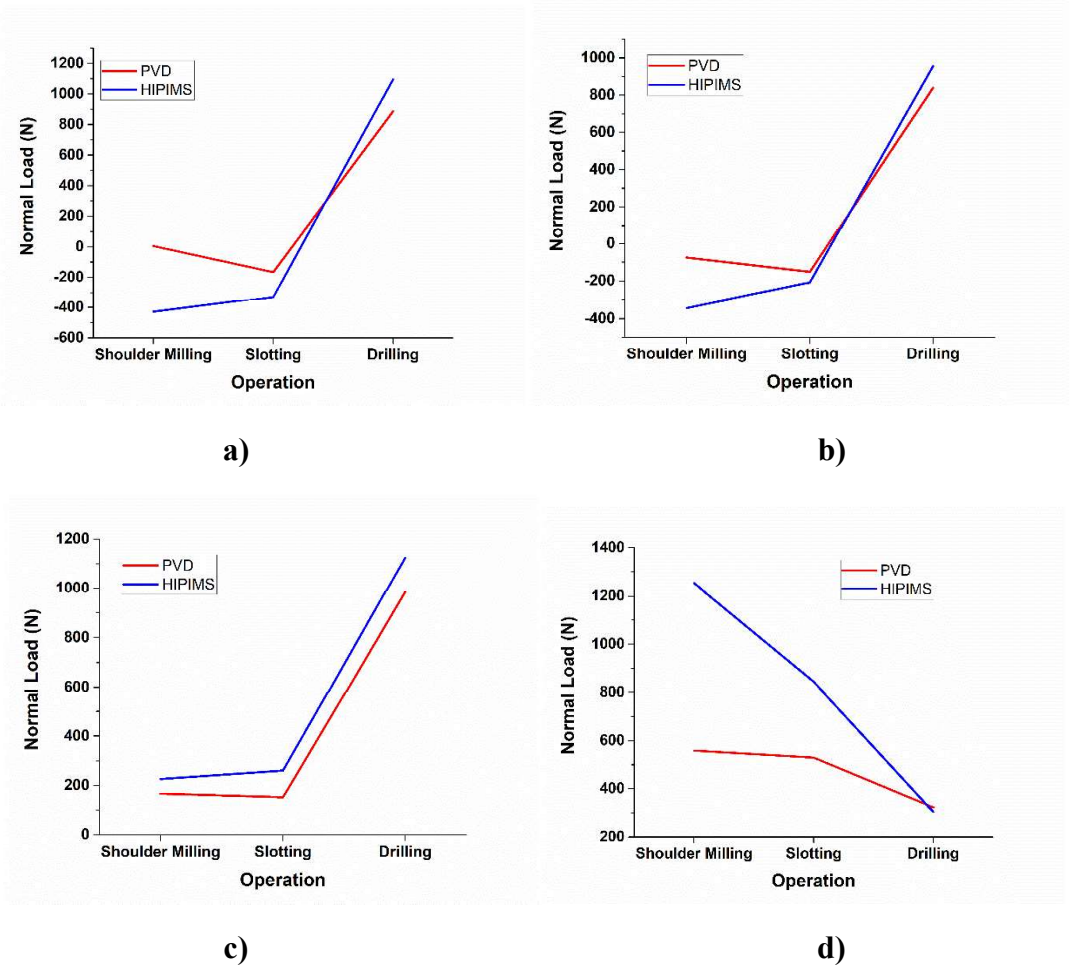


Figure 4.11. Interaction plot of normal load (a)Test end (b) Average (c) Max (d) Max-min of group 2

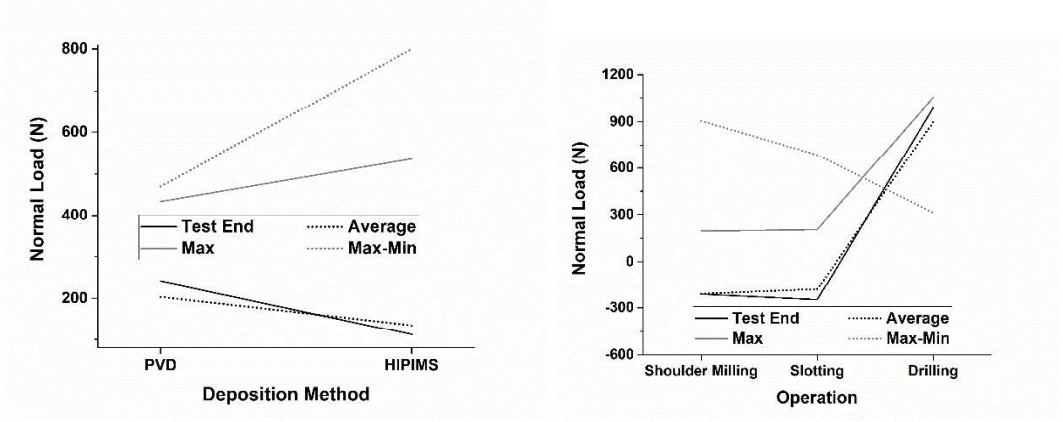


**a)** **b)**

Figure 4.12. Main effect graph of normal load and a) deposition method b) operation type

In figure 4.13 a, b, c, and d there is a strong interaction between operation type and coating technologies. In figure 4.14 a, there is a slight change in deposition methods and torsion force. On the other hand, in figure 4.14 b, the torsion force of drilling operation is much lower than the other operation types. Briefly, for drilling operation normal load is very distinguishing. Bending moment is highly effective for slotting and shoulder milling operations. Also, torsion force is really distinguishing for both drilling and slot operations.

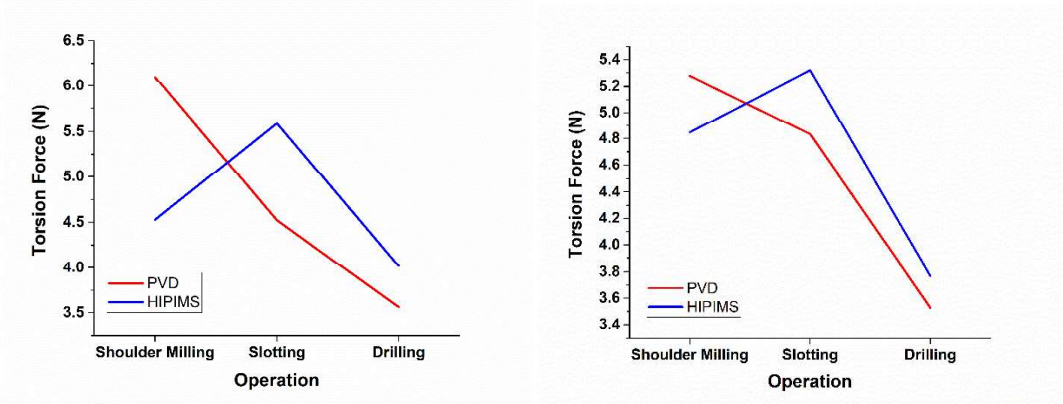


**a)** **b)**

Figure 4.13. Interaction plot of torsion force (a)Test end (b) Average (c) Max (d) Max-min of group 2 (cont. on next page)

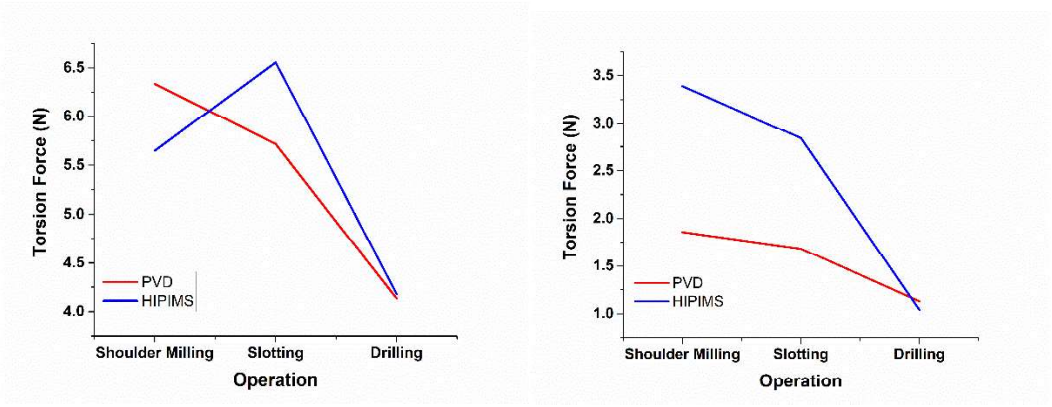


**c)** **d)**

Figure 4.13. (cont.)

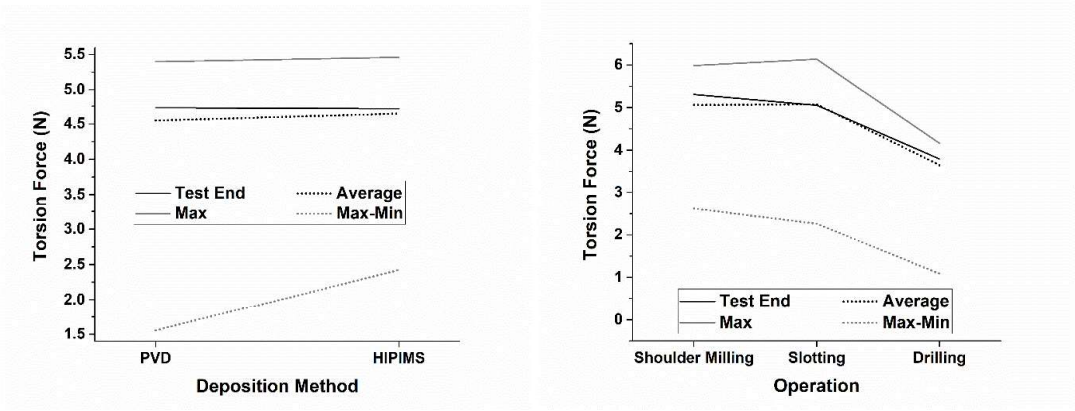


**a)** **b)**

Figure 4.14. Main effect plot of torsion force and a) deposition method b) operation type

In figure 4.15, the interaction plot of wear is given, there is little or no interaction between coating technologies and wear amount. In figure 4.16 a, the HIPIMS technology is less worn than cathodic arc technology regardless of operation. On the other hand, larger amount of wear belongs to the slotting operation in figure 4.16 b.

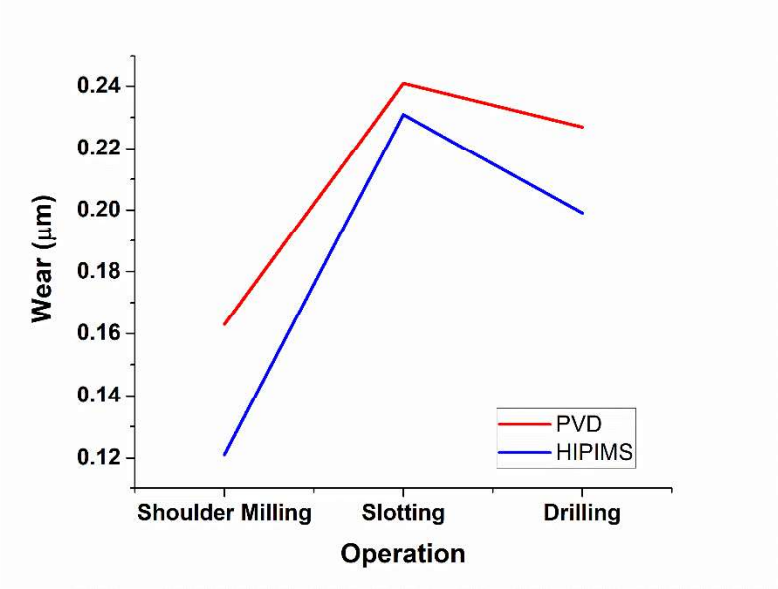


Figure 4.15. Interaction Plot of Wear Rate of group 2

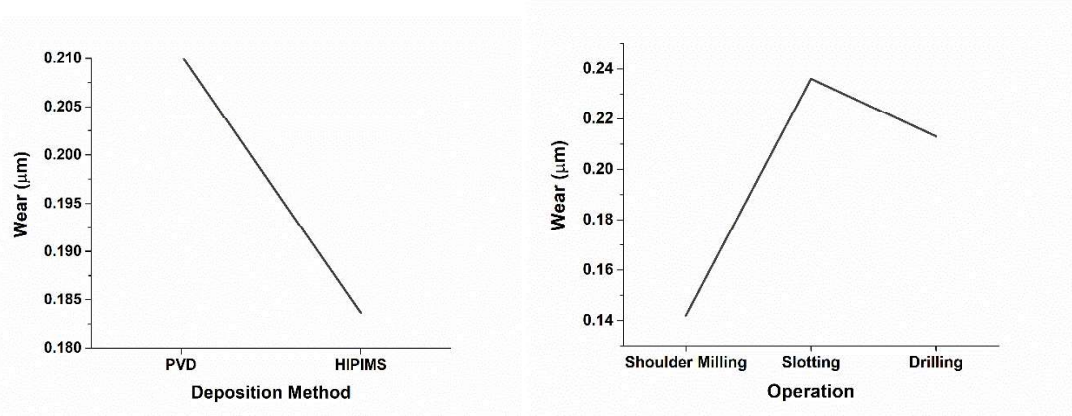


**a)** **b)**

Figure 4.16. Main effect plot of wear amount and a) deposition method b) operation type

Thirdly, group 3 interaction plots of bending moment are given and as it is seen figure 4.17 a, b, c there is little or no interaction between coating technologies and tool geometry. In figure 4.17 d, there is a strong interaction between both tool geometry bending moment and tool geometry coating technology in the terms of max-min values of bending moment this causes the instantly loading while machining. In figure 4.18 while the deposition technique does not affect the bending moment, different geometries are quite effective on the bending moment.

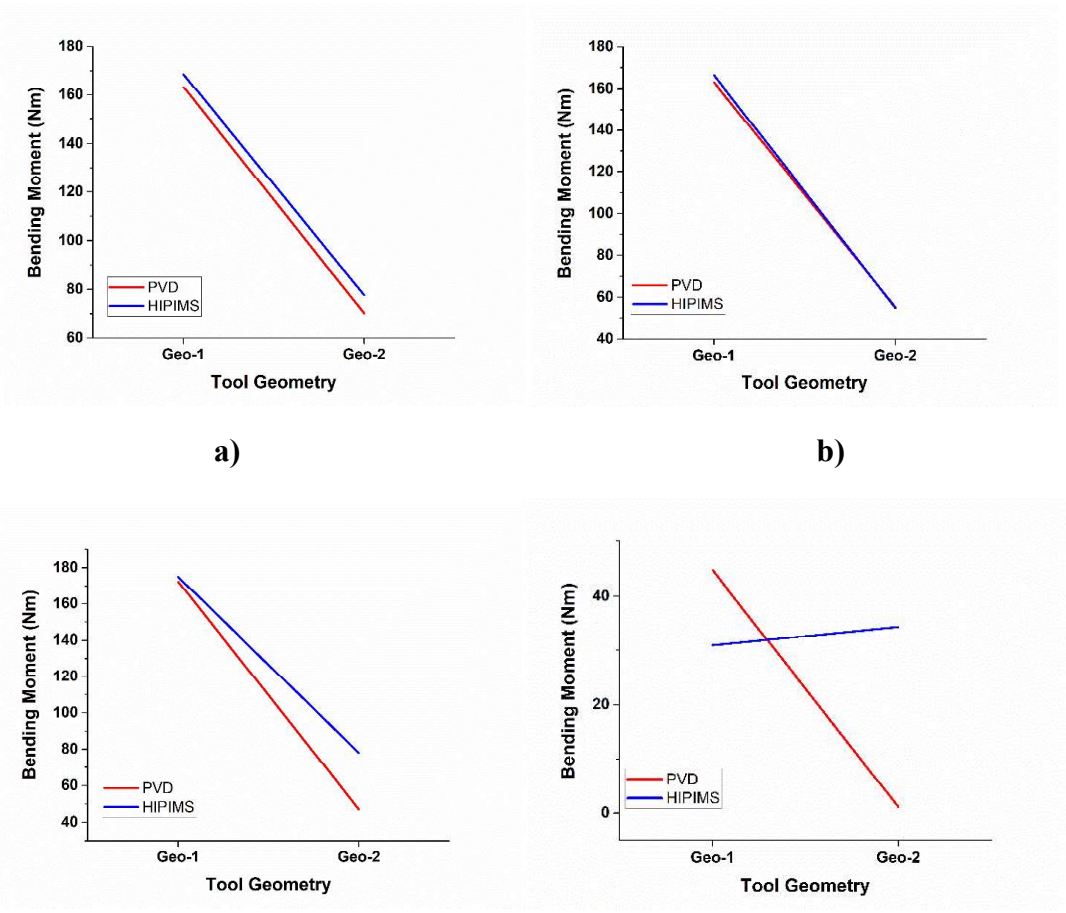


Figure 4.17. Interaction plot of bending moment (a)Test end (b) Average (c) Max (d) Max-min of group 3

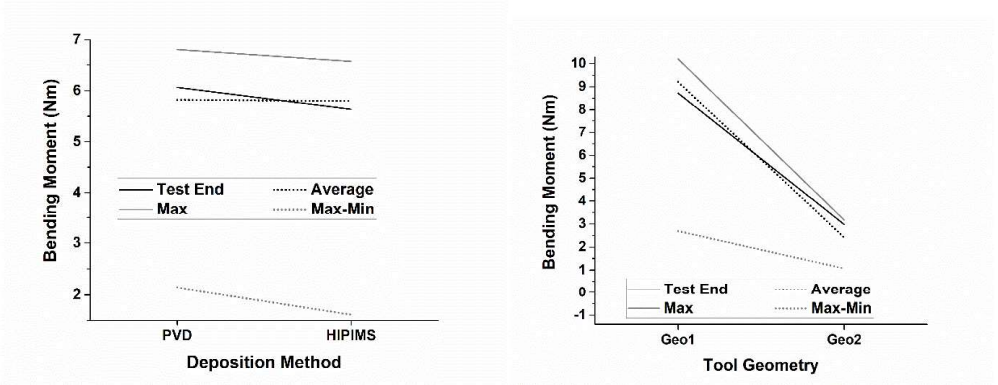


Figure 4.18. Main effect plot of bending moment and a) deposition method b) tool geometry

In figure 4.19 interaction plots of normal loads of group 3 are given and in all these graphs there is strong interaction between tool geometry and normal load and coating technologies.

PVD technology gave good results considering the maximum loading values but gave bad results when looking at the average and end values. In figure 4.20, while the normal load and deposition methods don't change much, there is an interaction between coating technologies and geometries. Geometry 2 gave very little normal load.

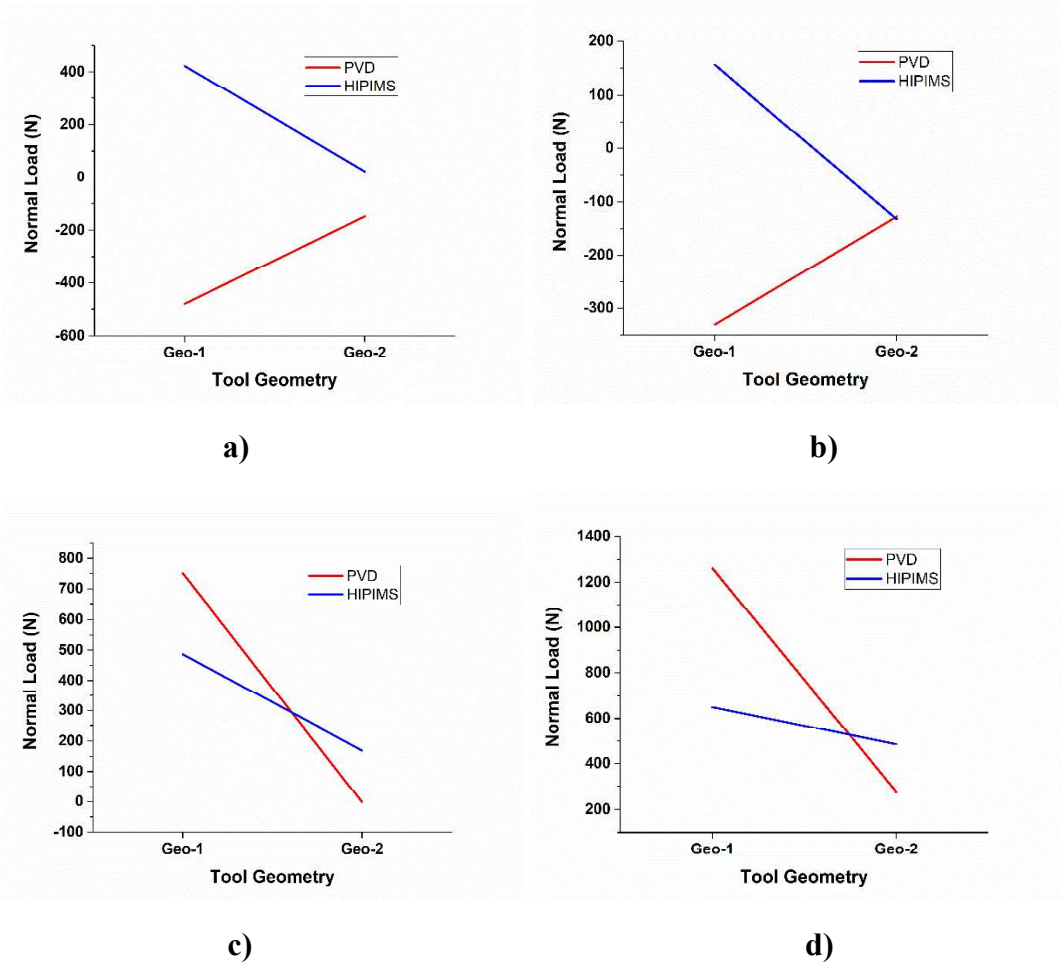


Figure 4.19. Interaction plot of normal load (a)Test end (b) Average (c) Max (d) Max-min of group 3

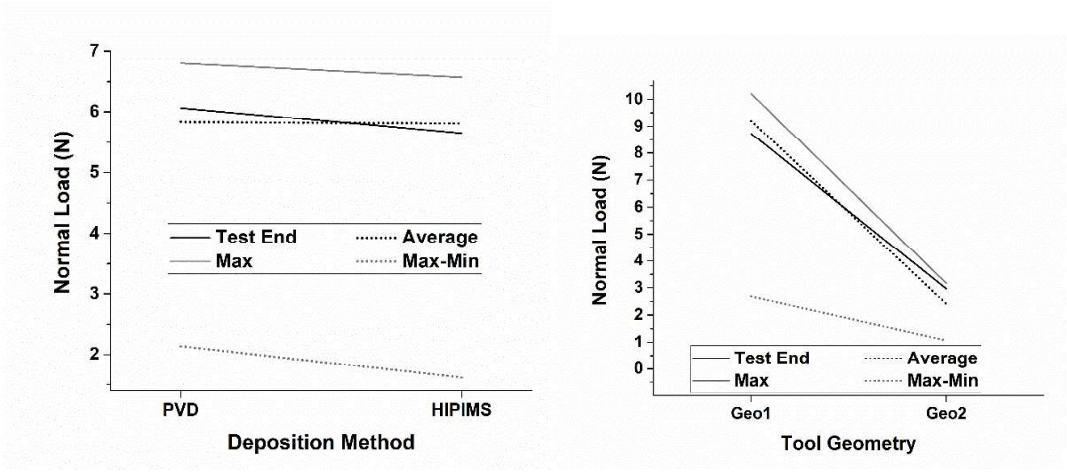


**a)** **b)**

Figure 4.20. Main effect plot of normal load and a) deposition method b) tool geometry

In figure 4.21 interaction plot of torsion forces of group 3 are given. There is little or no interaction between coating technologies. In figure 4.22 a, there is very little variation between the torsion force of coating technologies. In figure 4.22 b, there are significant different torsion forces between two different geometries. Geometry 2 has lower torsion force values.

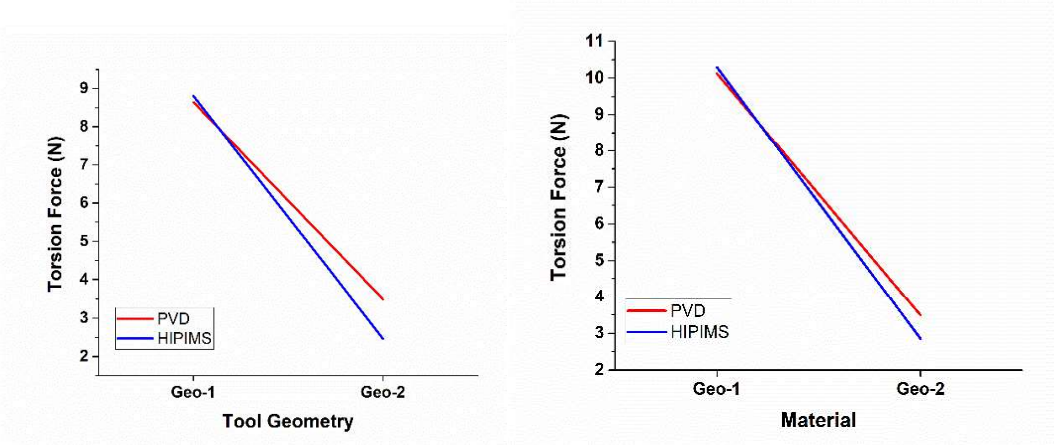


**a)** **b)**

Figure 4.21. Interaction plot of torsion force (a)Test end (b) Average (c) Max (d) Max-min of group 3 (cont. on next page)

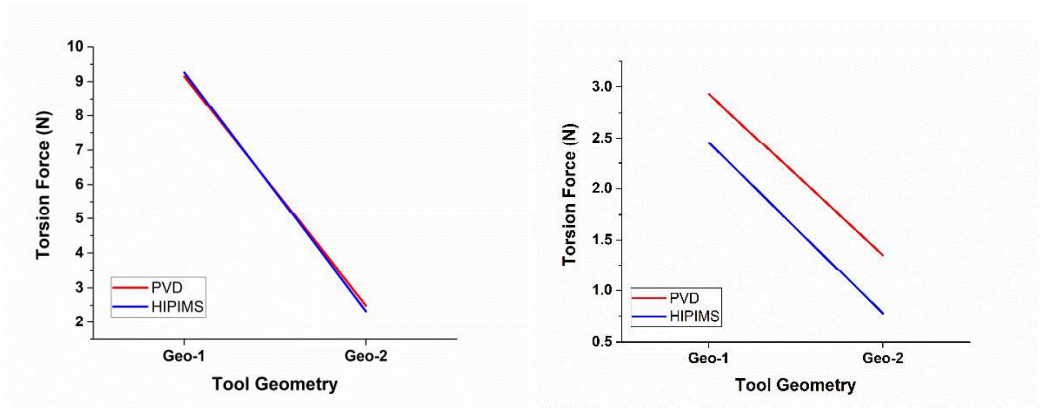


**c)** **d)**

Figure 4.21. (cont.)

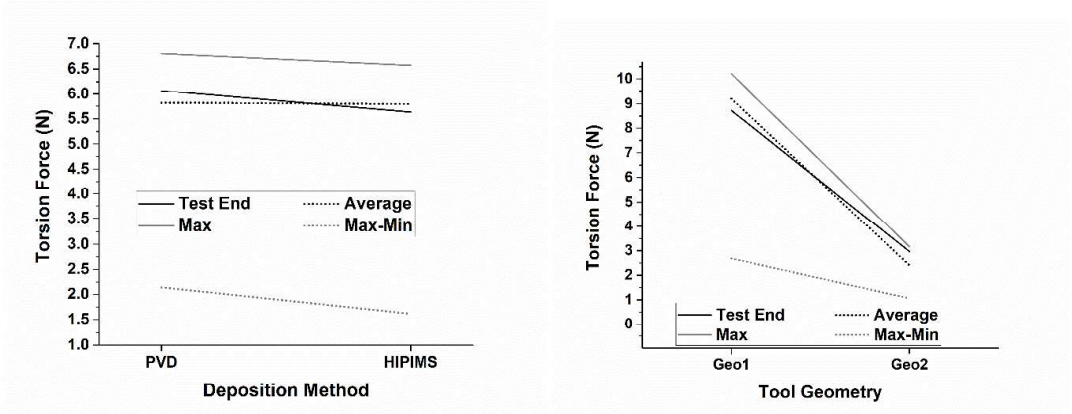


**a)** **b)**

Figure 4.22. Main effect plot of torsion forces and a) deposition method b) tool geometry

In figure 4.23 interaction plot of group 3 are given and there is a strong interaction between wear amount coating technology and tool geometry. Looking at figure 4.24 a and b, while the tools coated with HIPIMS technology are less worn than other techniques, the effect of geometry on tool wear is much less. In geometry 2, the HIPIMS wear much less, while the cathodic arc deposition wears much more.

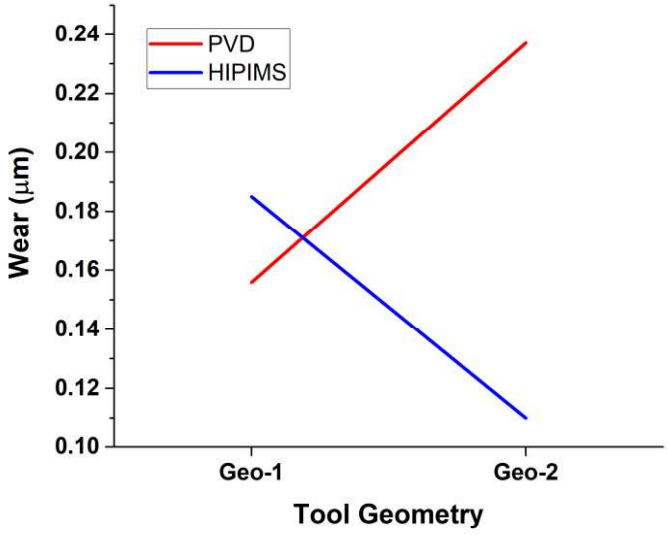


Figure 4.23. Interaction Plot of Wear Rate of group 3

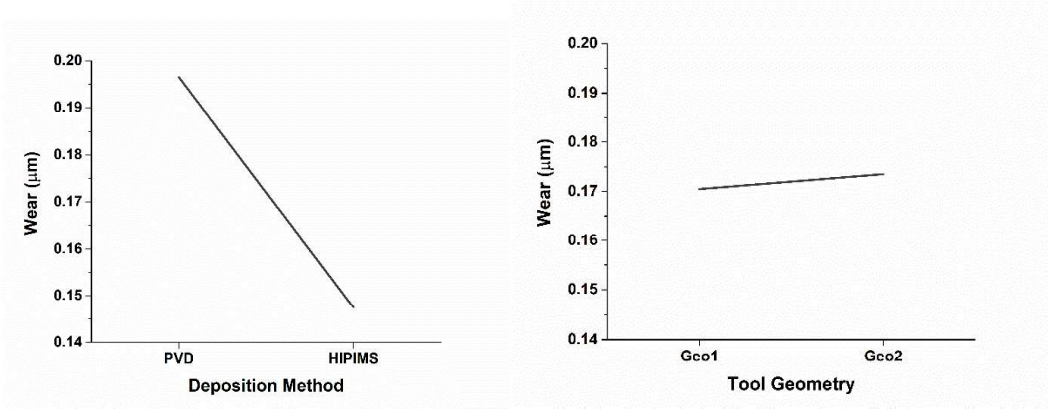


**a)** **b)**

Figure 4.24. Main effect of wear amount and a) deposition method b) tool geometry

Finally, since there was only one variable coating technique in group 4 tests, column charts were created. Looking at the bending moment graphs in figure 4.25, the average bending moment two coating types are head-to-head, while the other test end, max, and max min de perks have less load on the HIPIMS.

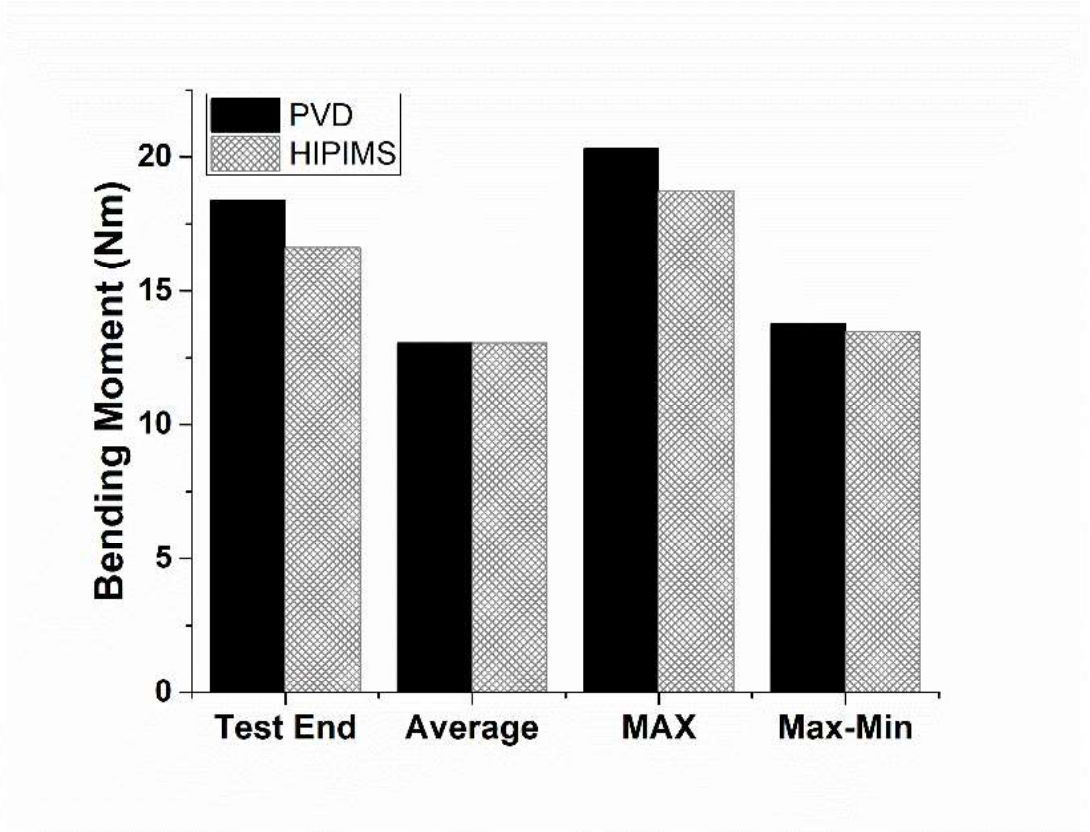


Figure 4.25. Column chart of group 4 bending moment

Looking at the normal load graphs in figure 4.26, the cathodic arc coating took less load in all normal load graphs. The reason for that since the cutting meter is higher in HIPIMS technology, the tool center wear has been less than the cathodic arc and it has drawn more normal load.

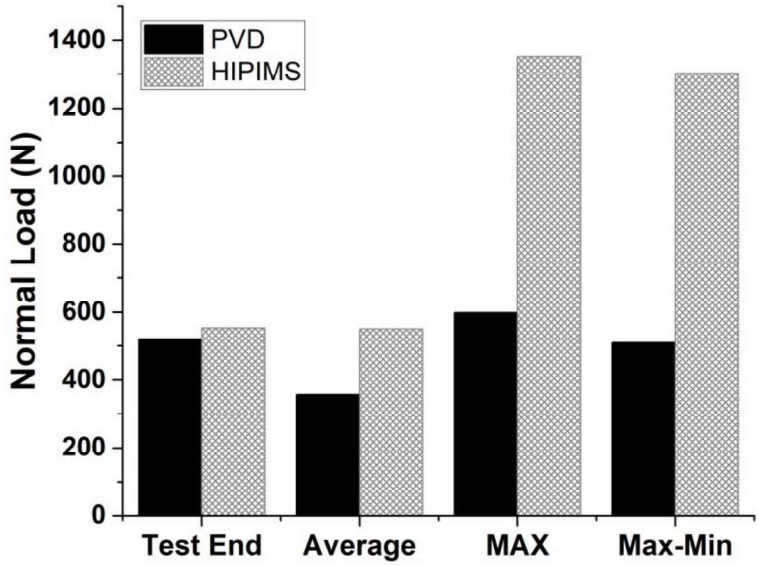


Figure 4.26. Column chart of group 4 normal load

In the test end and average torsion forces graphs in figure 4.27, HIPIMS takes more load while max and max-min graphics of torsion forces on HIPIMS has been exposed to less load.

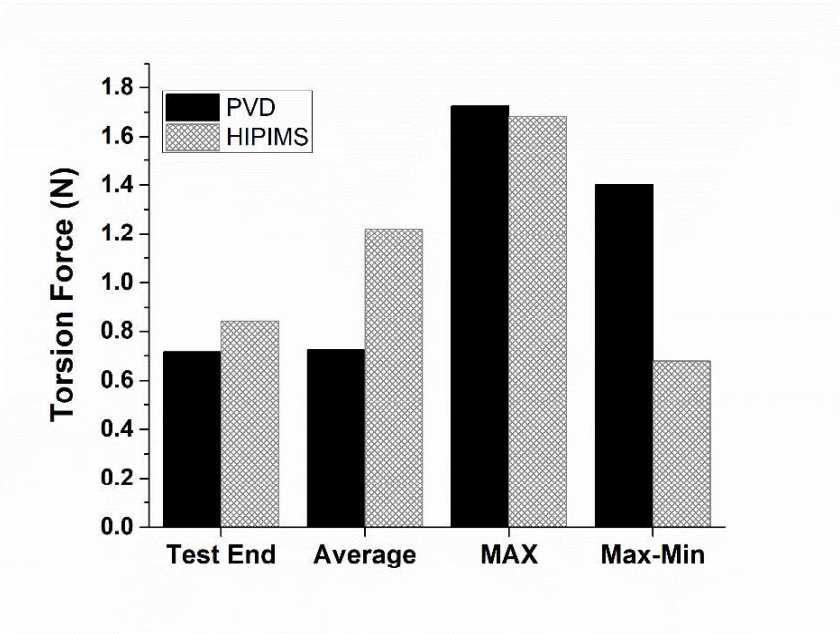


Figure 4.27. Column chart of group 4 torsion force

Looking at the wear graph in figure 9, the HIPIMS coated tool wears almost two times less than other coating technology.

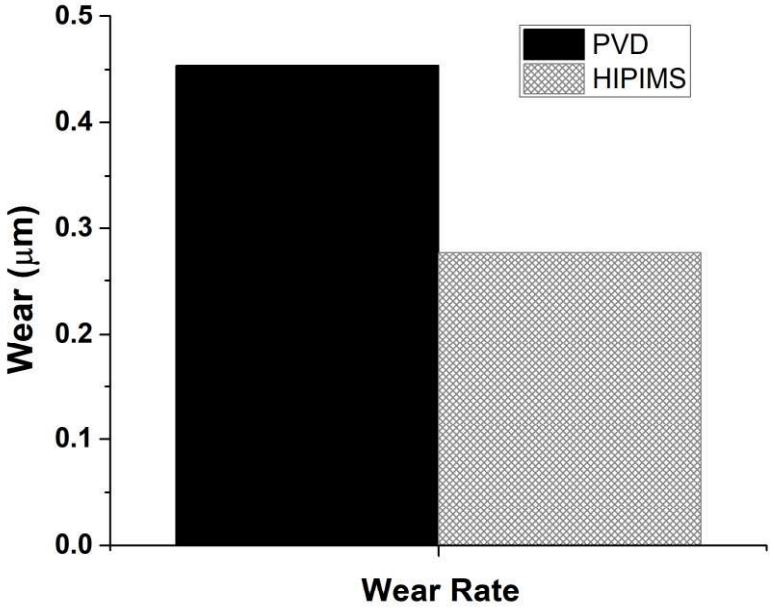


Figure 4.28. Column chart of group 4 wear

# CHAPTER 5

# CONCLUSIONS

Within the scope of this thesis, the effect of cathodic arc depositing and high-power impact magnetron putter coatings on the performance of tools in the machining of various ferrous materials and Ti6Al4V alloy. The results can be summarized as follows,

According to the SEM images, the number of droplets that affect the tool life is more in the cathodic arc deposition technique, while it is negligible in the HIPIMS technique. Different coating techniques give better performance on different coating types for the same material and operation.

Cutting forces are highly effective on the different materials, especially in GG25 material, the cutting forces are ~ %50 higher than the others. In addition, the amount of wear in group 1 is ~%55 higher in HIPIMS coating than in other group tests, because the HIPIMS coated tool in GG25 material has a lot of wear compared to the others. In short, GG25 material is not a very hard material and compared to other materials, the HIPIMS coated tool gave better results in hard materials.

Different types of operations strongly affect different cutting forces. HIPIMS technology is more effective in shoulder milling and HIPIMS performs better in operations where normal load is low and torsion force is high.

Considering all operation types in 4140 material, HIPIMS technology is ~%15 better than cathodic arc.

Tool geometry strongly influences cutting forces, but coating technology does not have much effect on forces. However, geometry affects tool wear a lot. HIPIMS technology suffers less wear when looking at the wear of coatings of different geometries.

Coating technologies give much better performance in hard materials. Even if there are significant differences between the cutting forces, HIPIMS technology coatings give up to ~50 better performance when looking at the amount of wear.

There are significant differences in all forces in the max-min graphs for all tests, these differences are due to the change point of the billet during the performance tests.

# REFERENCES


1. Chavoshi, S. Z., and Luo, X., **2015**, "Hybrid Micro-Machining Processes: A Review," *Precision Engineering*, **41**, pp. 1–23.

2. Ezugwu, E. O., **2005**, "Key Improvements in the Machining of Difficult-to-Cut Aerospace Superalloys," *International Journal of Machine Tools and Manufacture*, 45(12–13), pp. 1353–1367

3. Davim, J. P. (Ed.). **2008**. Machining: fundamentals and recent advances.

4. *Groover, Mikell P. **2007**,* "Theory of Metal Machining", *Fundamentals of Modern Manufacturing (3rd ed.), John Wiley & Sons, Inc., pp. 491–504, ISBN 978-0-471-74485-6*

5. Bourgoyne, A. T., Millheim, K. K., Chenevert, M. E., & Young, F. S. **1986**. Applied drilling engineering.

6. https://www.sandvik.coromant.com/en-us/knowledge/drilling

7. Practical treatise on milling and milling machines. Brown & Sharpe Manufacturing Company. 1914. Retrieved **2013**-01-28.

8. Gökçe, H., Ciftci, I., & Demir, H. *2018*. Cutting parameter optimization in shoulder milling of commercially pure molybdenum. *Journal of the Brazilian Society of Mechanical Sciences and engineering*, *40*, 1-11.

9. Mills, B. **2012**. *Machinability of engineering materials*. Springer Science & Business Media.

10. Childs, T. H., Arrazola, P. J., Aristimuno, P., Garay, A., & Sacristan, I. **2018**. *Ti6Al4V metal cutting chip formation experiments and modelling over a wide range of cutting speeds*. Journal of Materials Processing Technology, 255, 898-913.

11. Lawal, S. A., Choudhury, I. A., & Nukman, Y. **2012**. Application of vegetable oil-based metalworking fluids in machining ferrous metals—a review. *International Journal of Machine Tools and Manufacture*, 52(1), 1-12.

12. Rana, R. S., Purohit, R., & Das, S. **2012.** Reviews on the influences of alloying elements on the microstructure and mechanical properties of aluminum alloys and aluminum alloy composites. *International Journal of Scientific and research publications*, *2*(6), 1-7.

13. Armendia, M., Osborne, P., Garay, A., Belloso, J., Turner, S., & Arrazola, P. J. **2012**. Influence of heat treatment on the machinability of titanium alloys. *Materials and Manufacturing Processes*, *27*(4), 457-461.

14. Ahmed, W., Elhissi, A., Jackson, M., & Ahmed, E. **2012.** Precision machining of medical devices. *The design and manufacture of medical devices*, 59-113.

15. Ahmed, W., Hegab, H., Mohany, A., & Kishawy, H. **2021**. Towards Analysis and Optimization during Machining Hardened Steel AISI 4140 with Self-Propelled Rotary Tools

16. https://www.sandvik.coromant.com/tr-tr/knowledge/materials/workpiece-materials

17. https://www.ceratizit.com/

18. https://www.fivestartool.com/cutting-tools

19. Bouzakis, K. D., Michailidis, N., Skordaris, G., Bouzakis, E., Biermann, D., & M'Saoubi, R. **2012**. Cutting with coated tools: Coating technologies, characterization methods and performance optimization. CIRP annals, *61*(2), 703-723.

20. Sproul, W. D. **1996.** Physical vapor deposition tool coatings. Surface and Coatings Technology, *81*(1), 1-7.

21. Zhao, J., Liu, Z., Wang, B., & Hu, J. **2020**. PVD AlTiN coating effects on tool-chip heat partition coefficient and cutting temperature rise in orthogonal cutting Inconel 718. *International Journal of Heat and Mass Transfer*, *163*, 120449.

22. Deng, J., Liu, J., Zhao, J., & Song, W. **2008**. Wear mechanisms of PVD ZrN coated tools in machining. *International Journal of Refractory Metals and Hard Materials*, 26(3), 164-172.

23. Wang, C. Y., Xie, Y. X., Qin, Z., Lin, H. S., Yuan, Y. H., & Wang, Q. M. **2015**. Wear and breakage of TiAlN-and TiSiN-coated carbide tools during high-speed milling of hardened steel. *Wear*, 336, 29-42.

24. S. Zhang, D. Sun, Y.Q. Fu, and H.J. Du, Recent advances of superhard nanocomposite coatings: a review, *Surf. Coat. Technol.*, 167, **2003**, p. 113.

25. 1. Zhao, J., Liu, Z., Wang, B., Hu, J., & Wan, Y. **2021**. Tool coating effects on cutting temperature during metal cutting processes: Comprehensive review and future research directions. *Mechanical Systems and Signal Processing*, *150*, 107302.

26. 1. Sousa, V. F., & Silva, F. J. **2020**. Recent advances in turning processes using coated tools—A comprehensive review. *Metals*, *10*(2), 170.

27. Alfonso, E., Olaya, J., & Cubillos, G. **2012.** Thin film growth through sputtering technique and its applications. *Crystallization-Science and technology*, *23*, 11-12.

28. Panjan, P., Drnovšek, A., Gselman, P., Čekada, M., & Panjan, M. **2020.** Review of growth defects in thin films prepared by PVD techniques. *Coatings*, *10*(5), 447.

29. Sanders, D. M., & Anders, A. **2000**. Review of cathodic arc deposition technology at the start of the new millennium. *Surface and Coatings Technology*, *133*, 78-90.

30. Takikawa, H., & Tanoue, H. **2007**. Review of cathodic arc deposition for preparing droplet-free thin films. *IEEE transactions on plasma science*, *35*(4), 992-999.

31. Hecimovic, A. **2009**. *High power impulse magnetron sputtering (HIPIMS): Fundamental plasma studies and material synthesis*. Sheffield Hallam University (United Kingdom).

32. Lundin, D. **2010**. *The HIPIMS process* (Doctoral dissertation, Linköping University Electronic Press).

33. BAĞCI, M. **2018**. Optimization of Solid Particle Erosion by ZrN Coating Applied Fiber Reinforced Composites by Taguchi Method. *Academic Platform-Journal of Engineering and Science*, *6*(2), 185-194.

34. 1. Antonin, O., Tiron, V., Costin, C., Popa, G., & Minea, T. M. **2014**. On the HIPIMS benefits of multi-pulse operating mode. *Journal of Physics D: Applied Physics*, *48*(1), 015202.

35. Bobzin, K. **2017**. High-performance coatings for cutting tools. *CIRP Journal of Manufacturing Science and Technology*, *18*, 1-9.

36. Sarakinos, K., Alami, J., & Konstantinidis, S. **2010**. High power pulsed magnetron sputtering: A review on scientific and engineering state of the art. *Surface and coatings technology*, *204*(11), 1661-1684.

37. Marchin, N., & Ashrafizadeh, F. **2021**. Effect of carbon addition on tribological performance of TiSiN coatings produced by cathodic arc physical vapour deposition. *Surface and Coatings Technology*, *407*, 126781.

38. Yi, J., Chen, K., & Xu, Y. **2019**. Microstructure, properties, and titanium cutting performance of AlTiN–Cu and AlTiN–Ni coatings. *Coatings*, *9*(12), 818.

39. He, Q., DePaiva, J. M., Kohlscheen, J., Beake, B. D., & Veldhuis, S. C. **2021**. Study of wear performance and tribological characterization of AlTiN PVD coatings with different Al/Ti ratios during ultra-high speed turning of stainless steel 304. *International Journal of Refractory Metals and Hard Materials*, *96*, 105488.

40. Kumar, A., Bauri, R., Naskar, A., & Chattopadhyay, A. K. **2021**. Characterization of HIPIMS and DCMS deposited TiAlN coatings and machining performance evaluation in high-speed dry machining of low and high carbon steel. *Surface and Coatings Technology*, *417*, 127180.

41. Sousa, V. F., Silva, F. J., Lopes, H., Casais, R. C., Baptista, A., Pinto, G., & Alexandre, R. **2021**. Wear Behavior and Machining Performance of TiAlSiN-Coated Tools Obtained by dc MS and HIPIMS: A Comparative Study. Materials, 14(18), 5122.

42. Reolon, L. W., Aguirre, M. H., Yamamoto, K., Zhao, Q., Zhitomirsky, I., Fox-Rabinovich, G., & Veldhuis, S. C. **2021**. A comprehensive study of Al0. 6Ti0. 4N coatings deposited by cathodic arc and HIPIMS PVD methods in relation to their cutting performance during the machining of an inconel 718 alloy. Coatings, 11(6), 723.